Phase transformations in additive manufacturing of tool steels materials

Francisca G. Caballero

National Centre for Metallurgical Research (CENIM)

Spanish Research Council (CSIC)

Madrid, Spain

Formation of Bainite in Steels

Jiaqing Yin

Doctoral Thesis in
Department of Materials Science and Engineering
School of Industrial Engineering and Management
KTH Royal Institute of Technology
Stockholm, Sweden, 2017

A Symposium in Memory of Prof. Mats Hillert

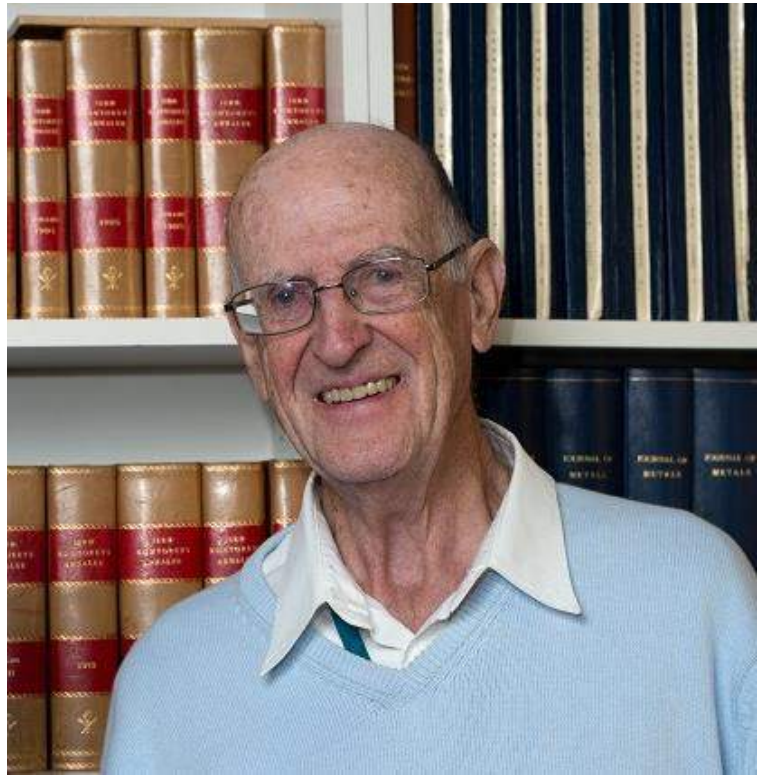

Phase transformations in additive manufacturing of tool steels materials

In collaboration with:

Adriana Eres-Castellanos, Los Alamos National Lab, NM, USA

Jonathan D. Poplawsky, Oak Ridge National Laboratory, TN, USA.

Aleksandra Królicka, Politechnika Wroclawska, PL.

Rosalia Rementeria, ArcelorMittal Global R&D SLab—Steel Labs, Avilés, Spain

Acknowledge funding sources:

European Commission, Research Fund for Coal and Steel Programme. Ref. RFCS-2022-101112371.
Center for Nanophase Materials Sciences-DOE Office of Science User Facility, Ref. CNMS2022-B-01449 and CNMS2024-B-02594.

New Approach to Additive Manufacturing of Microstructurally Optimized Steels (NewAIMS)

RFCS-2022-101112371

The main objective of NewAIMS is to demonstrate strategies to obtain cost-effective high-performance steel through concepts of modified AM with integrated heat treatments.

NewAIMS will propose two high-performing steel grades and a demonstration of printing solutions based on laser powder bed fusion (LPBF) while linking processes and microstructures to their final performance.

Involving all steps in the technological and value chain, NewAIMS will demonstrate these solutions in a tool steels-based use case, with high requirements that imply great technological transferability.

eurecat Centre Tecnològic de Catalunya

Mittuniversitetet MID SWEDEN UNIVERSITY

INNOMAQ21

CSIC Consejo Superior de Investigaciones Científicas

AMAZEMET

Ana Santana

Nisrine Elhamouchi

Content:

- ✓ Revealing the complexity of non-equilibrium, and non-uniform microstructures formed during LPBF process of maraging steels.
- ✓ Precipitation of intermetallic phases and austenite growth/reversion during ageing of LPBF maraging steels.
- ✓ Promoting thermal stabilization of austenite in microstructure by preheating and/or post-heat-treatment in a specially designed tool steels for LPBF manufacturing.

Content:

- ✓ Revealing the complexity of non-equilibrium, and non-uniform microstructures formed during LPBF process of maraging steels.
- ✓ Precipitation of intermetallic phases and austenite growth/reversion during ageing of LPBF maraging steels.
- ✓ Promoting thermal stabilization of austenite in microstructure by preheating and/or post-heat-treatment in a specially designed tool steels for LPBF manufacturing.

Laser Powder Bed Fusion of Maraging Steel

EOS cylinders (Ref. Material)

Under N2 atmosphere

Volume rate of 3 mm³/s

Continuous Wave Emission

Layer thickness: 40 μm

Hatch spacing: 100 μm

Hatch angle: 67°

RENISHAW cubes

Under Ar atmosphere

Laser power: 250 W

Laser speed: 1000 mm/s

Continuous and Pulsed Wave Emission

Layer thickness: 50 and 100 μm

Hatch spacing: 80 μm

Hatch angle: 67°

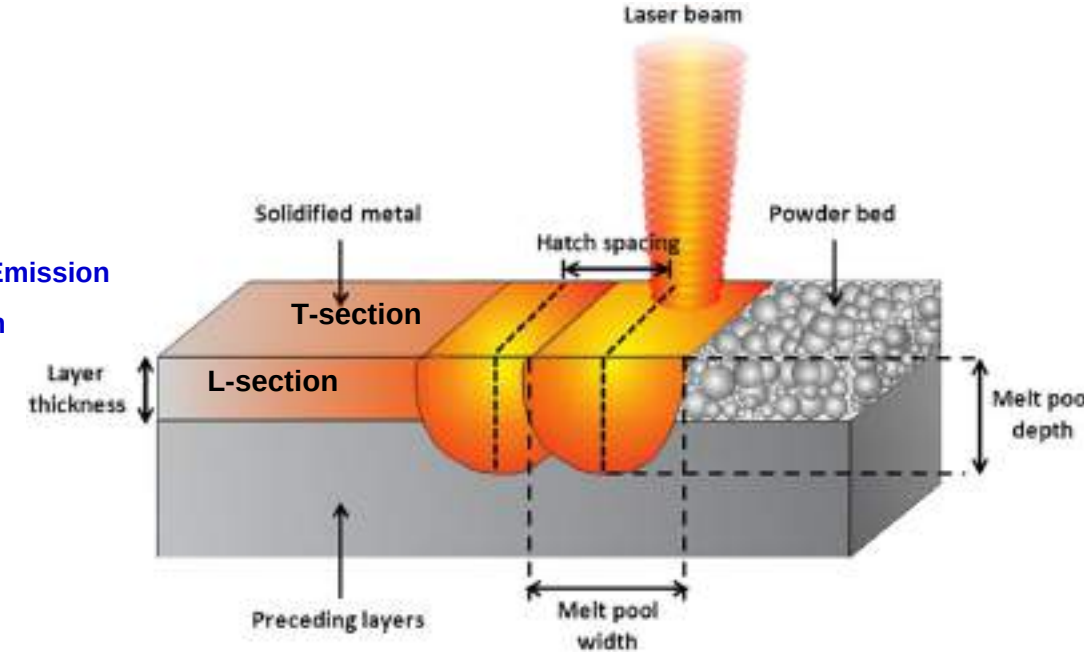

Element	Wt. %
Fe	66.38
Ni	18.35
Co	8.64
Mo	5.45
Ti	0.87
Cr	0.15
Si	0.11
Mn	0.05

Renishaw- 100 μm-PW laser

Transverse section	Longitudinal section

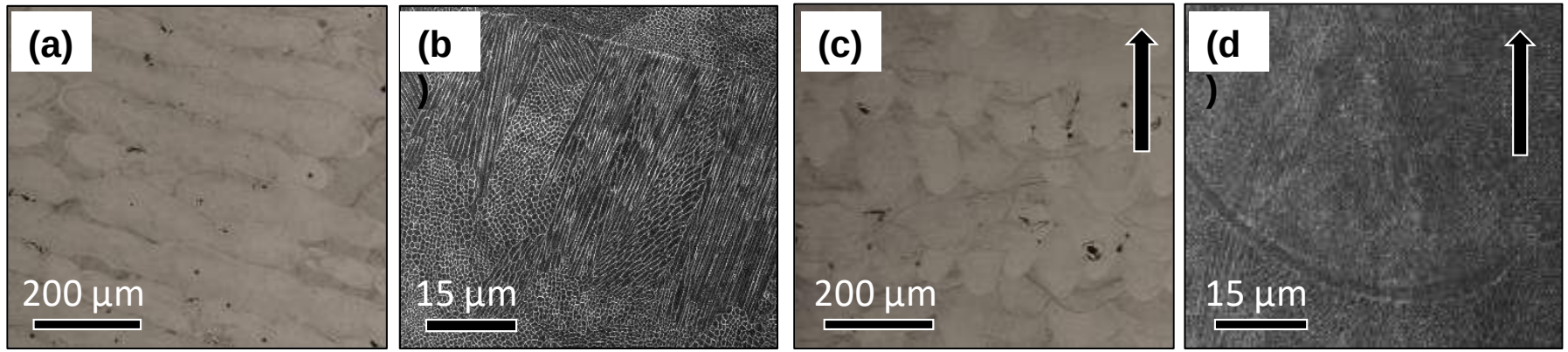

Thermal history experienced by the material during the build process

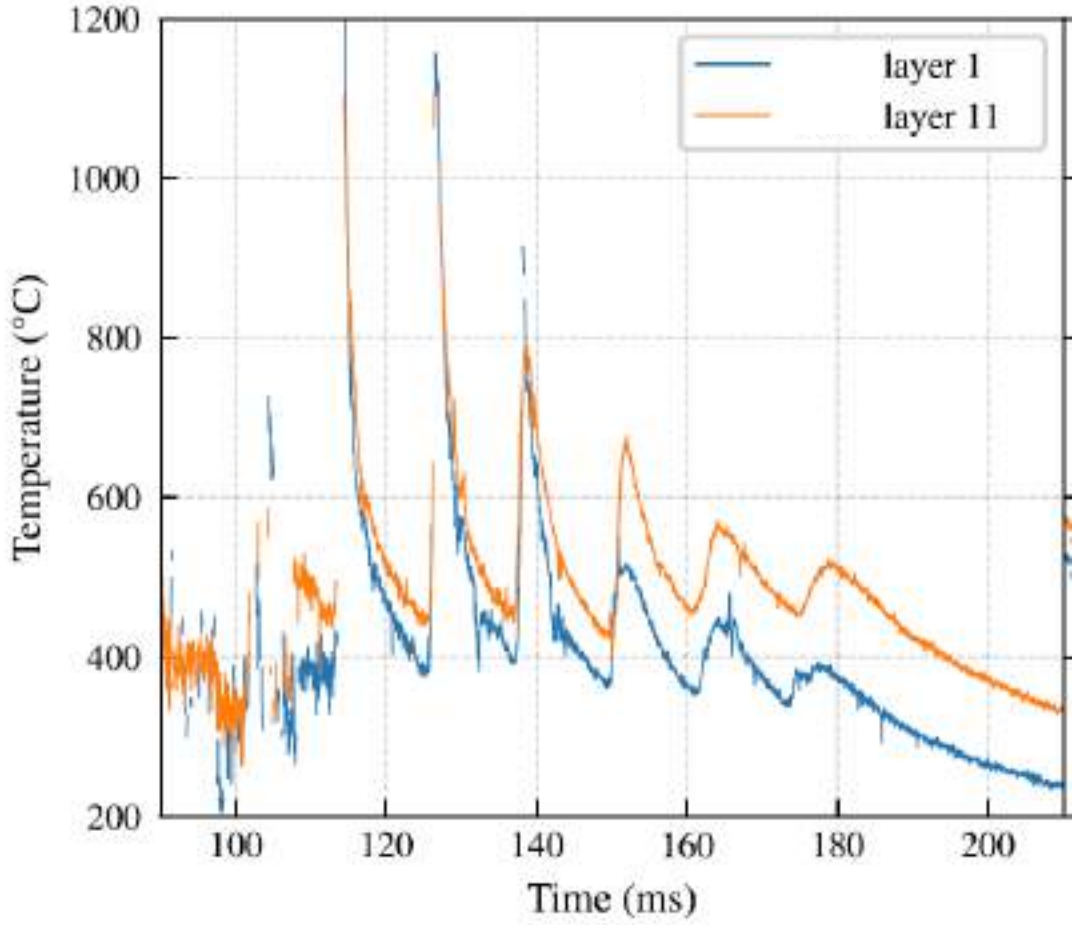

Temperature profiles for layers 1 and 11 based on measurements using *operando* X-ray diffraction

Scheel et al., Additive Manufacturing Letters 6 (2023) 100150

Thermal cycles simulation in a quenching dilatometer (Bahr 805A)

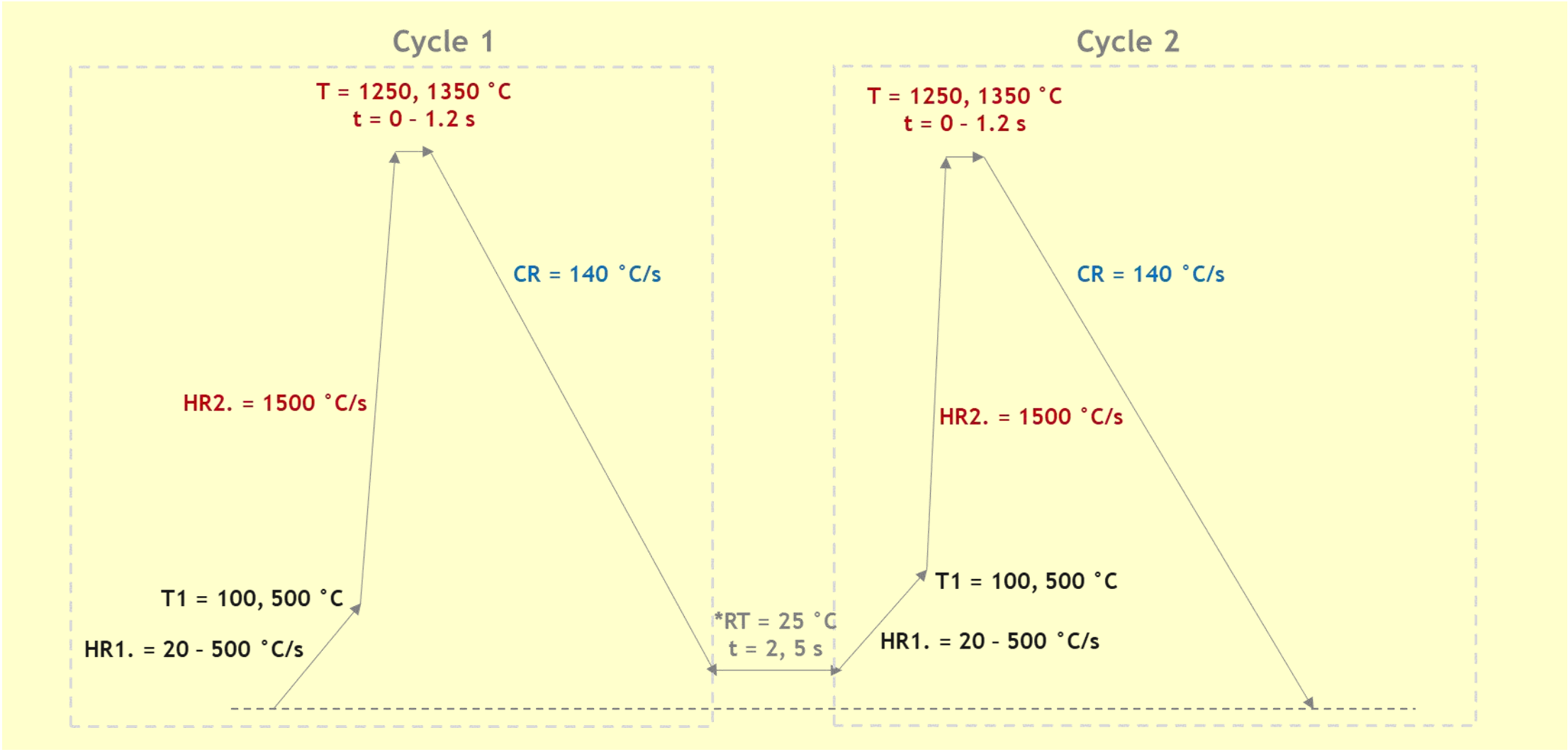

Thermal cycles simulation in a quenching dilatometer (Bahr 805A)

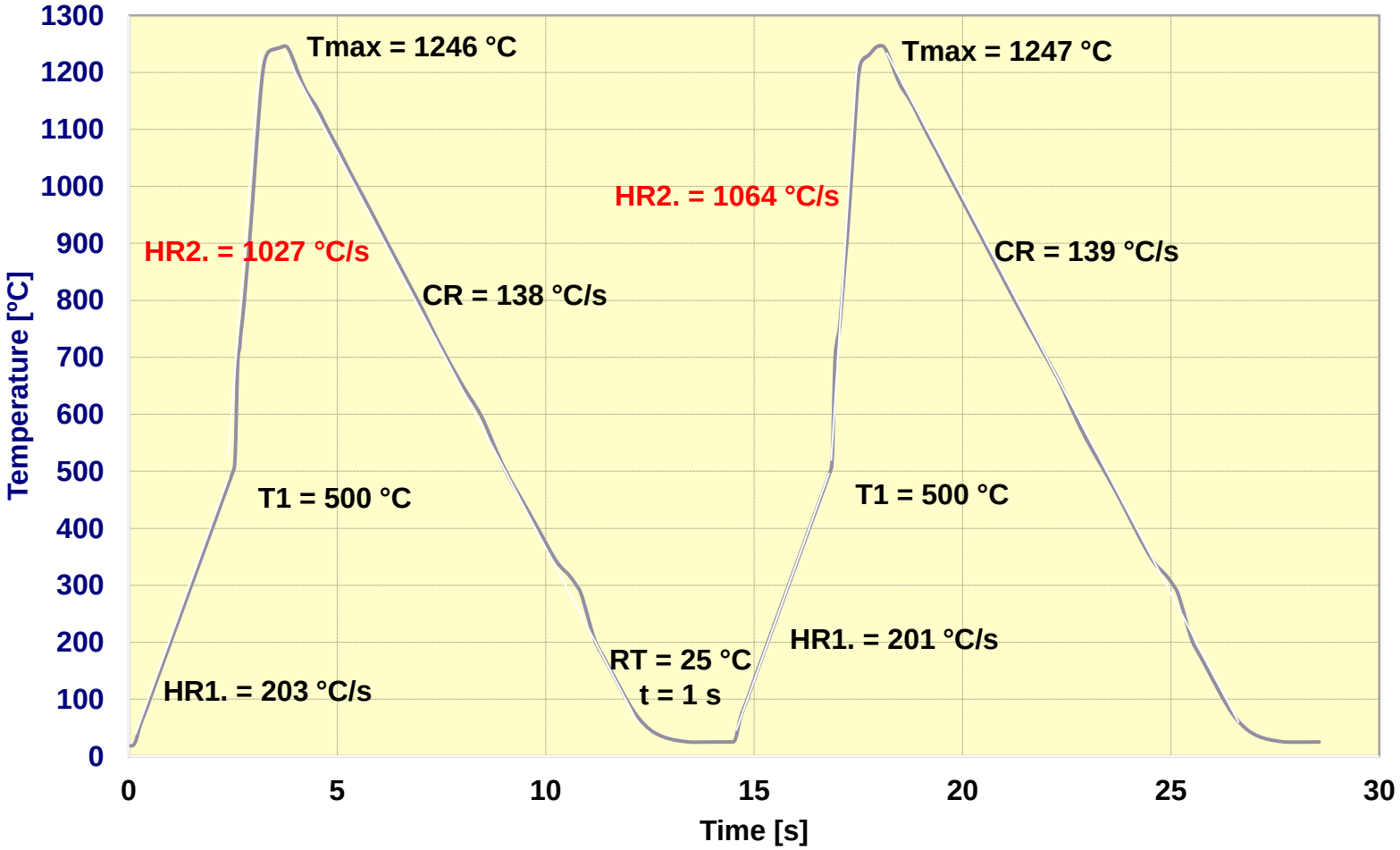

Setup

- Preheating step: HR1 (20 – 500 °C) = 200 °C/s
- Isothermal process at 1250 °C for 0.7 s
- Teflon coil was used

Observations

- HR1. and T1 are achieved
- HR2. average is not achieved
- Tmax and CR programmed are both achieved

High thermal conductivity tool steel

Thermal cycles simulation in a quenching dilatometer (Bahr 805A)

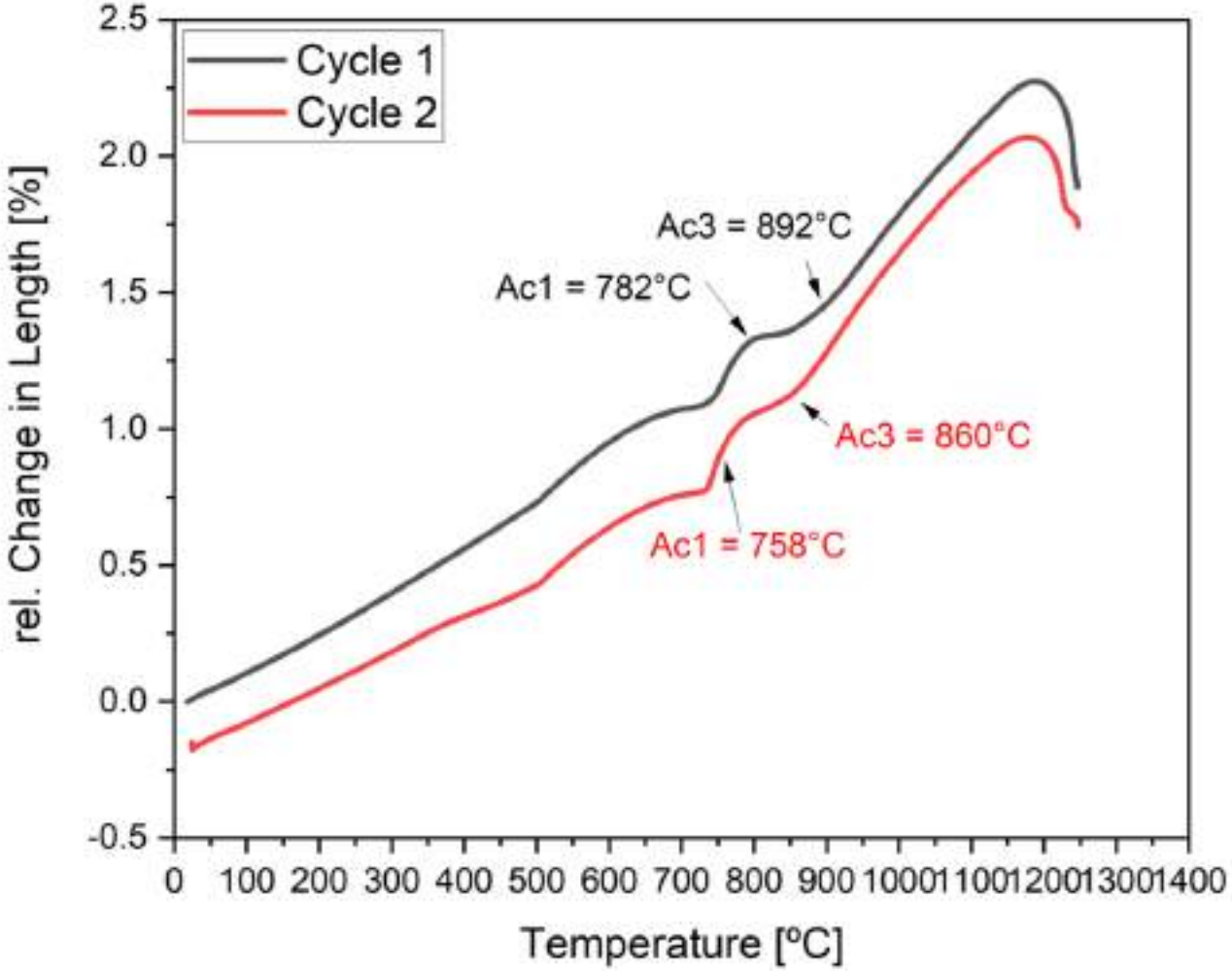

Cellular Structure of Maraging Steel

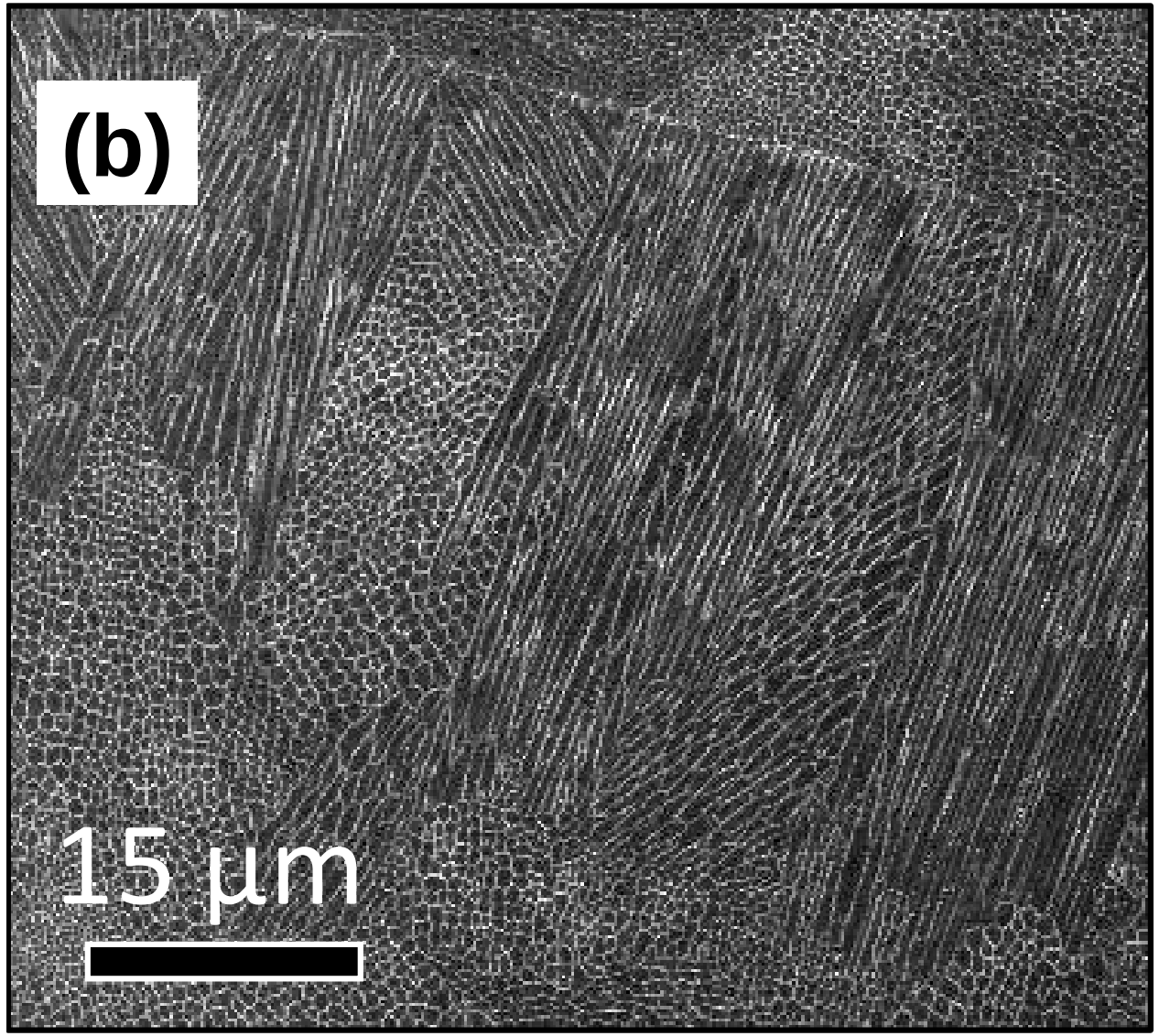

Transverse section

Cellular Structure of Maraging Steel

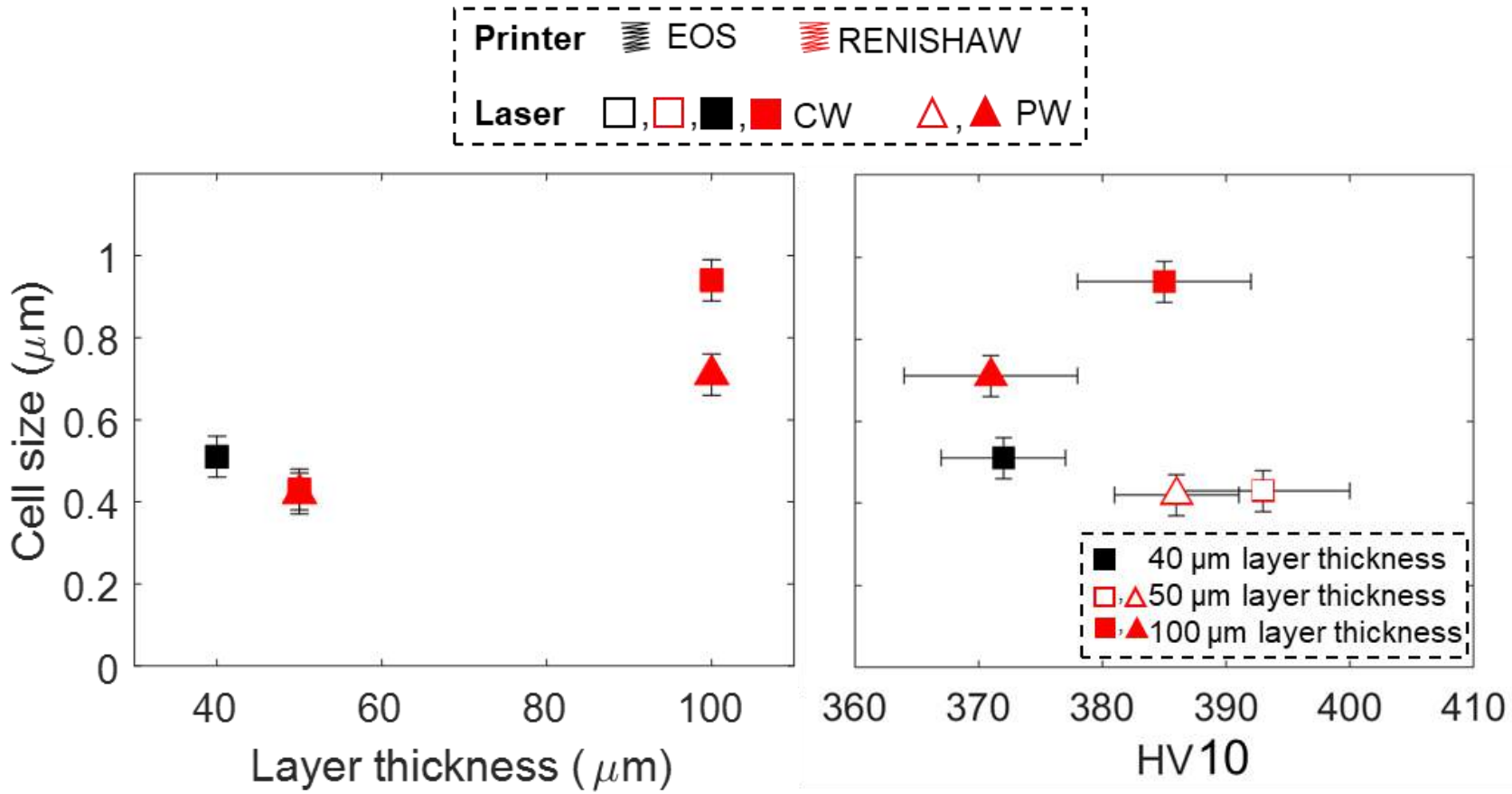

Cellular Structure of Maraging Steel

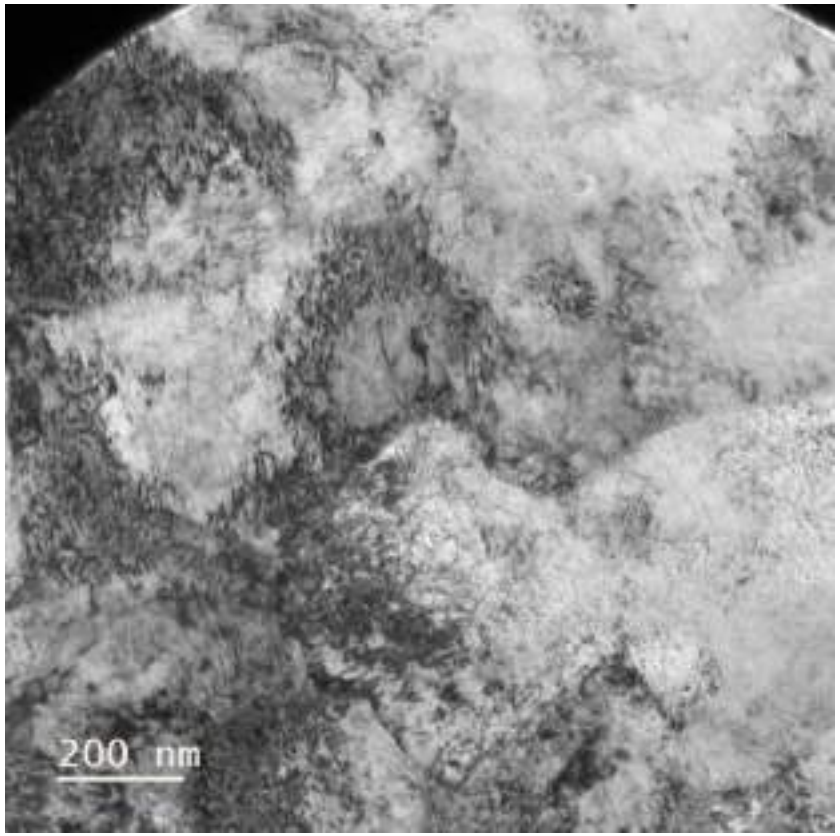

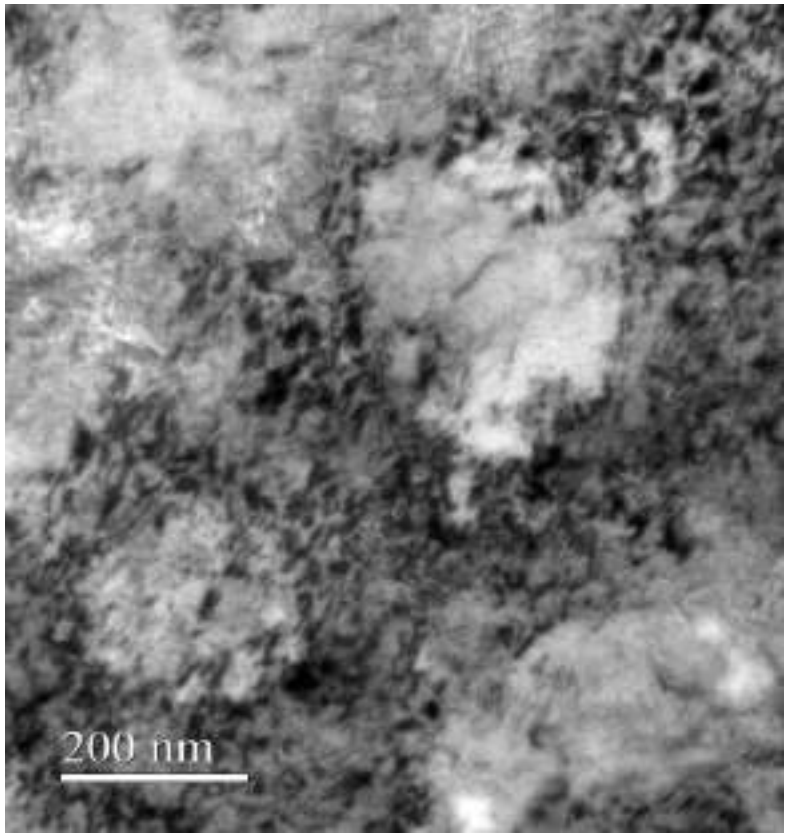

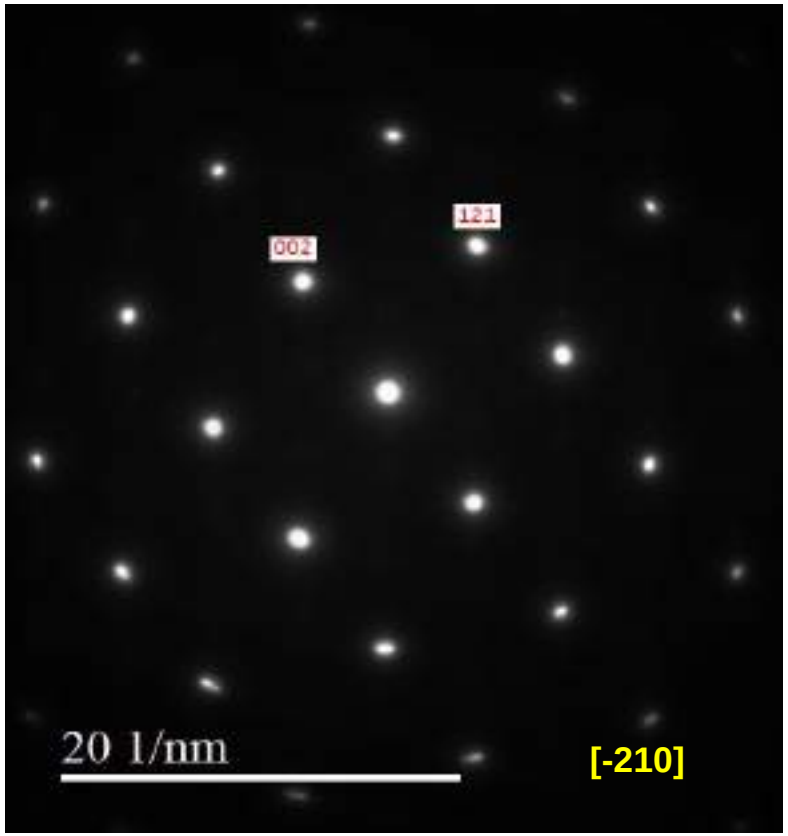

EOS - 40 microns - CW laser mode

Retained Austenite in As-Built Structure

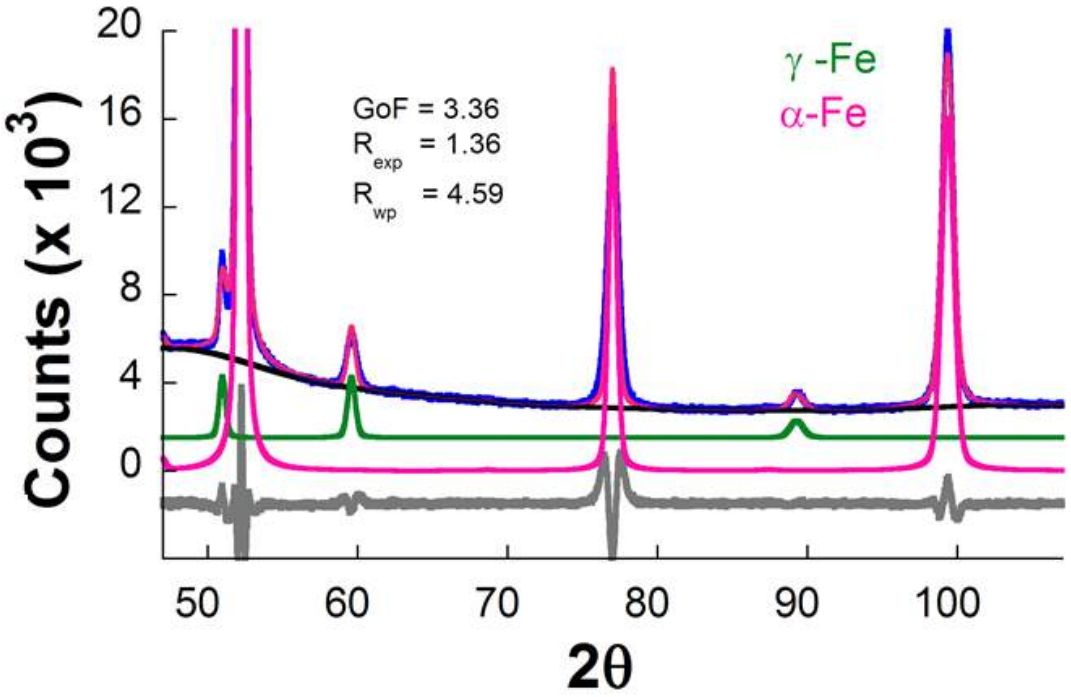

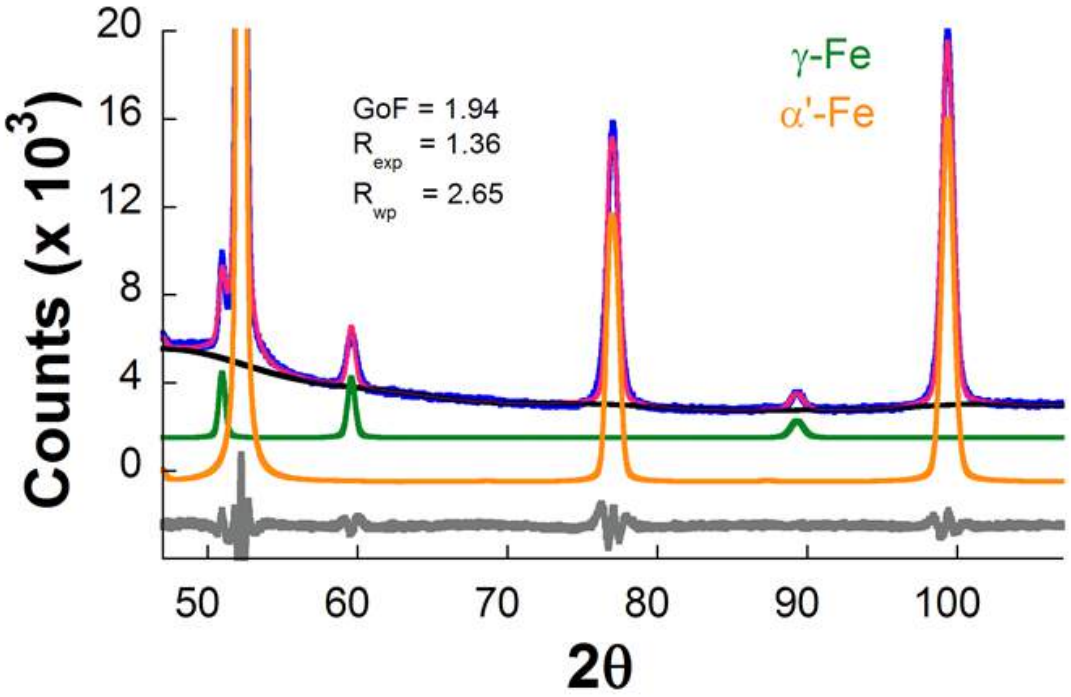

Rwp: weighted summation of residual of the least squares fit,
Rexp: statistically expected least squares fit,
GoF: goodness of fit (sometimes referred as chi-squared); GoF=Rwp/Rexp; a GoF=1.0 means a perfect fitting.

Journal of Materials Research and Technology, 2023; 25: 6898-6912

Retained Austenite in As-Built Structure

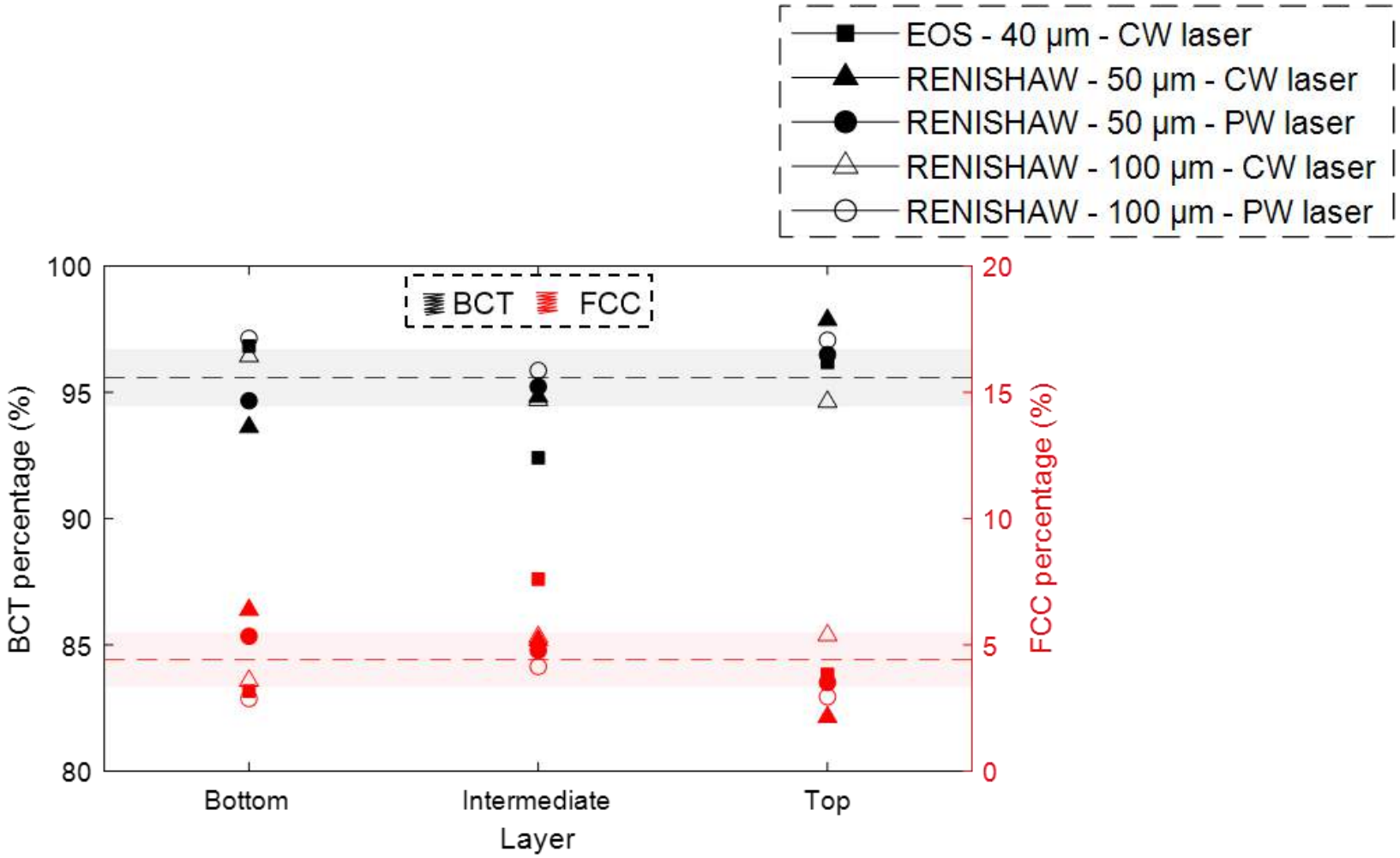

Retained Austenite in As-Built Structure

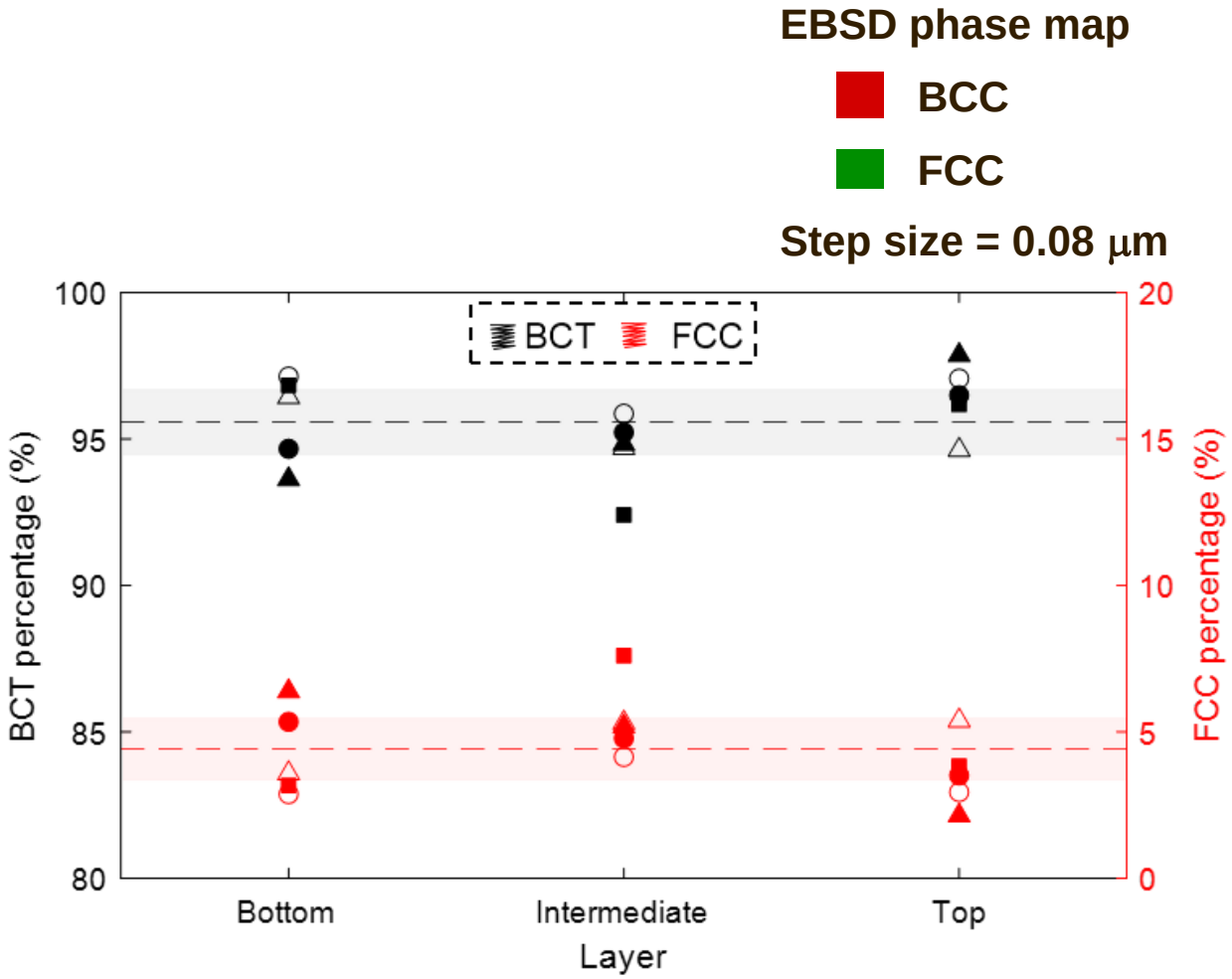

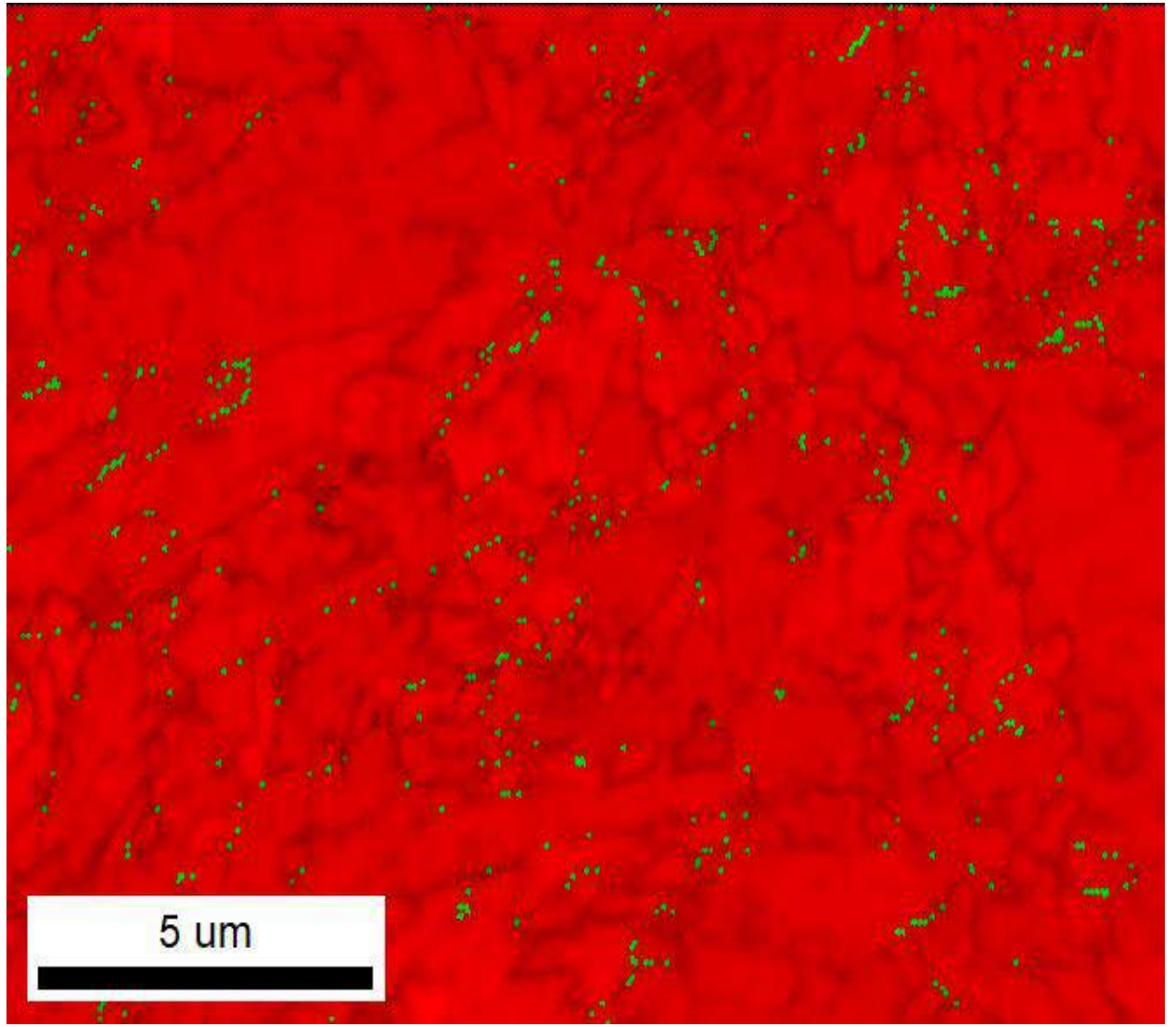

Retained Austenite in As-Built Structure

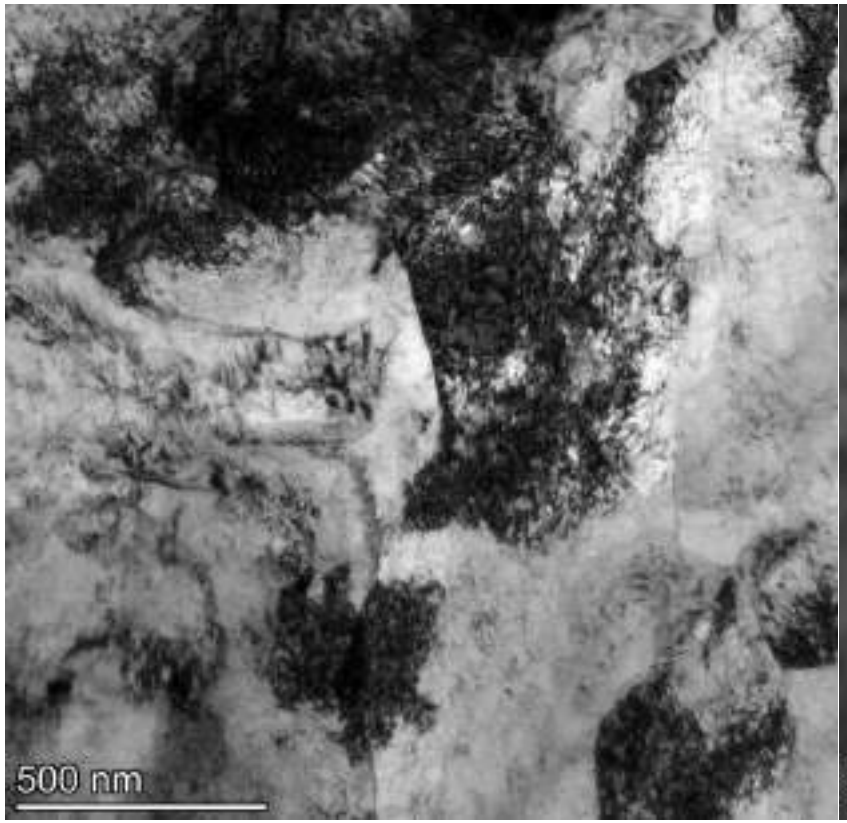

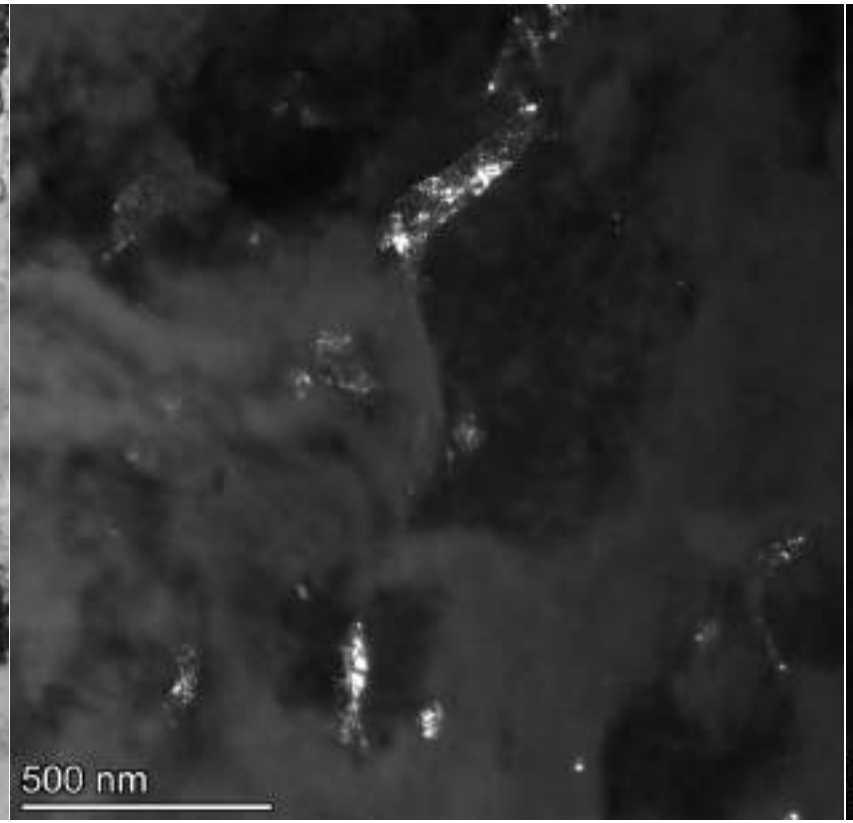

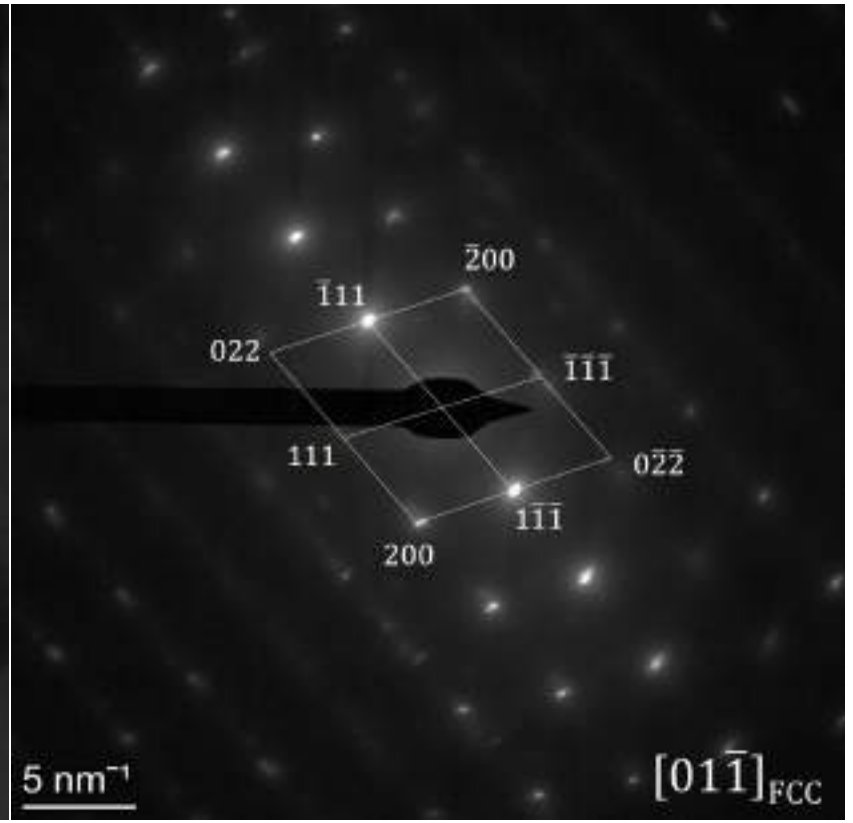

EOS - 40 microns - CW laser mode

Austenite at celular boundaries

Solute Distribution in As-Built Structure

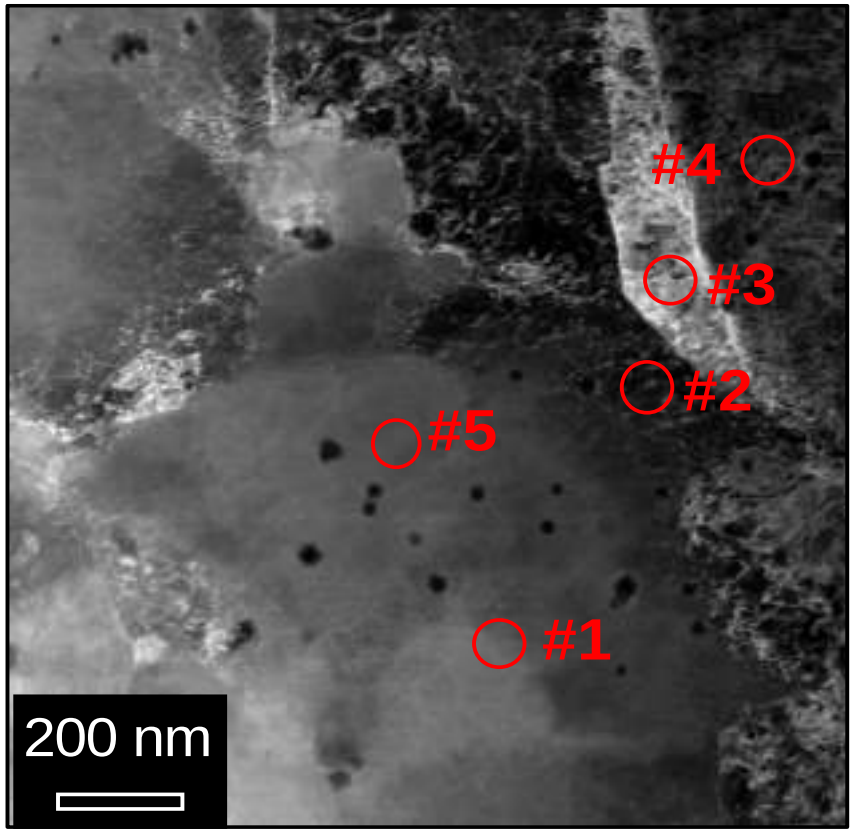

	Chemical composition (at. %)					
	Al	Ti	Cr	Fe	Ni	Mo
Matrix #1	0.18	0.88	0.25	76.79	18.16	3.74
Intercellular #2	0.15	0.84	0.21	75.46	19.03	4.31
Intercellular #3	0.07	0.75	0.21	76.48	18.71	3.78
Intercellular #4	0.21	0.78	0.23	76.00	18.54	4.24
Matrix #5	0.11	0.61	0.20	76.98	18.23	3.87

Solute Distribution in As-Built Structure

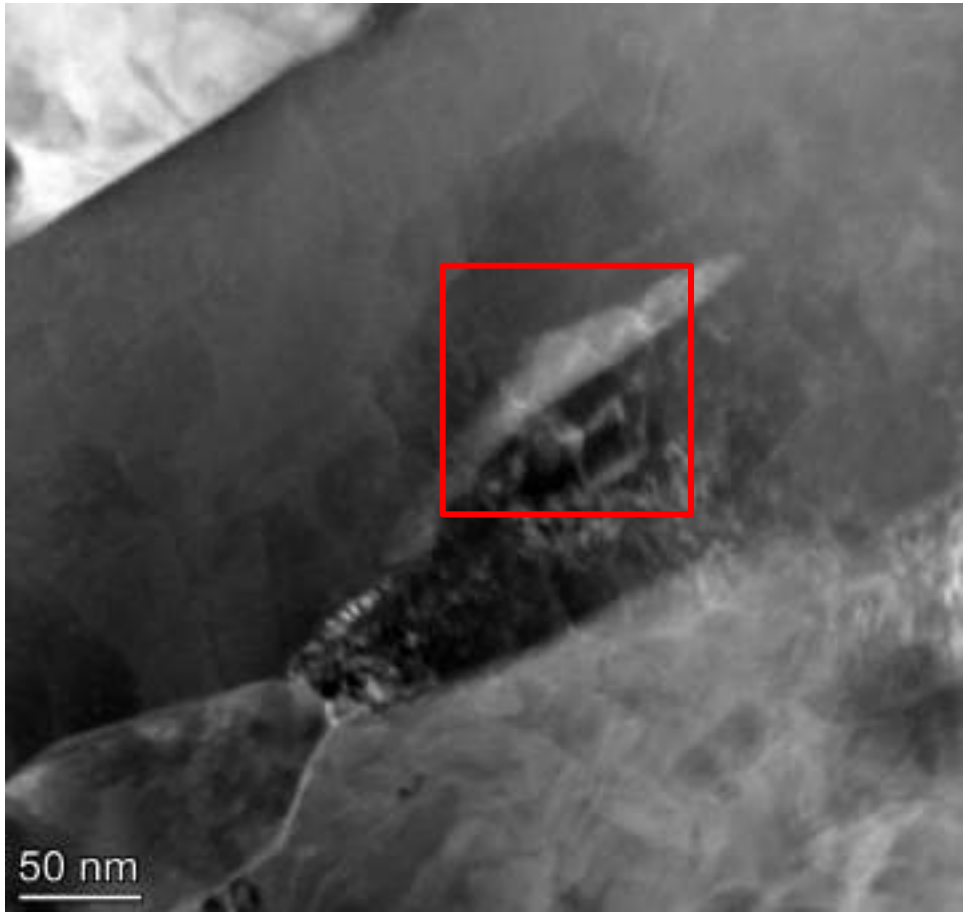

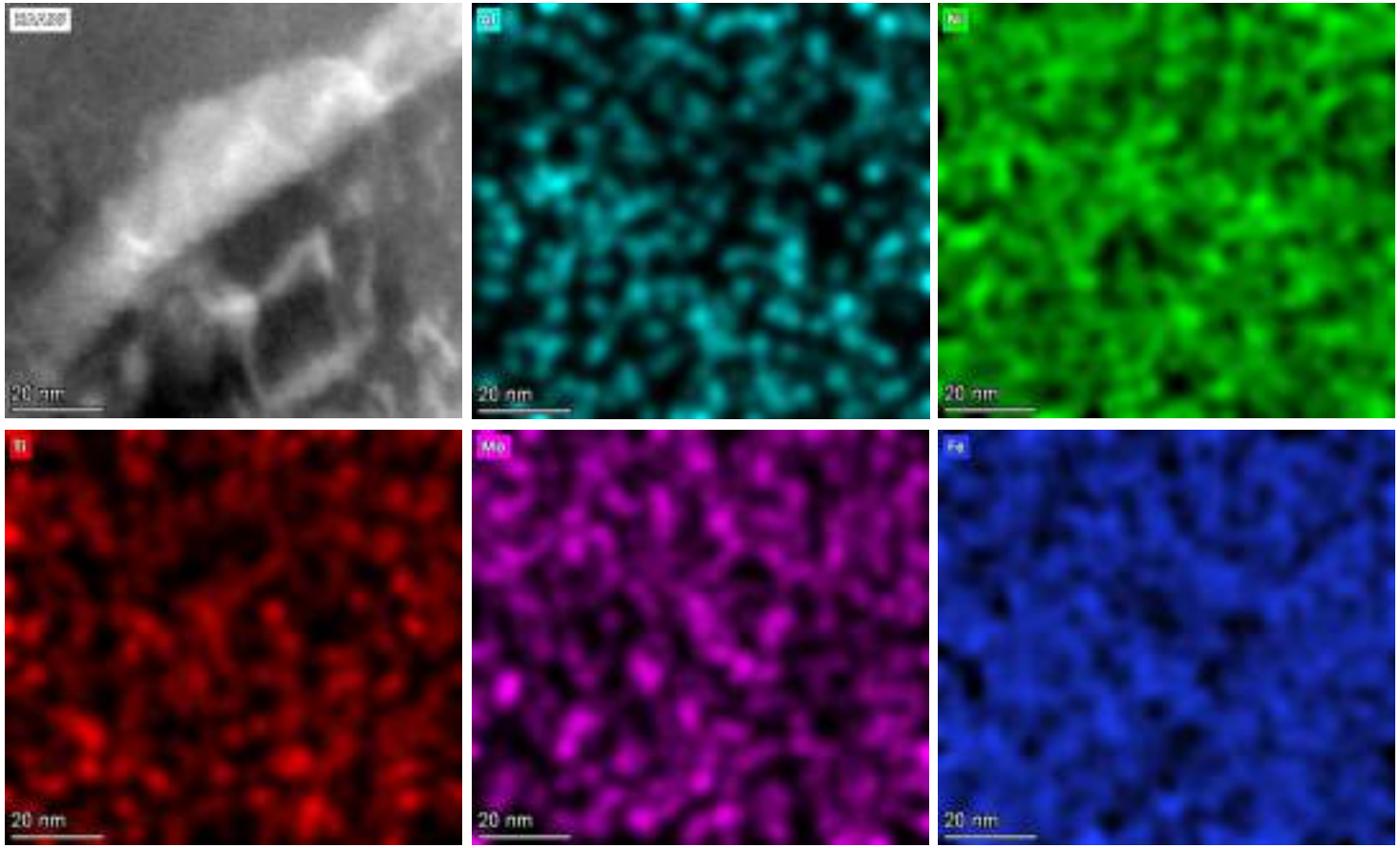

Retained Austenite in As-Built Structure

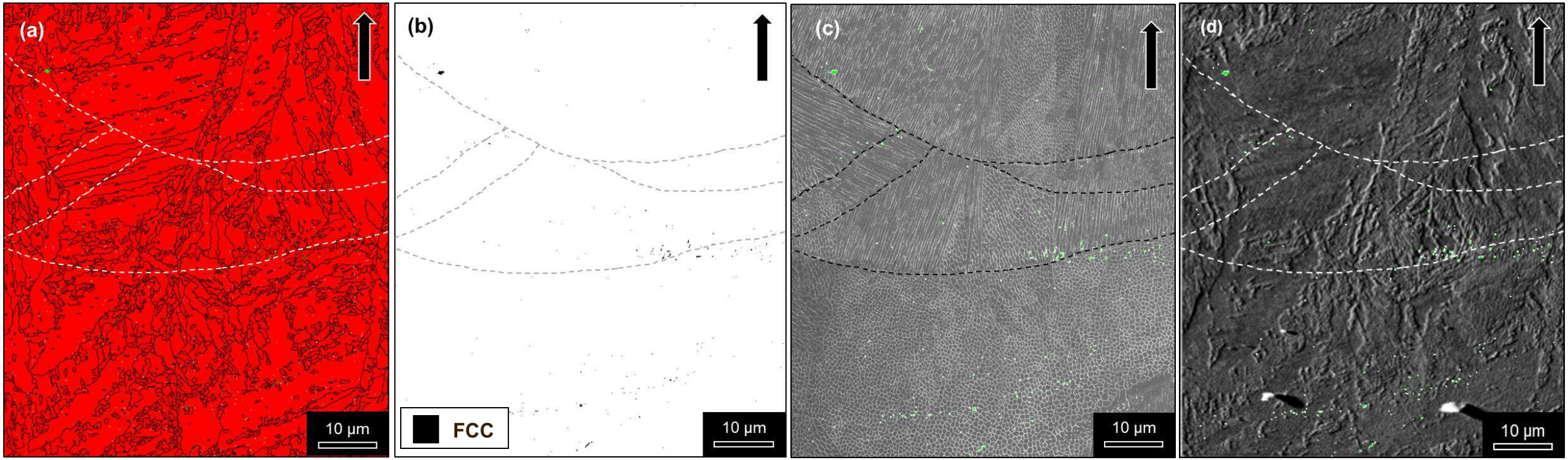

BCC

FCC

Step size = 0.2 µm

Correlative of (a) EBSD phase distribution map with retained austenite (green), BCT (red) and high angle grain boundary (black); (b) FCC phase (black) distribution; (c) SE micrograph with the FCC phase (green) overlaid and (d) BSE micrograph with FCC phase (green) overlaid. For all micrographs, the arrows on the top right show the BD, and the dotted lines represent the MP boundaries. L section.

Solute Distribution in As-Built Structure

EOS condition

40 microns

CW laser mode

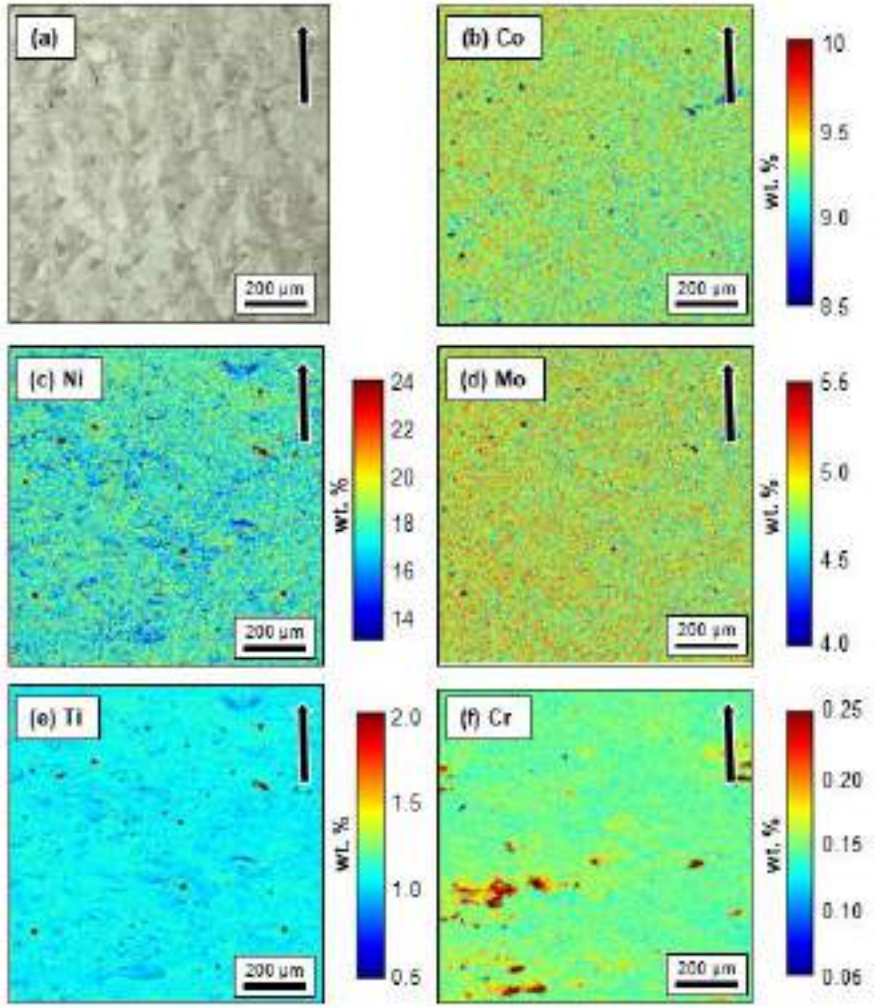

Area: 1000 µm x 1000 µm; Step size: 1 µm

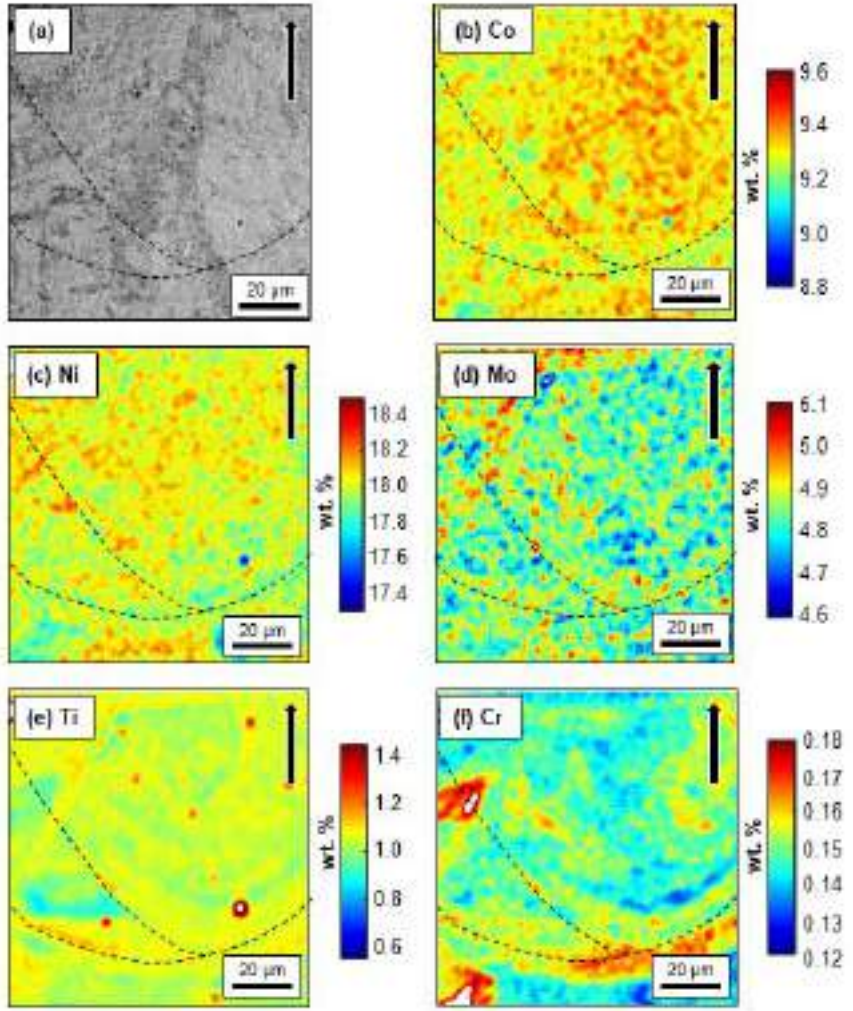

Area: 100 µm x100 µm; Step size: 0.2 µm

L-section

Tetragonality of Martensite in As-Built Structure

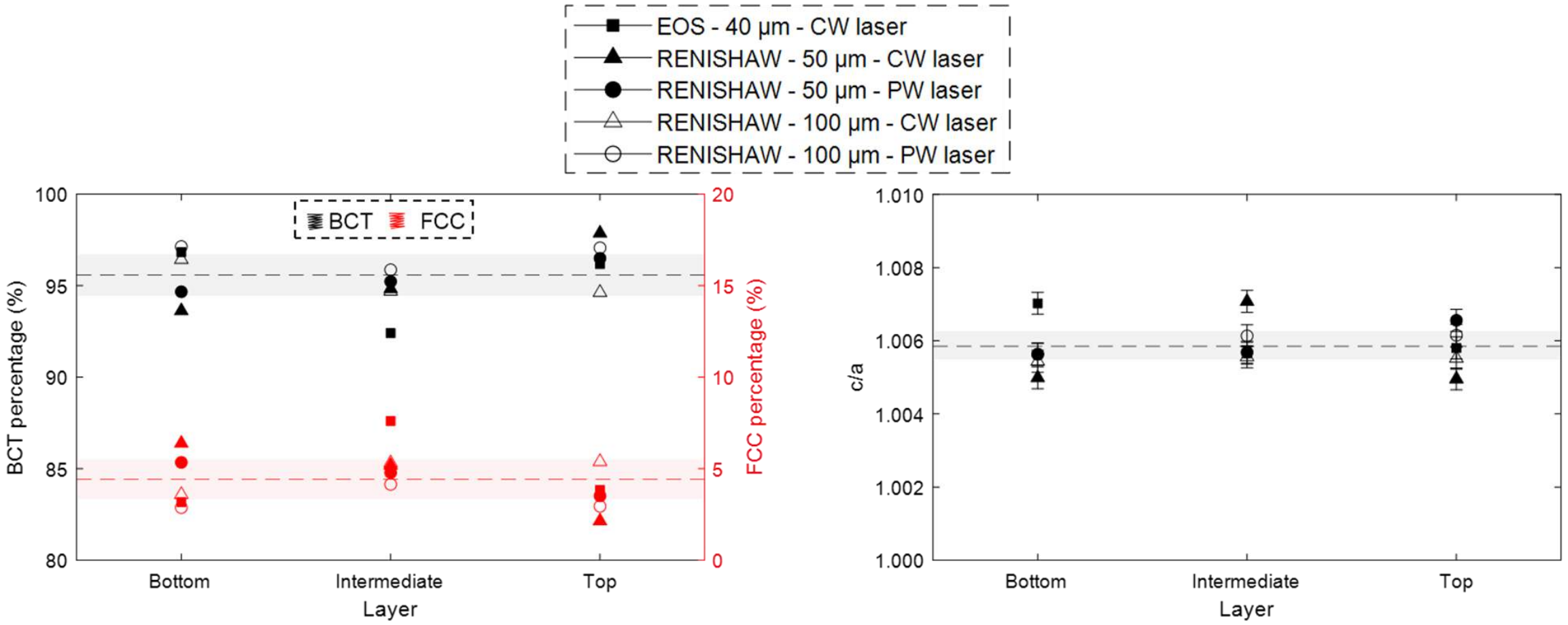

Texture in As-Built Structure

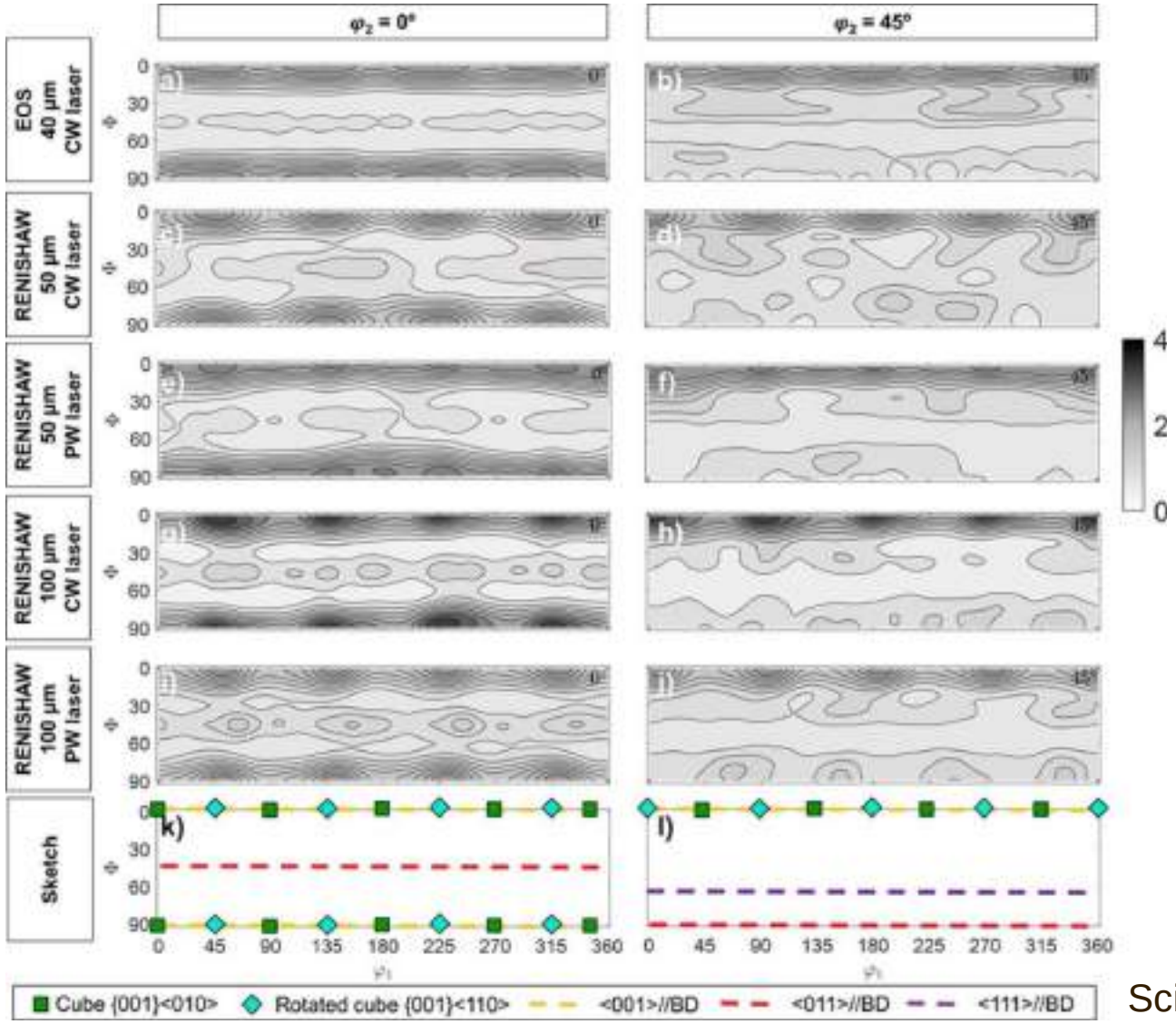

Multiples of Random Distribution (MRD)

Scientific Reports, 2022; 12: 16168

Texture in As-Built Structure

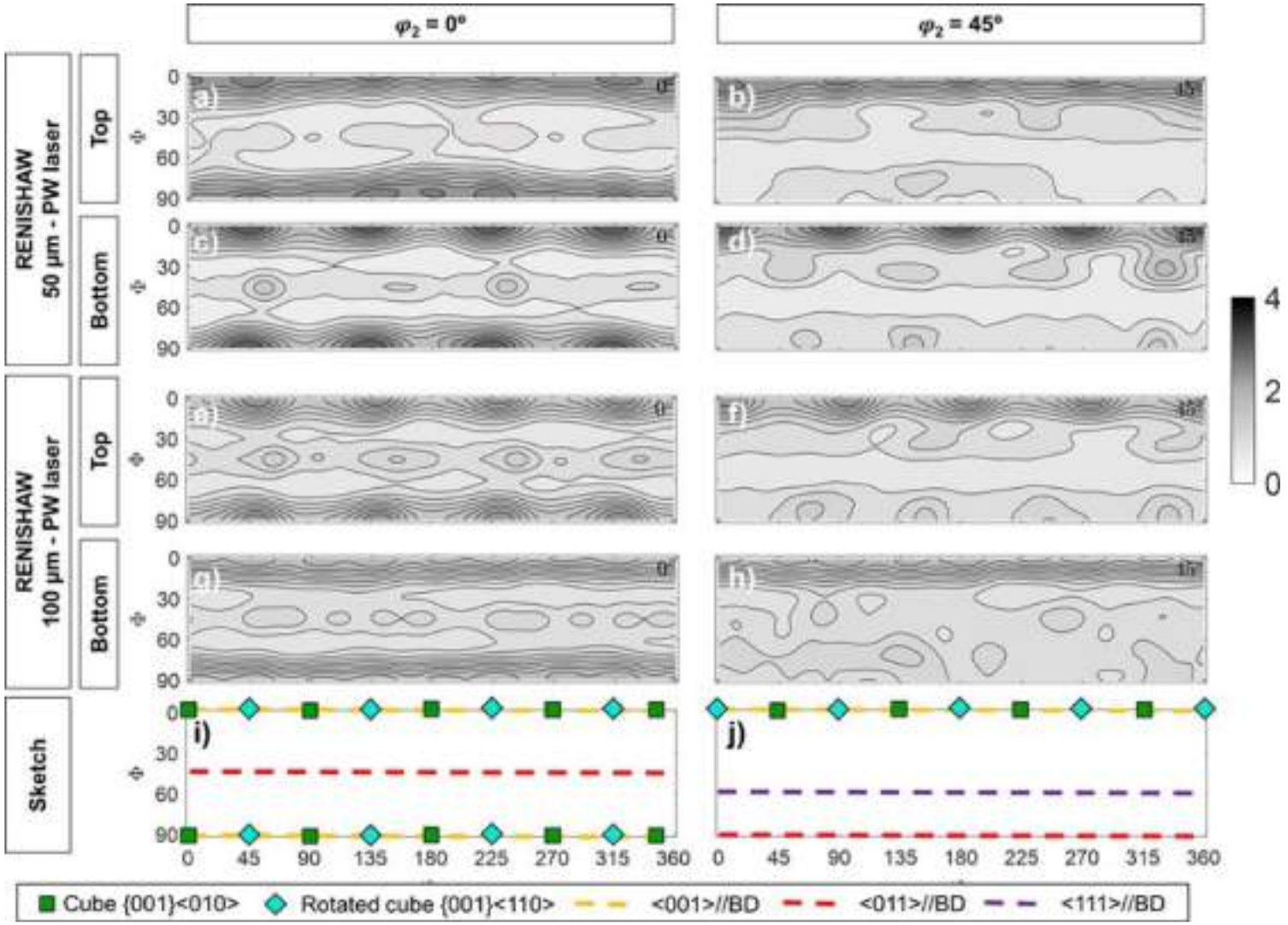

Multiples of Random Distribution (MRD)

Microtexture in As-Built Structure

EOS condition

40 microns

CW laser mode

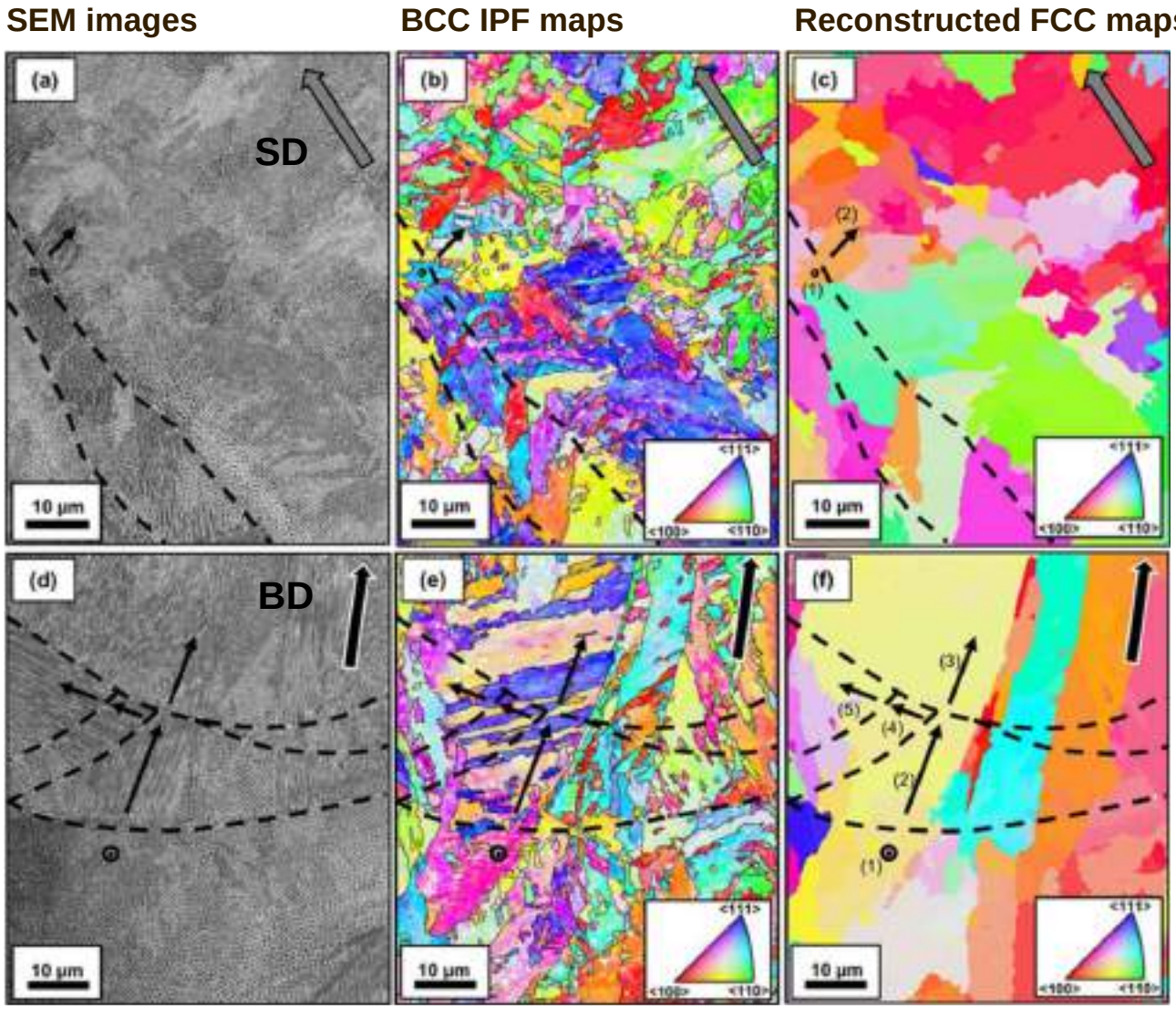

Content:

- ✓ Revealing the complexity of non-equilibrium, and non-uniform microstructures formed during LPBF process of maraging steels.
- ✓ Precipitation of intermetallic phases and austenite growth/reversion during ageing of LPBF maraging steels.
- ✓ Promoting thermal stabilization of austenite in microstructure by preheating and/or post-heat-treatment in a specially designed tool steels for LPBF manufacturing.

Microstructure Evolution during Aging

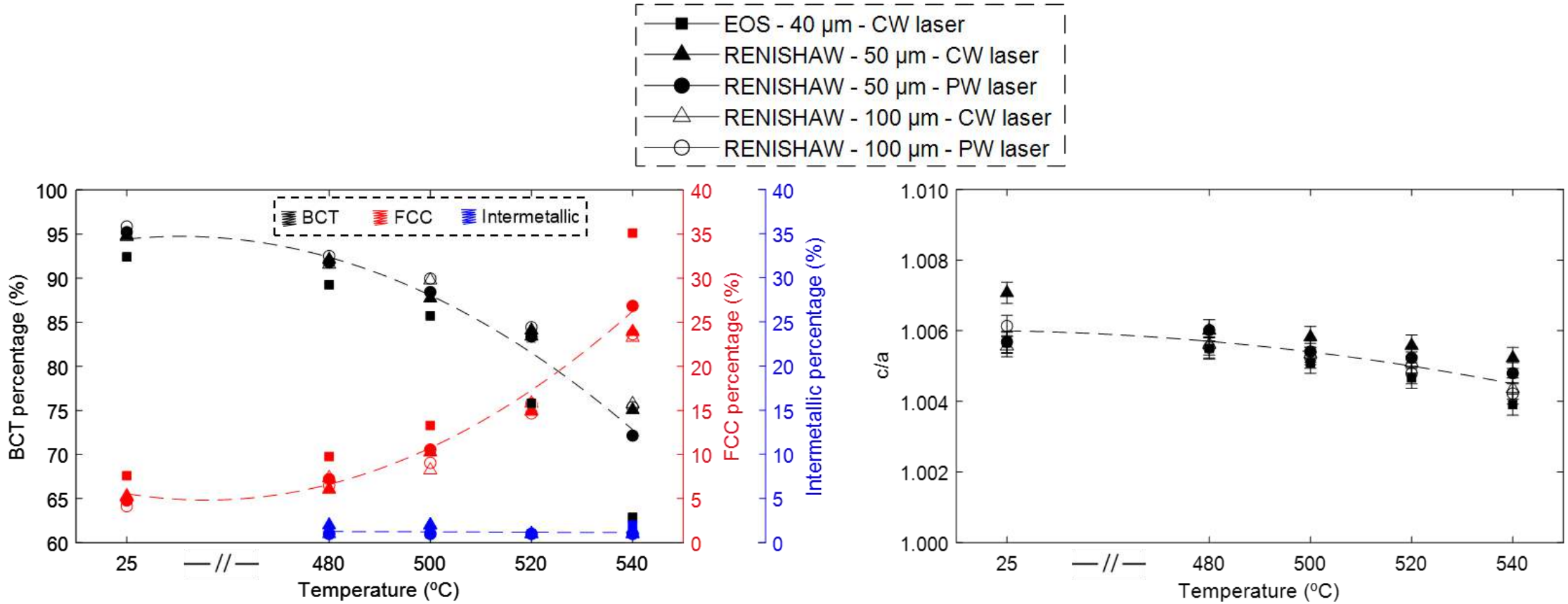

Microstructure Evolution during Aging

	As-built	Tag = 480 ºC	Tag = 540 ºC
LOM	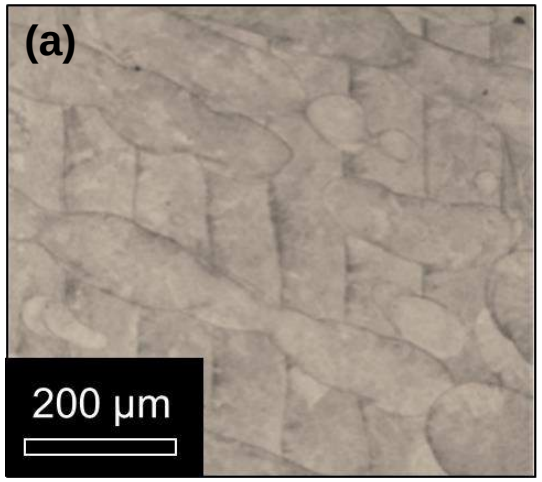	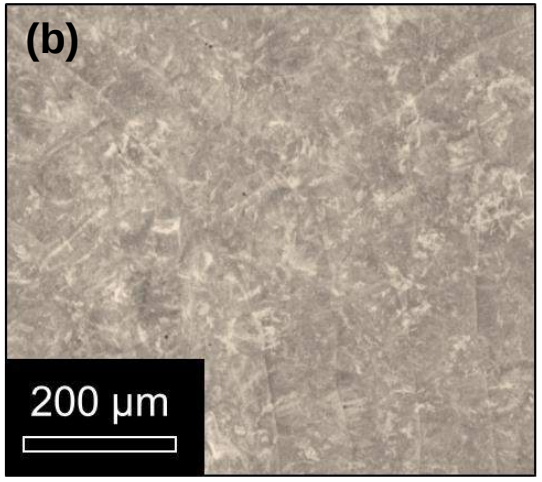	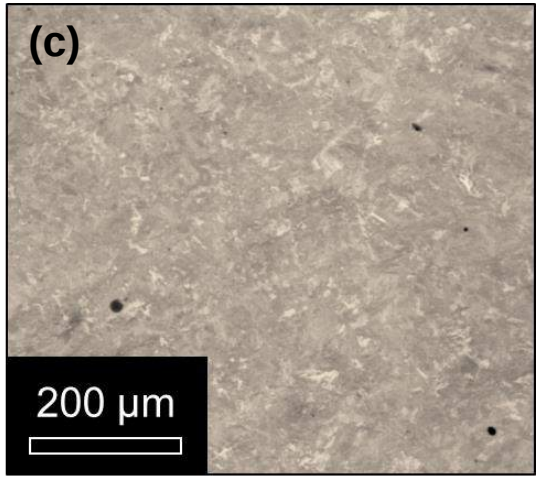
SEM	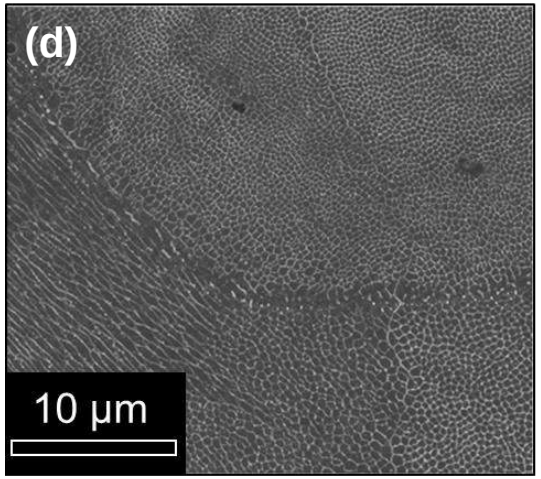	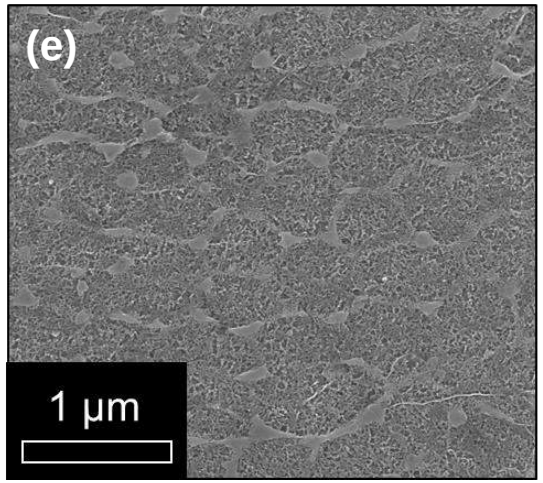	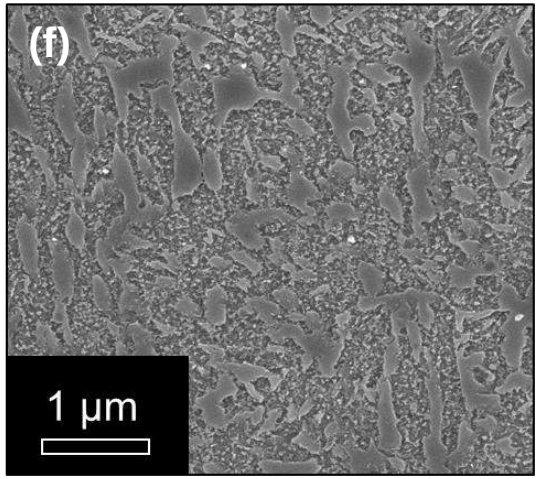

EOS condition

40 microns

CW laser mode

T-section

Solute Segregation during Aging

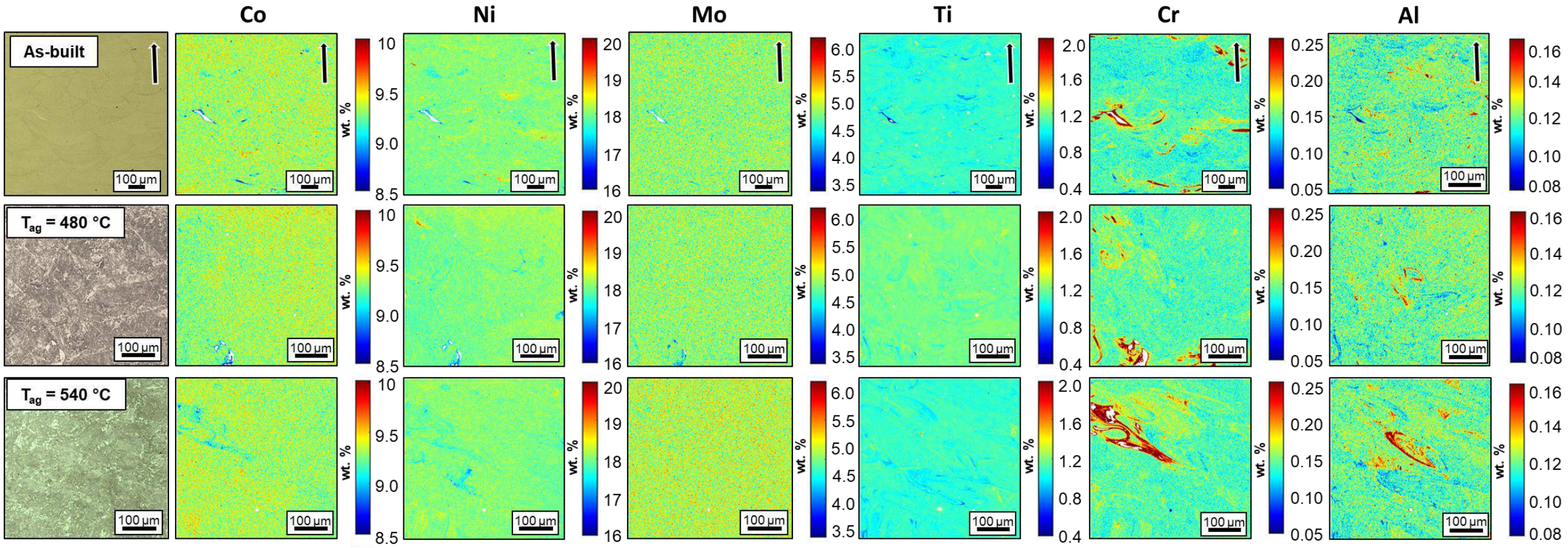

As-built = L-section

T_{ag} 480 and 540 ºC = T-section

Area: 500 µm x 500 µm; Step size: 0.5 µm

Precipitation Processes during Aging

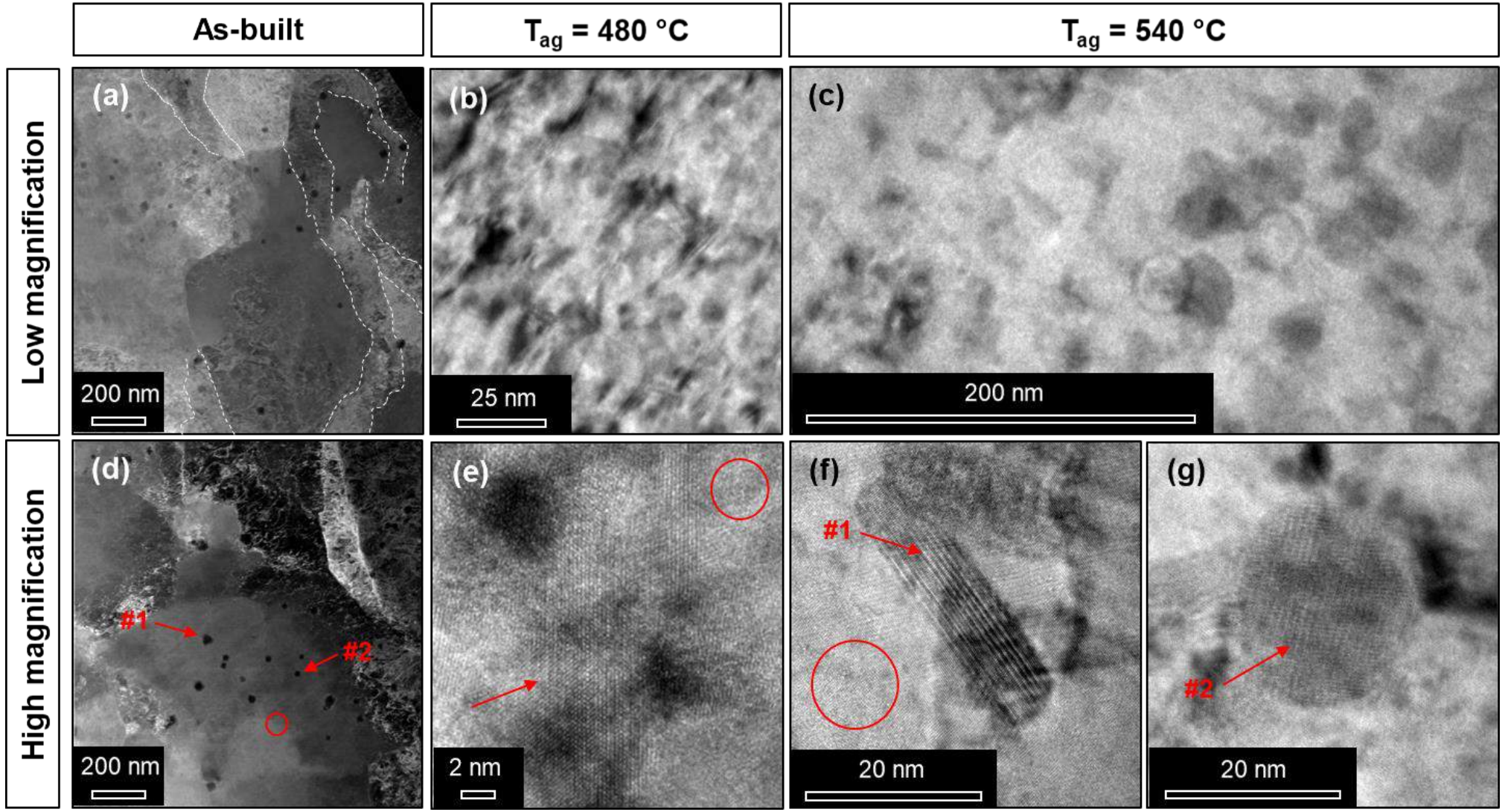

EOS condition

40 microns

CW laser mode

Precipitation Processes during Aging. As Built

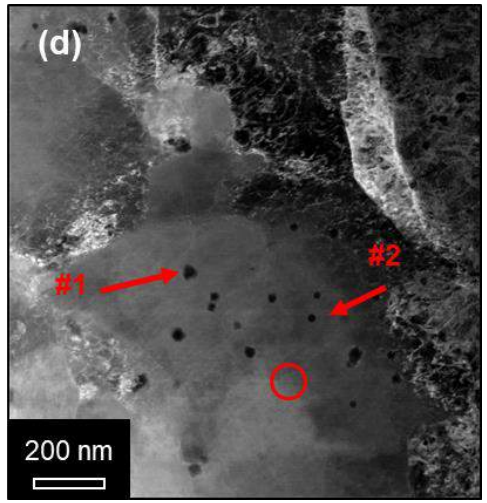

Randomly distributed Ti and Al enriched particles

		Al	Ti	Cr	Fe	Ni	Mo
As-built	Matrix	0.18	0.88	0.25	76.79	18.16	3.74
	Nanoparticle #1	3.48	4.29	0.17	71.69	16.75	3.13
	Nanoparticle #2	2.57	8.46	0.20	69.15	16.22	3.40

EOS condition

40 microns

CW laser mode

Precipitation Processes during Aging. As Built

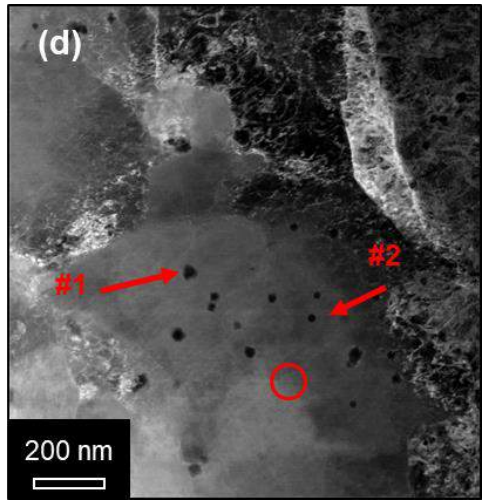

Randomly distributed Ti and Al enriched particles

Ti and Al enriched particles

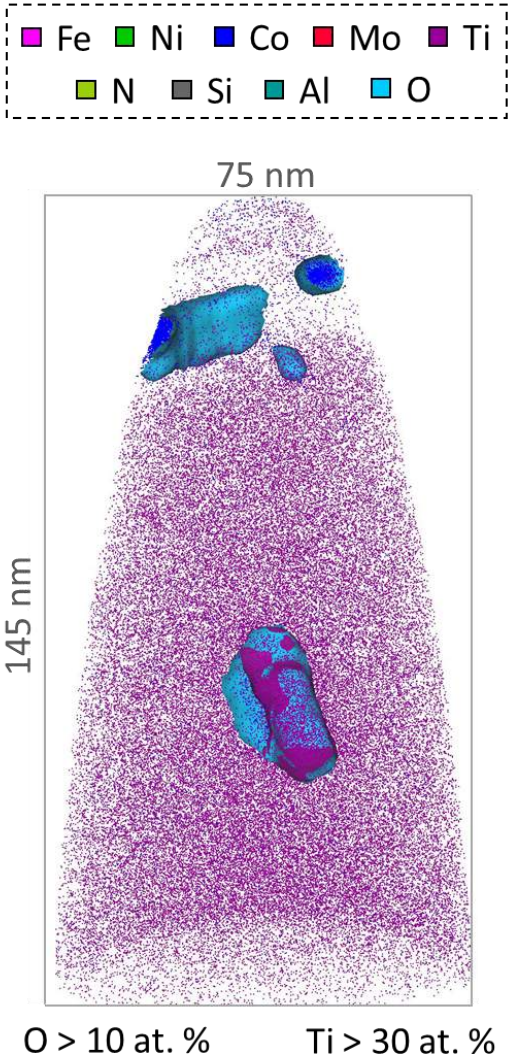

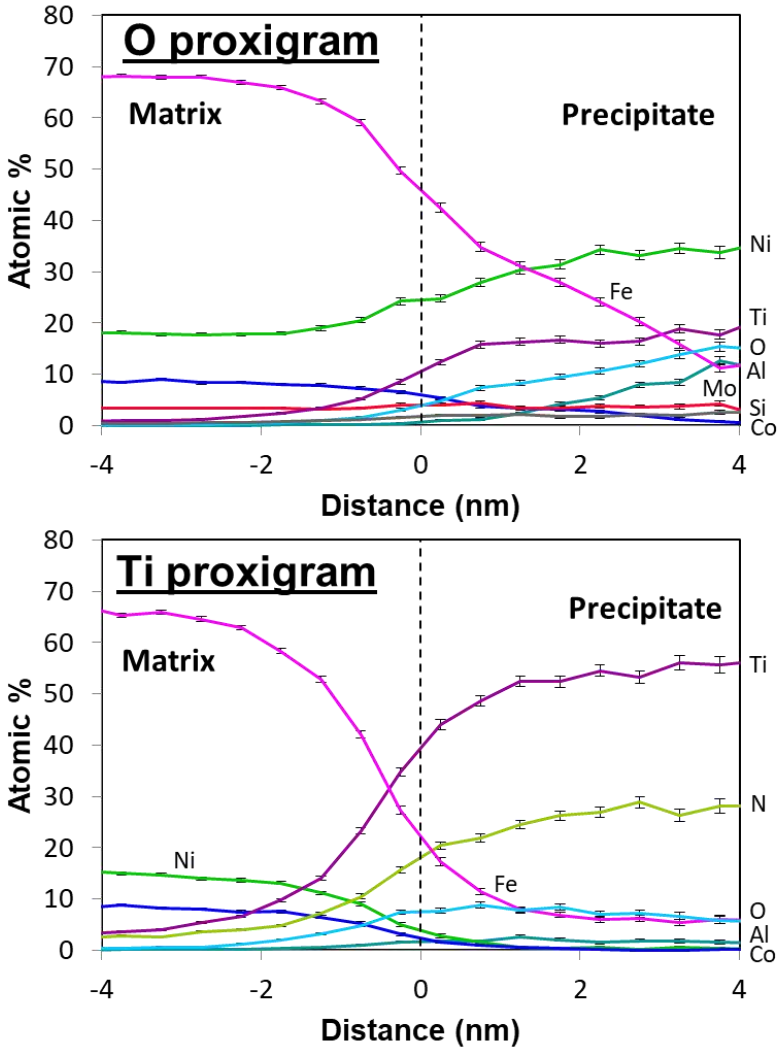

EOS condition

40 microns

CW laser mode

Precipitation Processes during Aging. As Built

Spherical Ti oxides (TiO and TiO2)

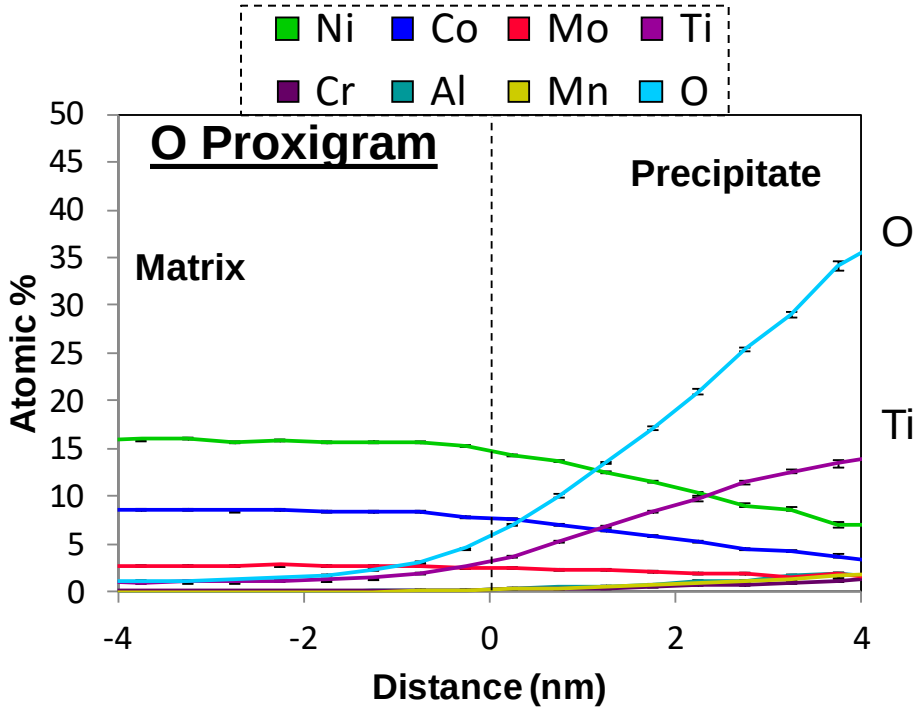

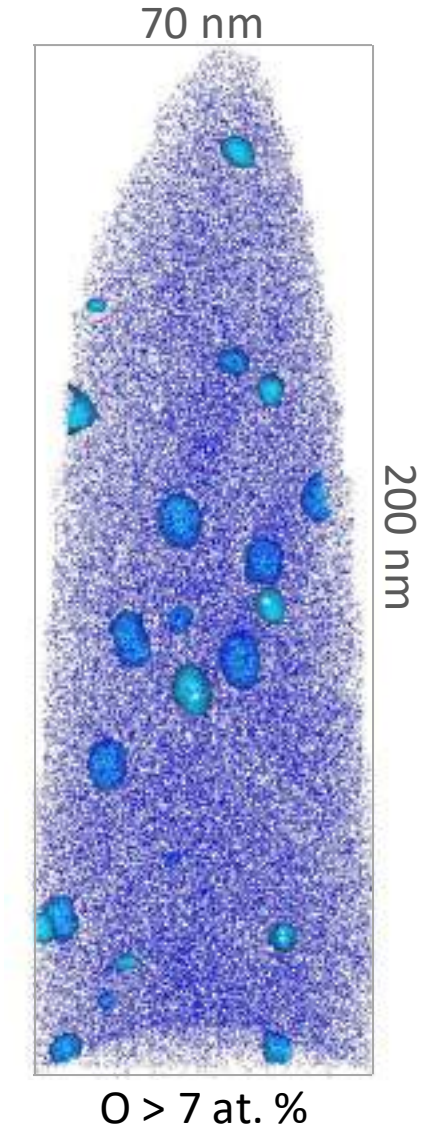

EOS condition

40 microns

CW laser mode

Precipitation Processes during Aging. 480 and 540 ºC

#1: Ni, Ti enriched rod-like phases
#2: Mo enriched spherical phases

Ni, Ti, Mo precipitates

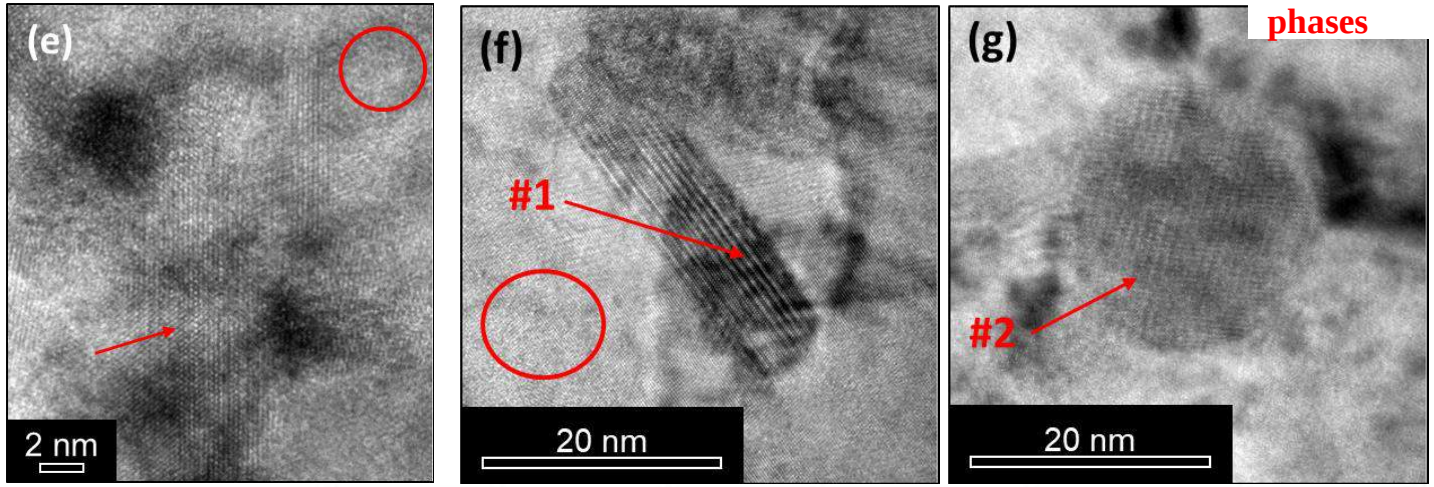

		Al	Ti	Cr	Fe	Ni	Mo
T_{ag} = 480 ºC	Matrix	-	0	-	85.00	14.20	0.80
	Nanoparticle #1	-	1.60	-	68.50	24.70	5.20
T_{ag} = 540 ºC	Matrix	-	0.50	-	84.50	8.90	6.10
	Nanoparticle #1	-	3.00	-	78.10	17.10	1.80 ↓
	Nanoparticle #2	-	0.20	-	71.60	11.30	16.90

EOS condition

40 microns

CW laser mode

Precipitation Processes during Aging. 480ºC

EOS condition

40 microns

CW laser mode

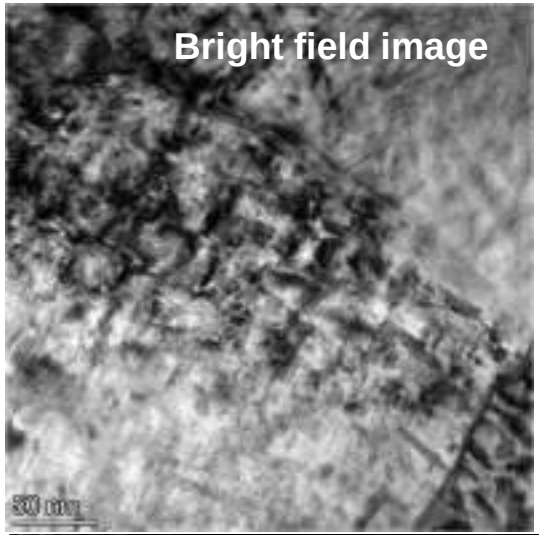

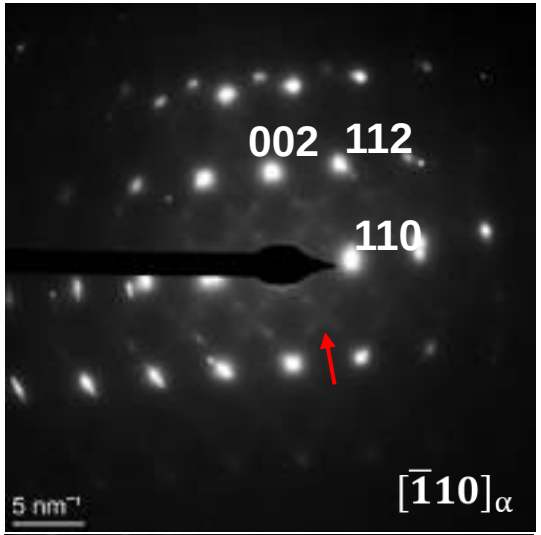

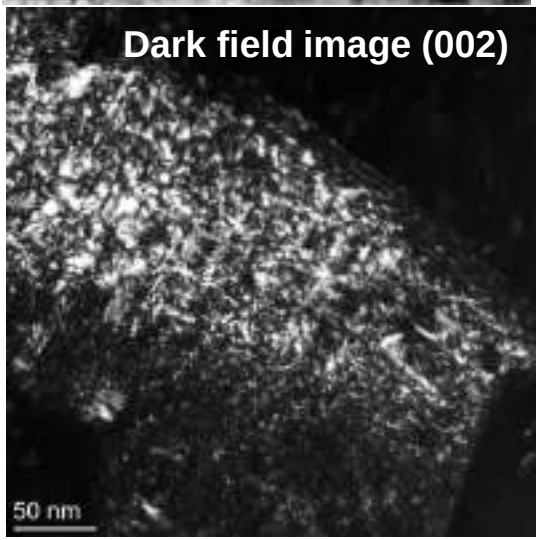

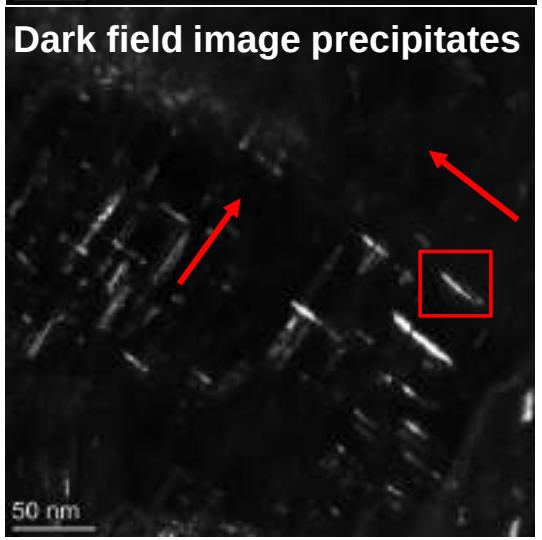

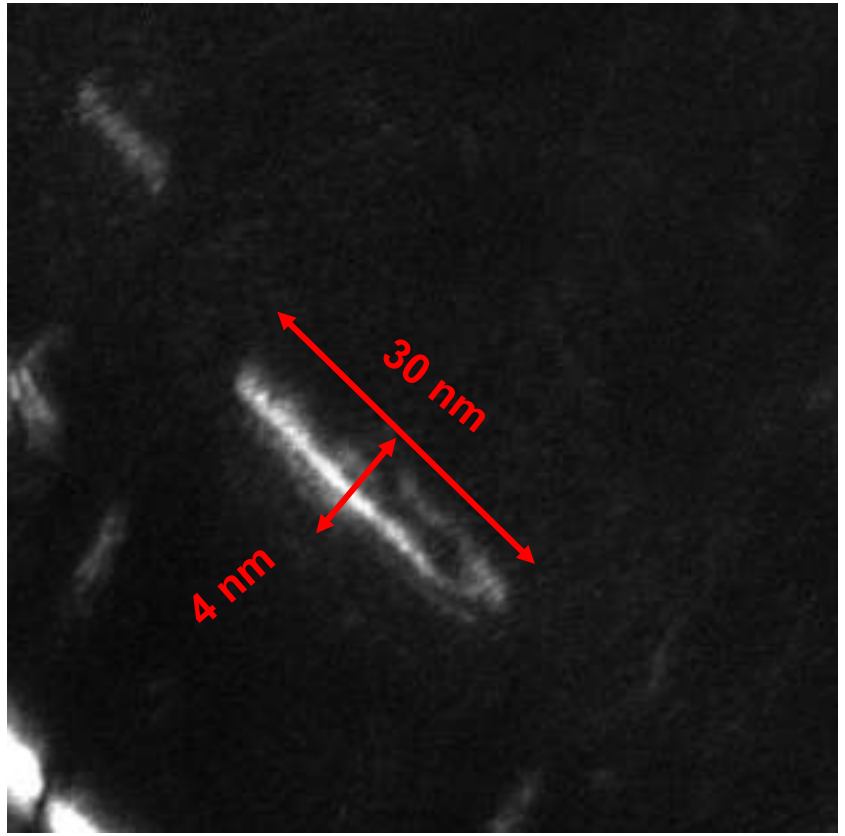

Ni, Ti enriched rod-like particles

Precipitation Processes during Aging. 480ºC

Ni, Ti enriched rod-like particles

STEM mode

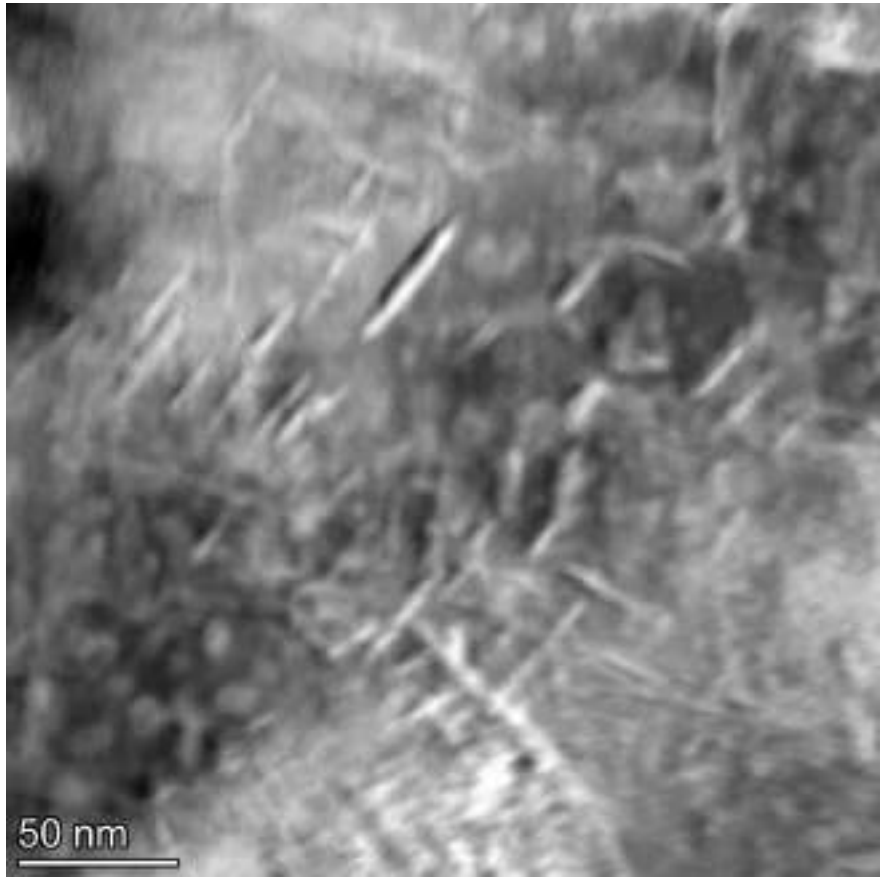

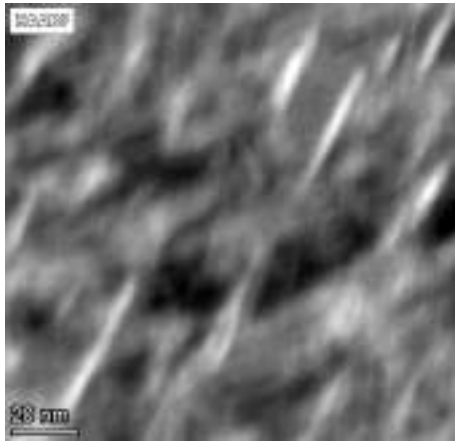

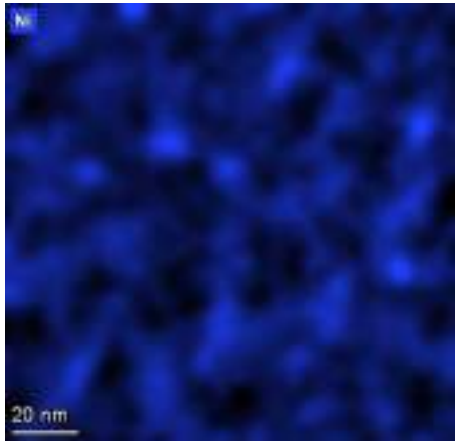

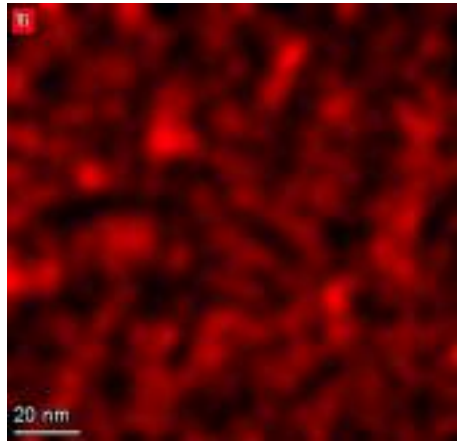

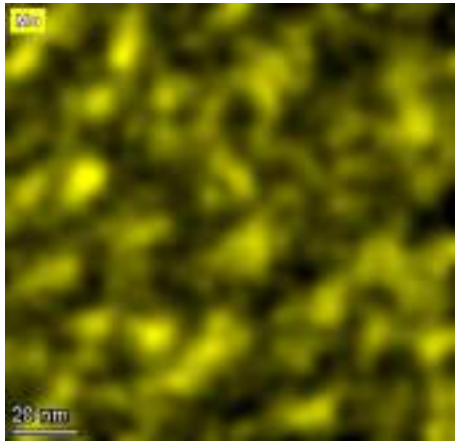

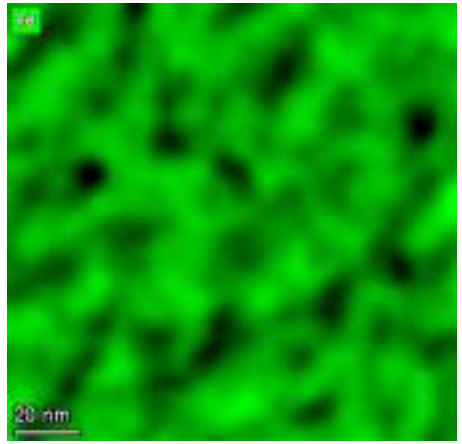

EOS condition

40 microns

CW laser mode

Precipitation Processes during Aging. 480ºC

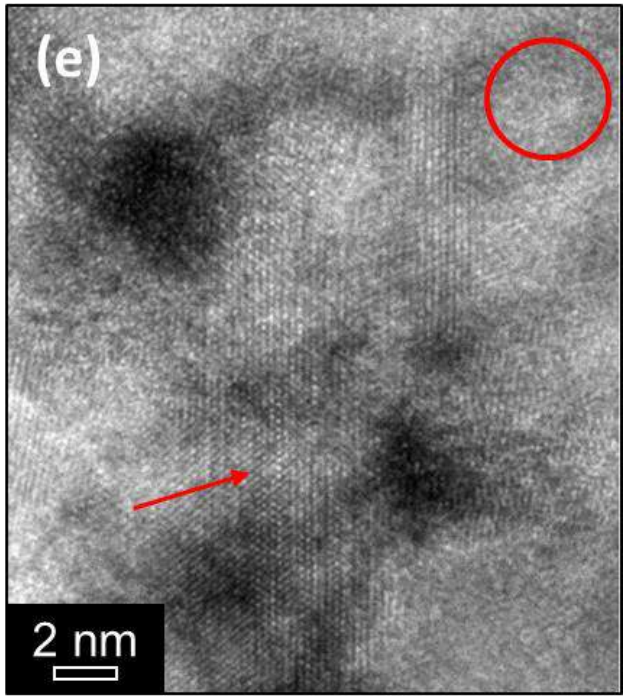

EOS condition

40 microns

CW laser mode

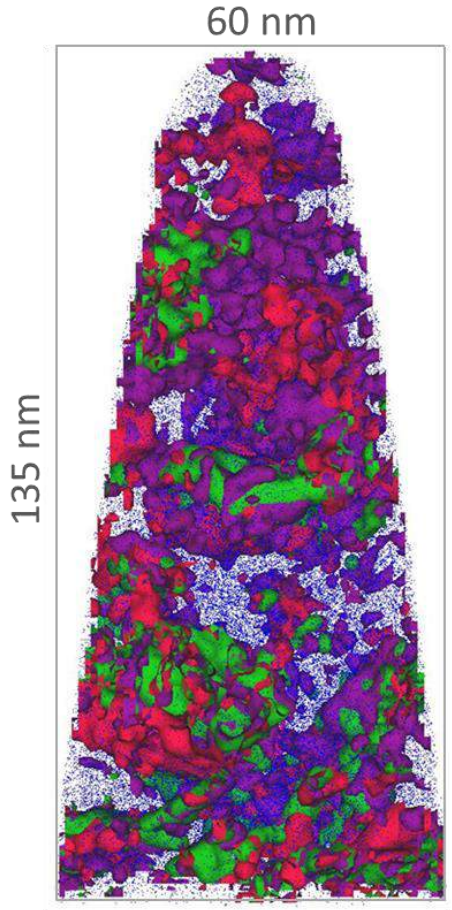

Ni > 20 at. % Mo > 4 at. %

Ti > 1 at. %

Clusters enriched in Ni, Ti and Mo

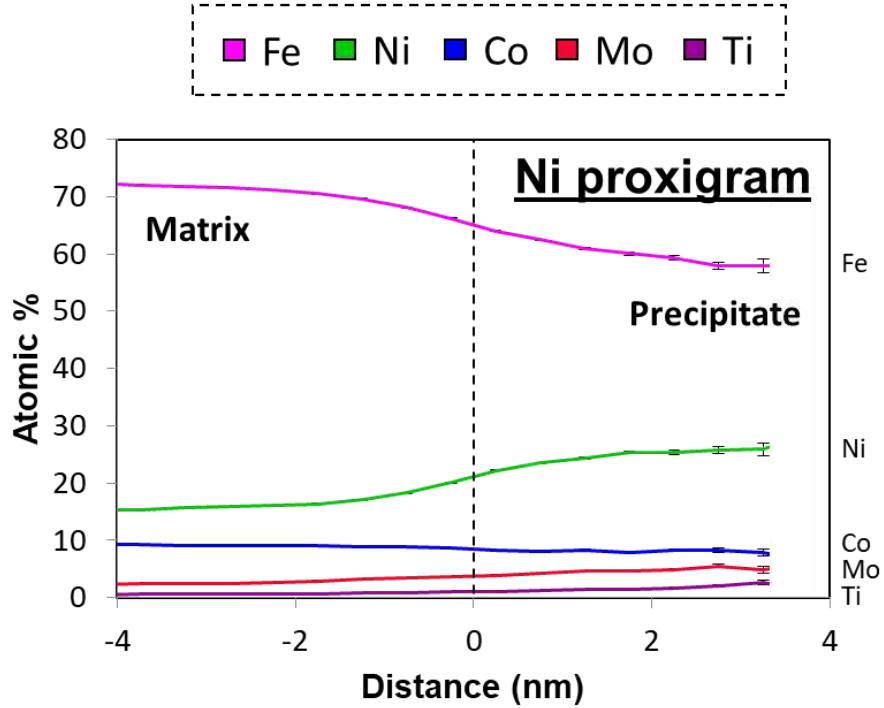

Precipitation Processes during Aging. 540ºC

EOS condition

40 microns

CW laser mode

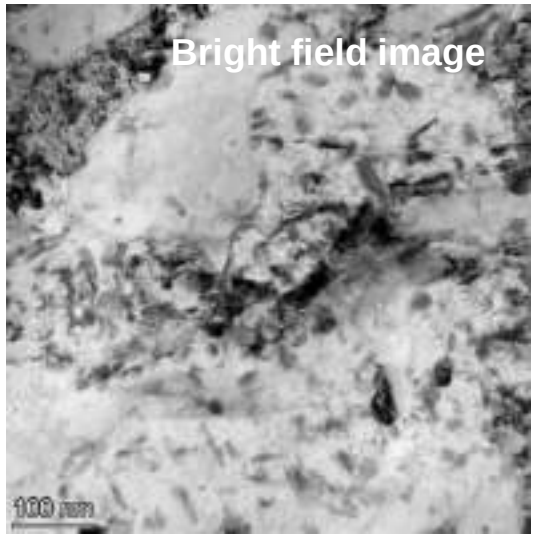

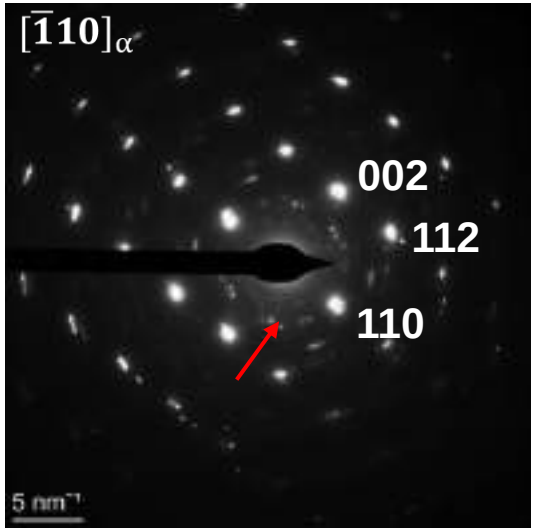

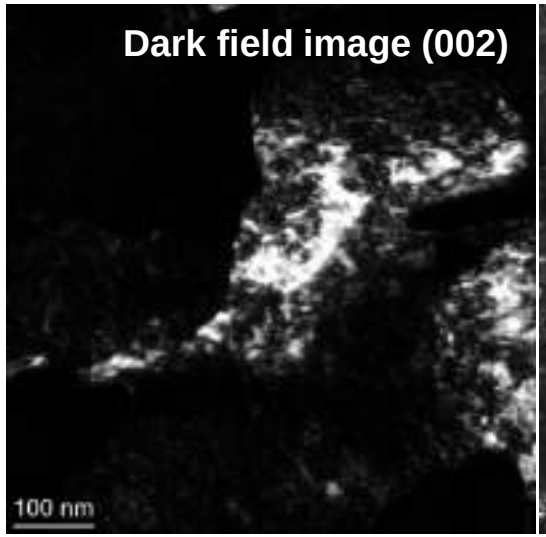

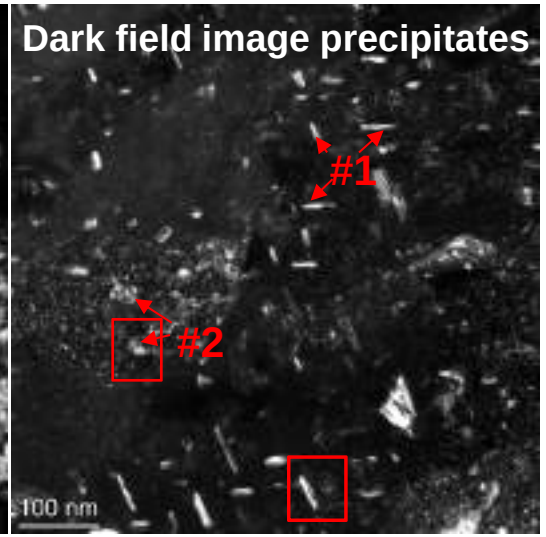

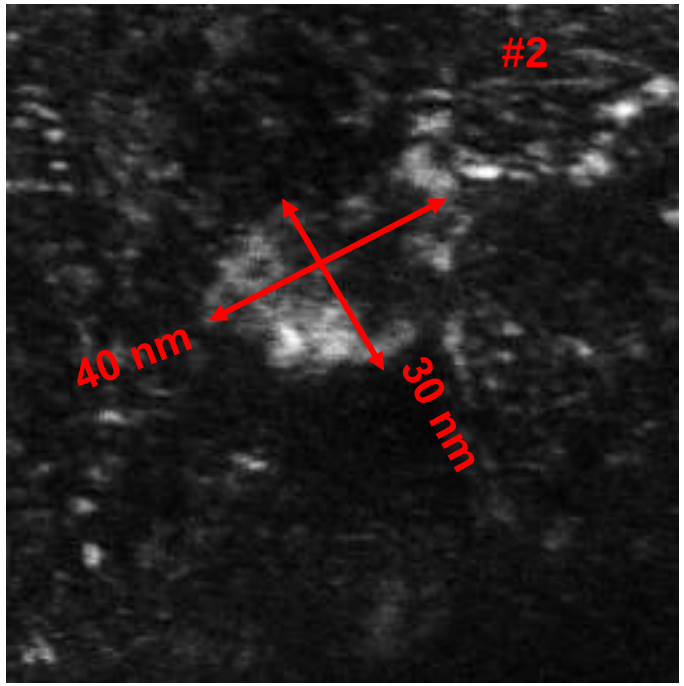

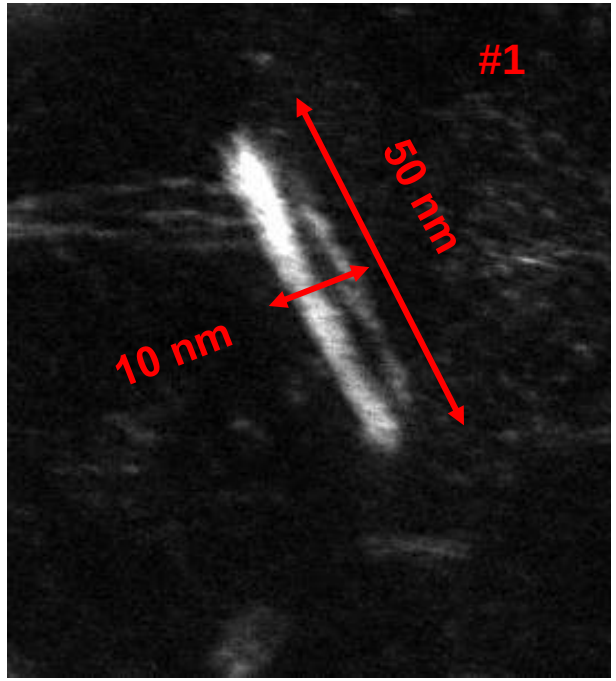

#1: Ni, Ti enriched rod-like phases

#2: Mo enriched spherical phases

Precipitation Processes during Aging. 540ºC

EOS condition

40 microns

CW laser mode

STEM Mode

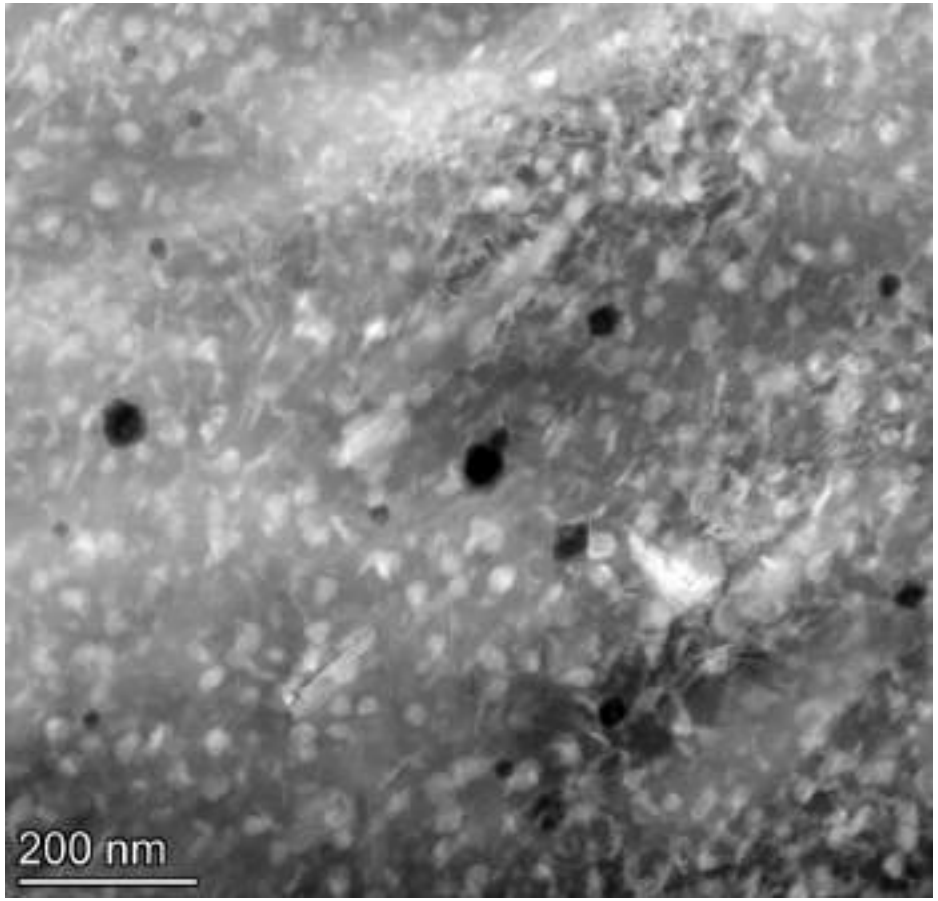

Mo enriched spherical phases

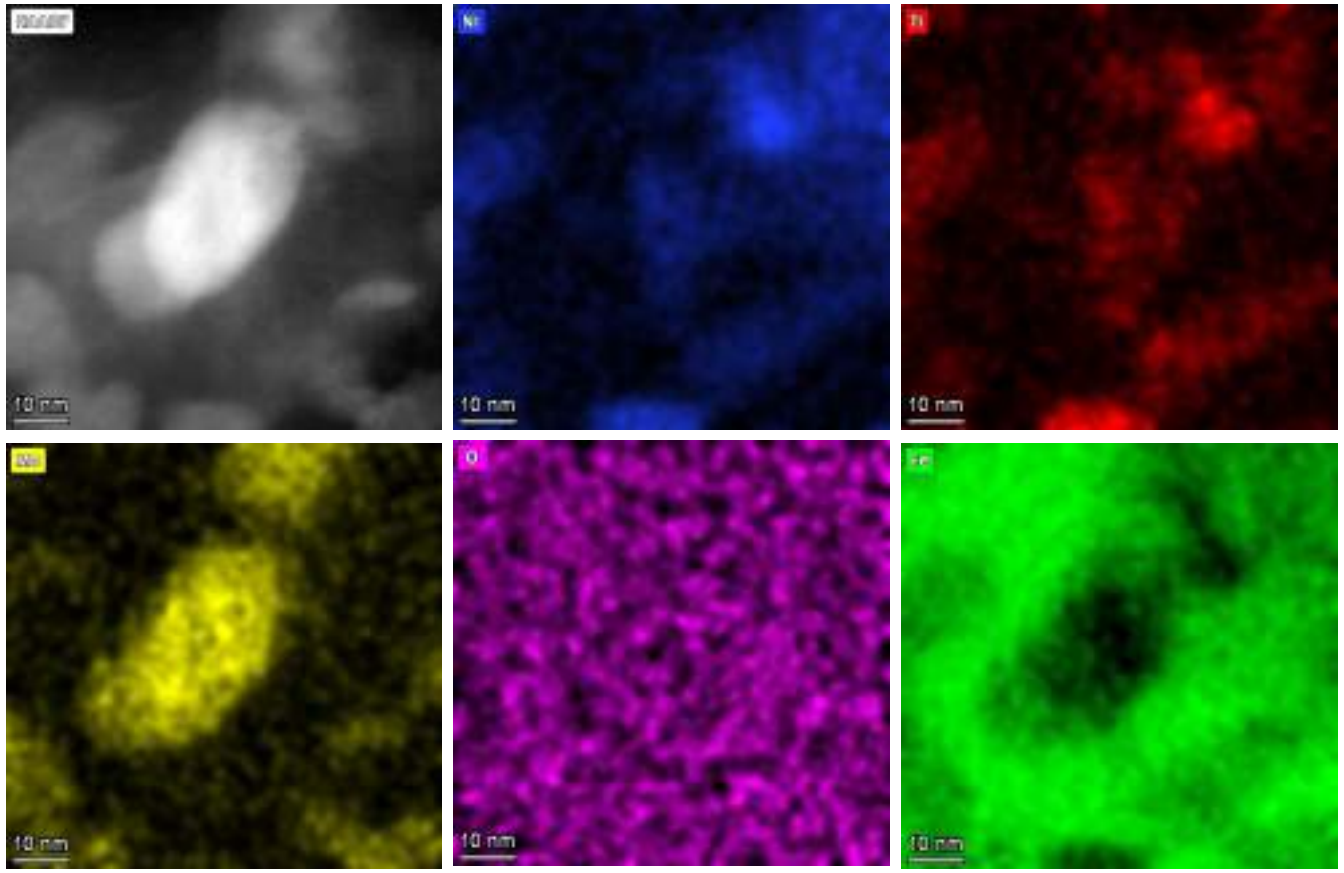

Precipitation Processes during Aging. 540ºC

Ni, Ti enriched rod-like and Mo enriched spherical phases

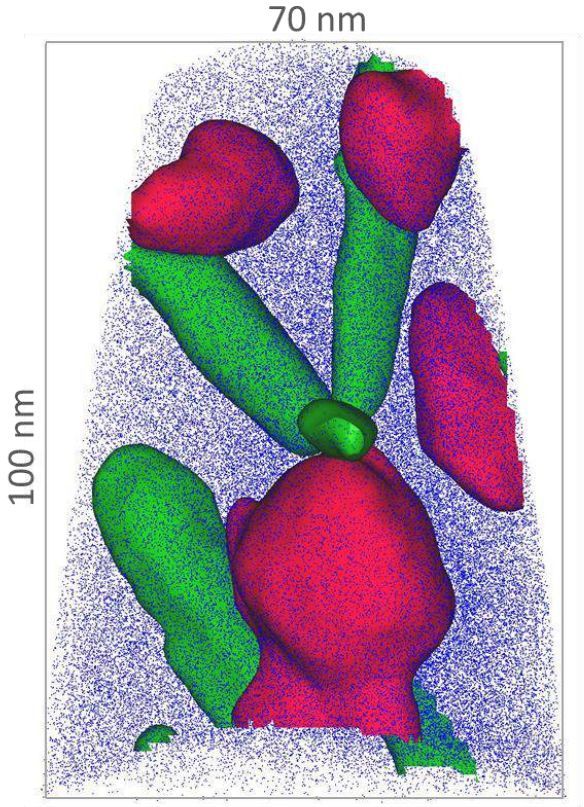

Ni > 40 at. % Mo > 15 at. %

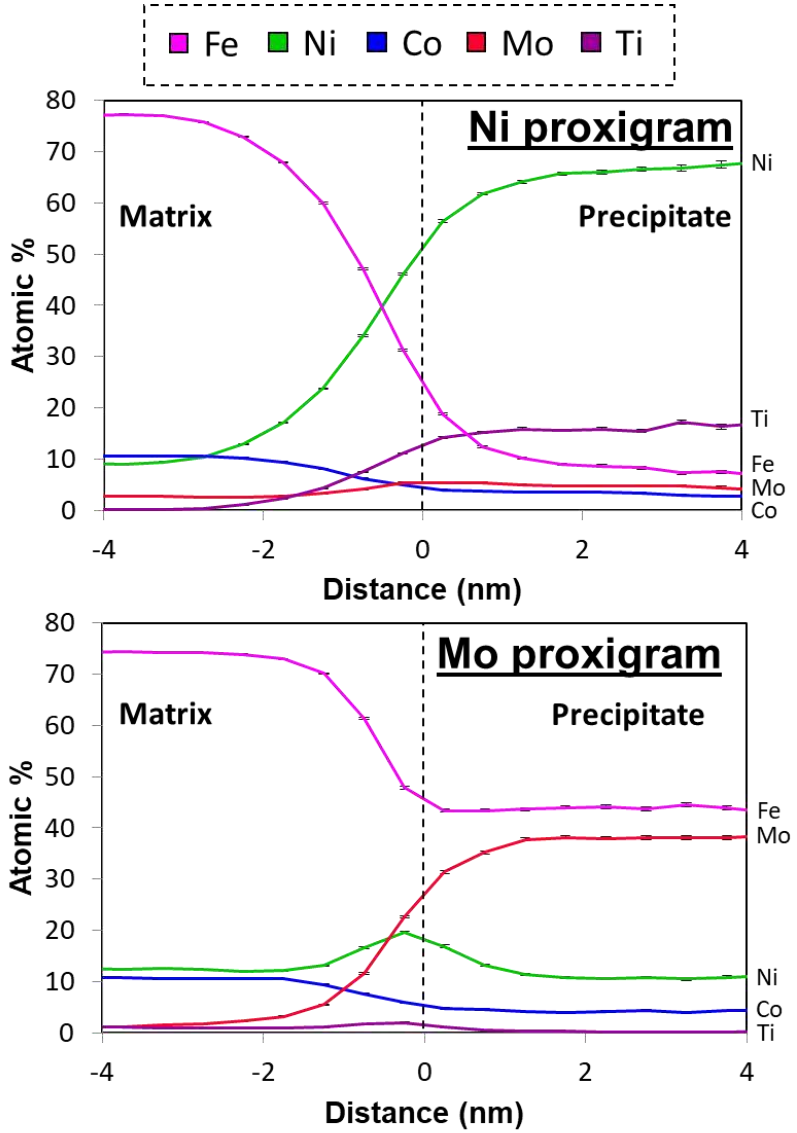

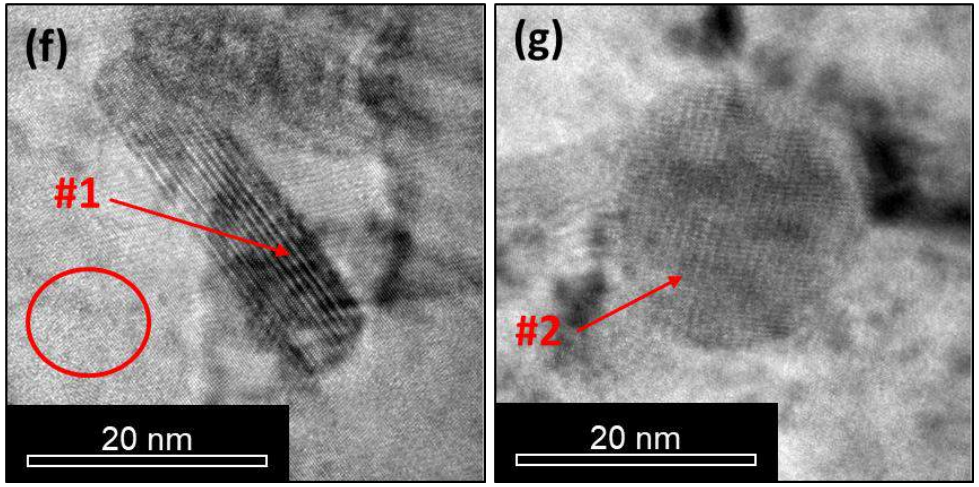

Ni, Ti enriched rod-like and Mo enriched spherical phases

EOS condition

40 microns

CW laser mode

Austenite Reversion during Aging. As built

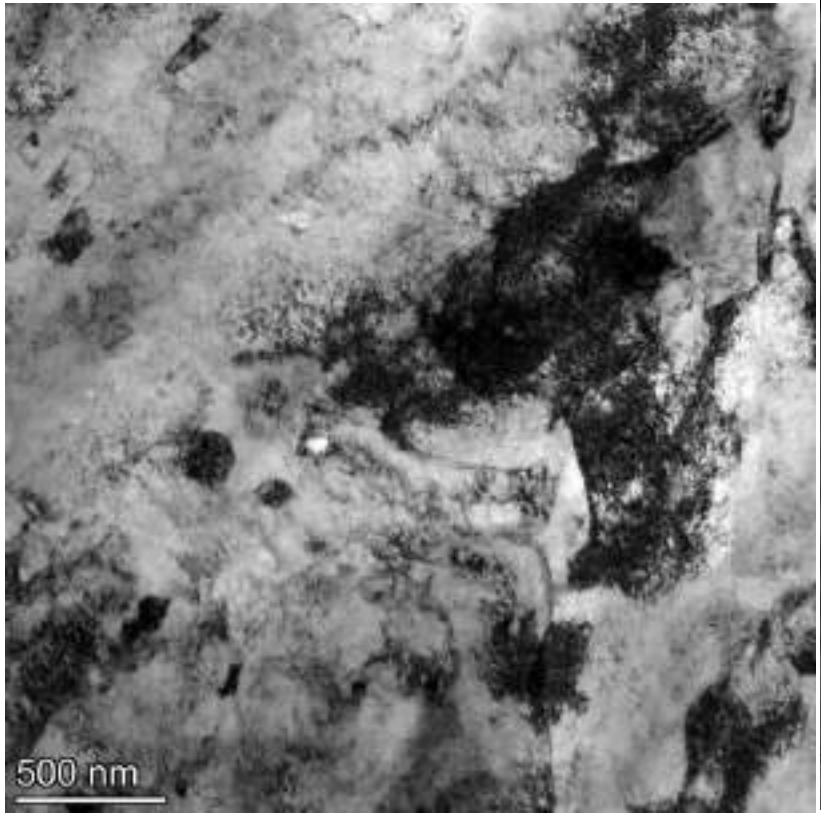

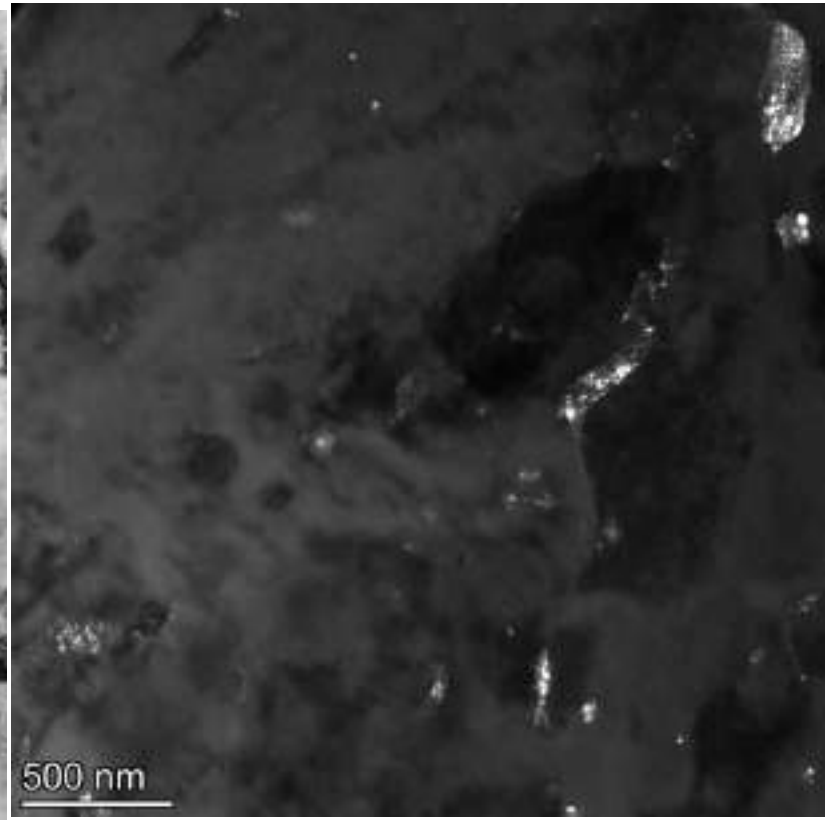

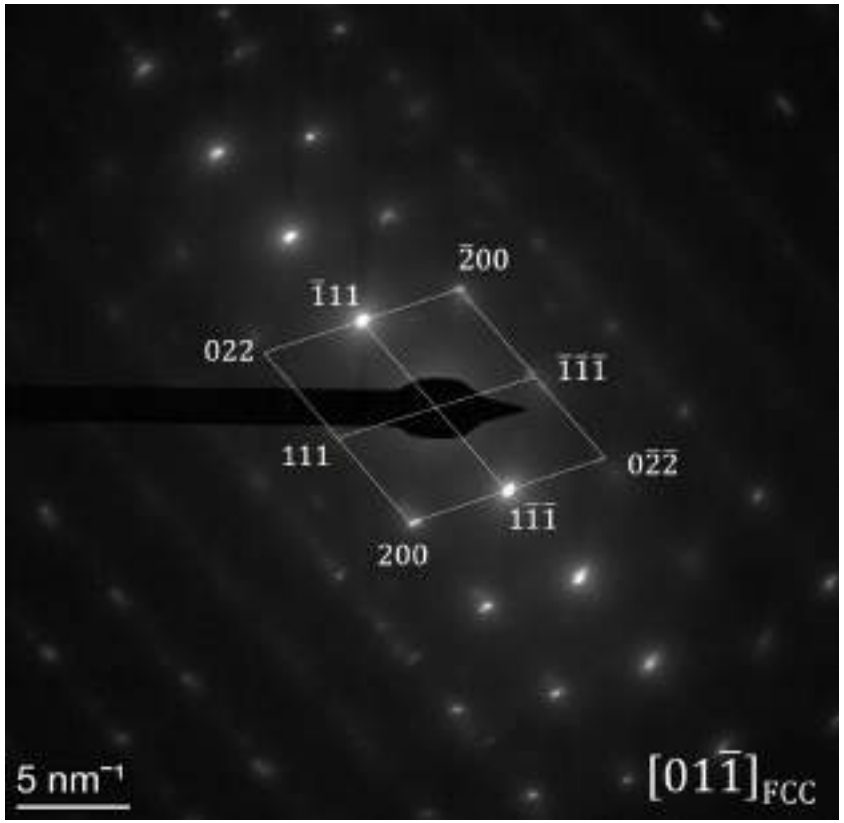

EOS - 40 microns - CW laser mode

Austenite Reversion during Aging. 480ºC

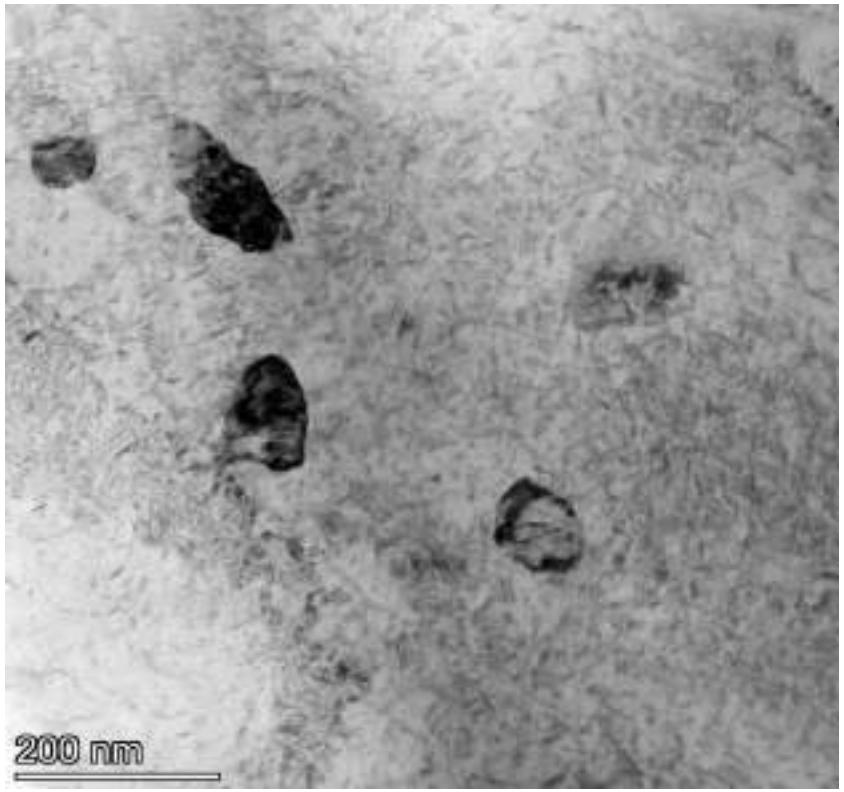

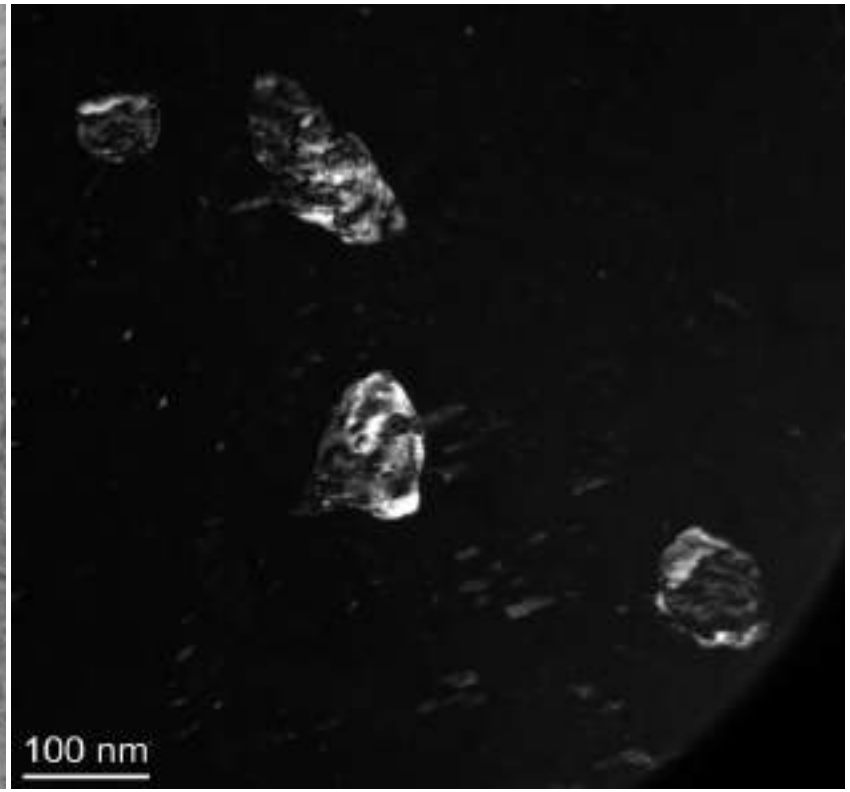

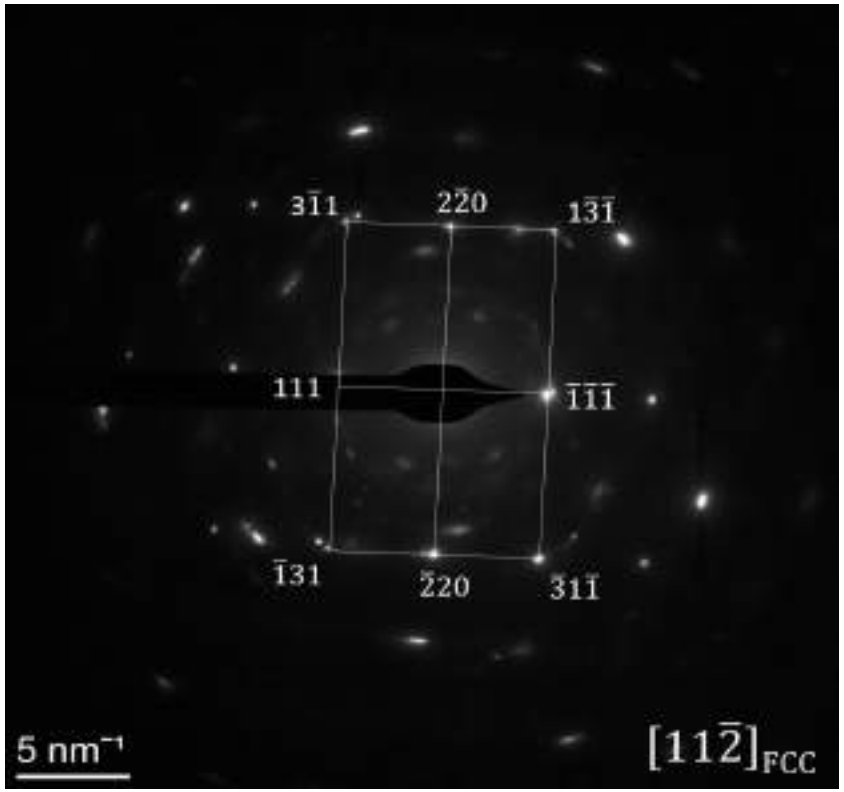

EOS - 40 microns - CW laser mode

Austenite Reversion during Aging. 540ºC

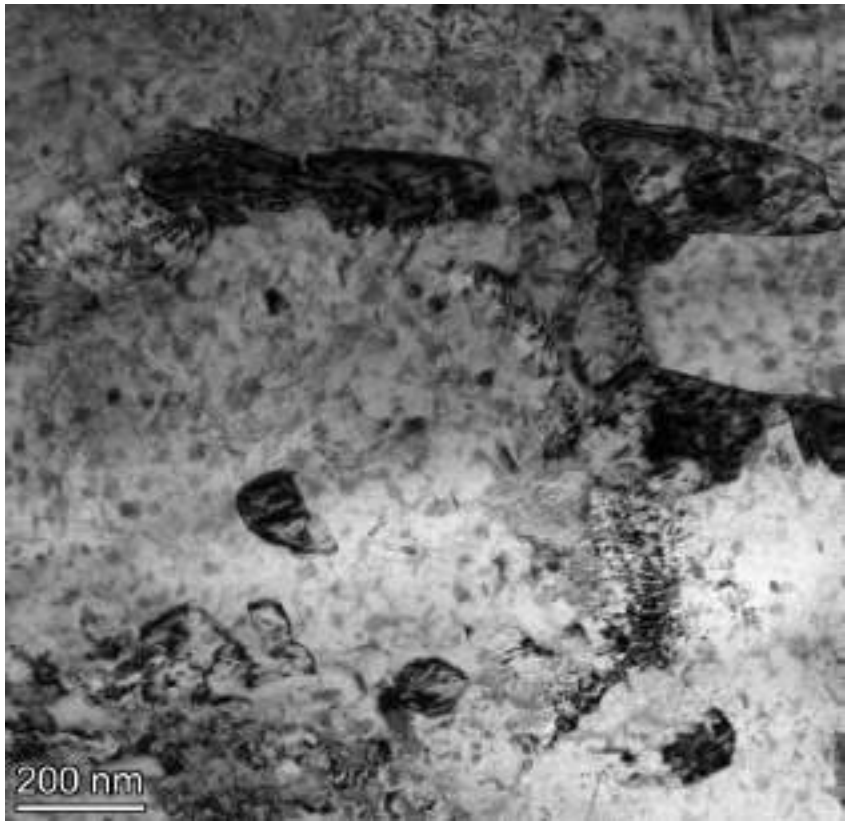

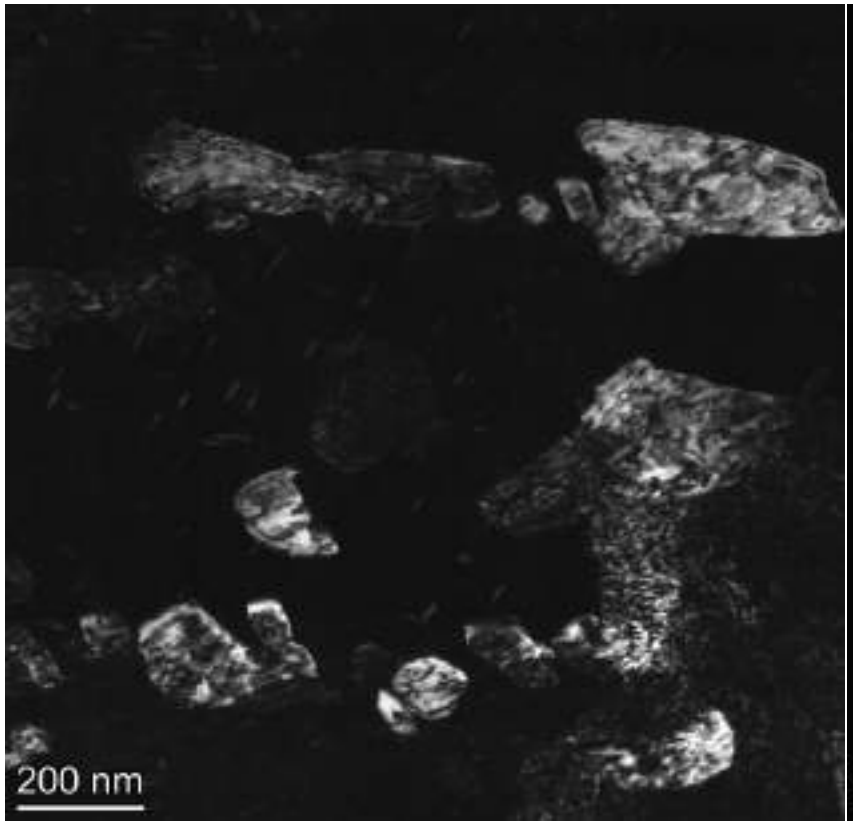

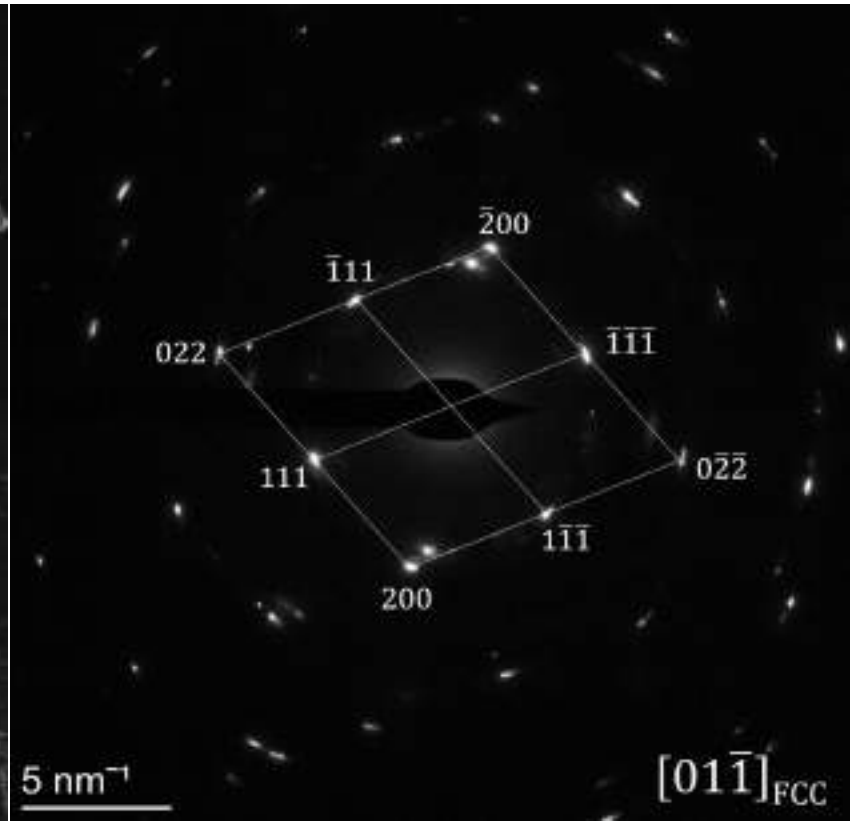

EOS - 40 microns - CW laser mode

Austenite Reversion during Aging. As built

EOS condition

40 microns

CW laser mode

STEM mode

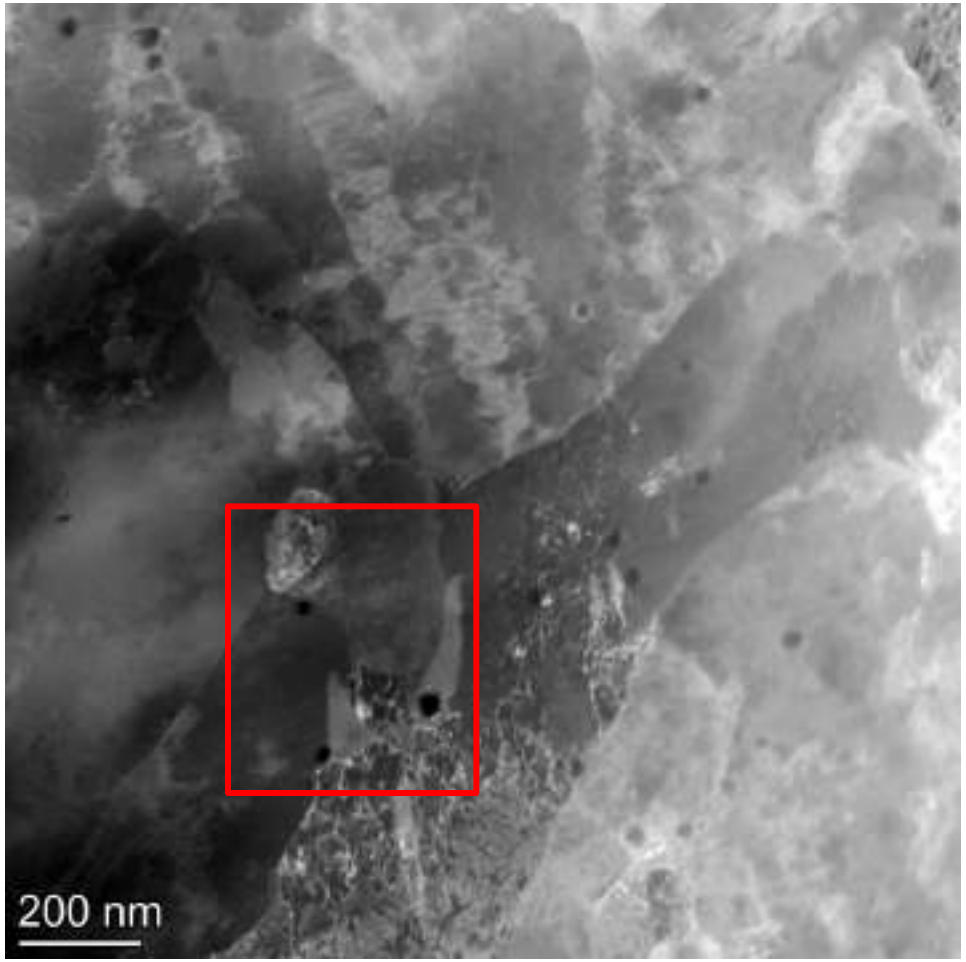

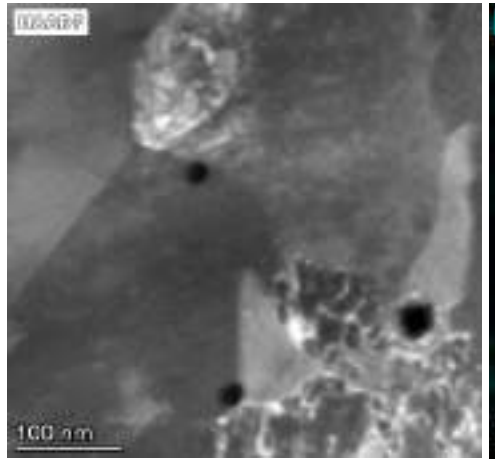

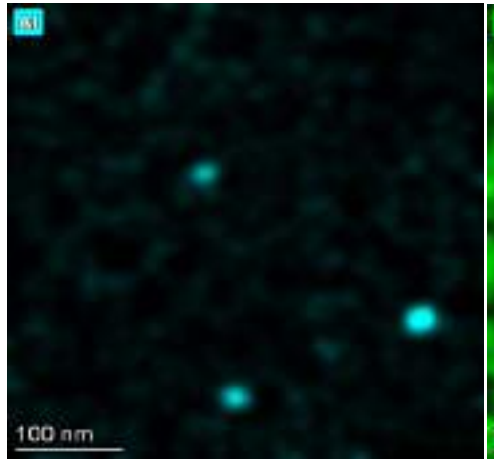

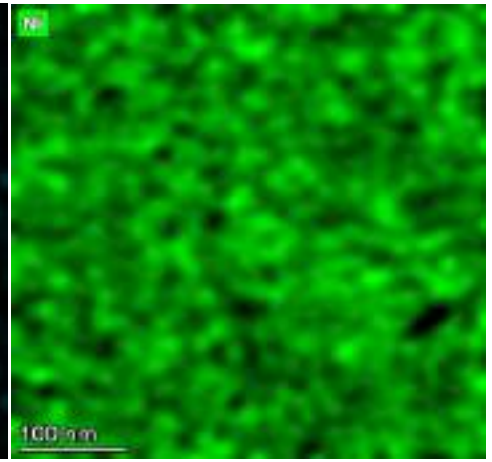

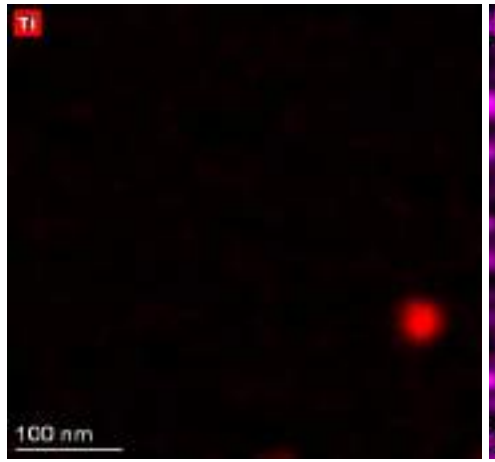

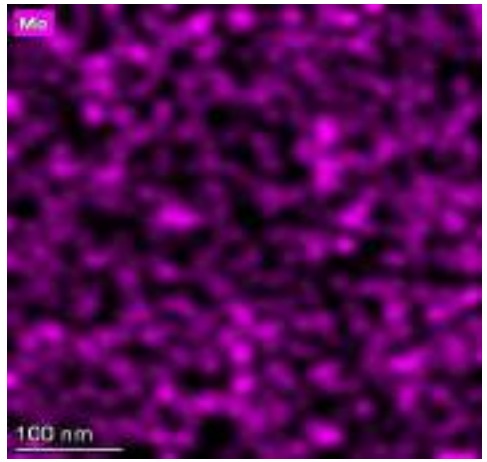

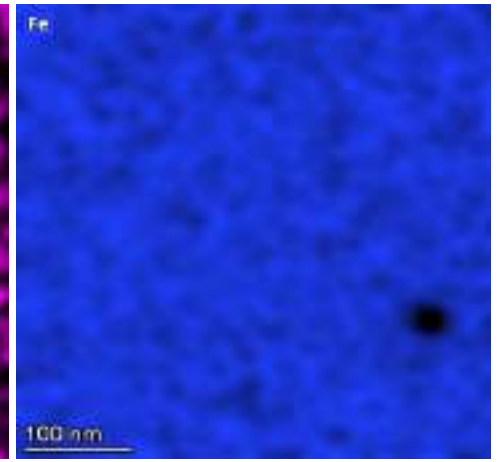

Austenite Reversion during Aging. 480ºC

EOS condition

40 microns

CW laser mode

STEM mode

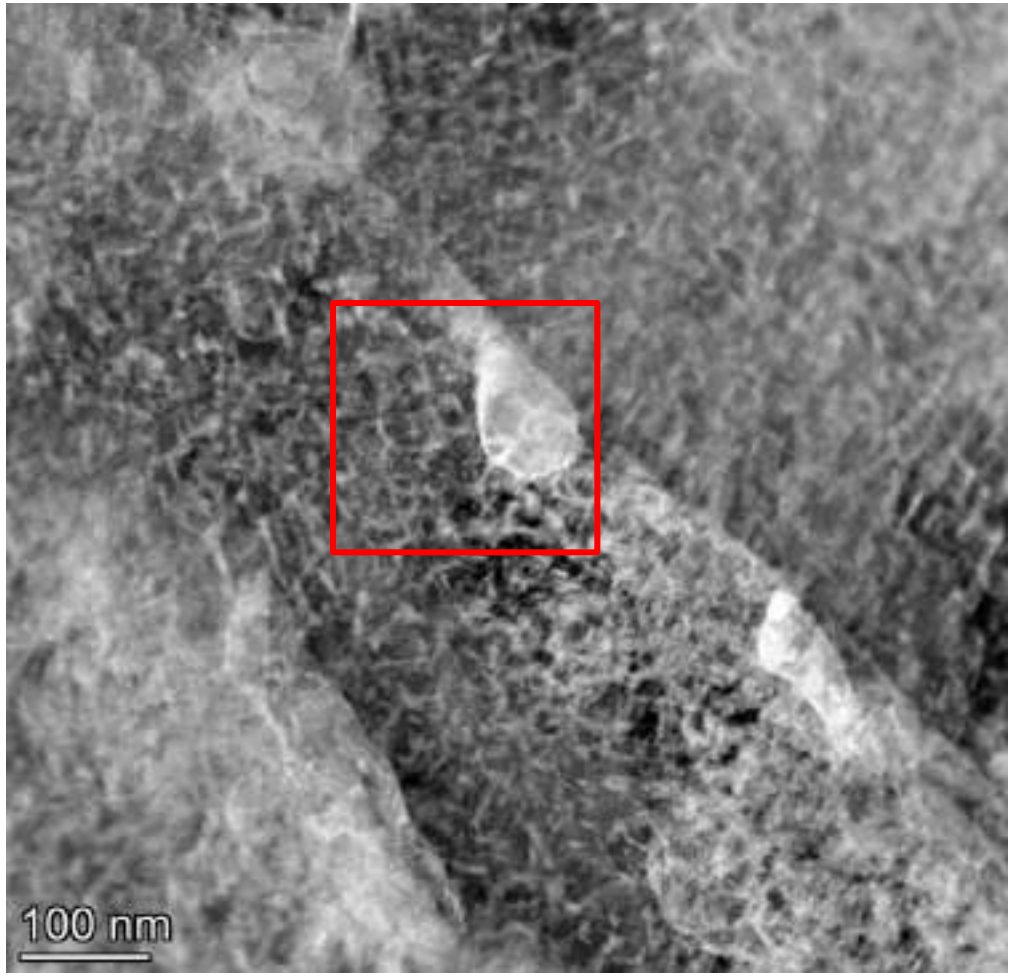

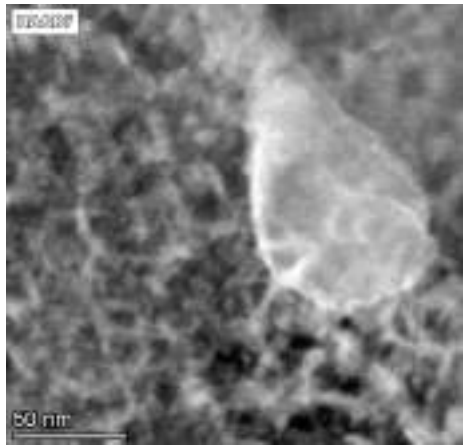

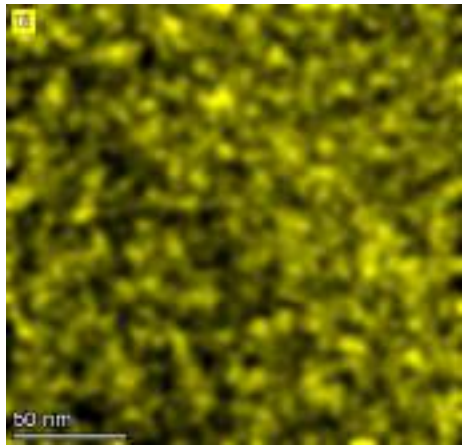

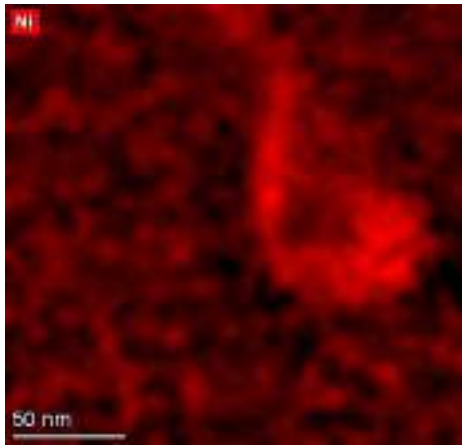

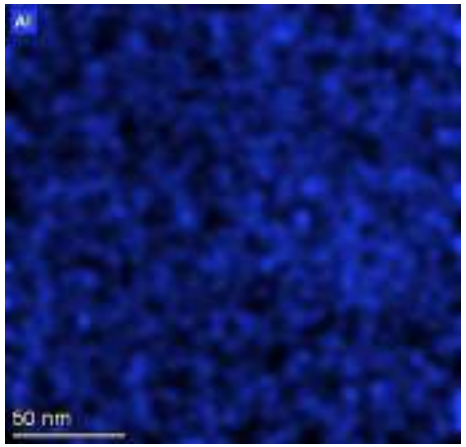

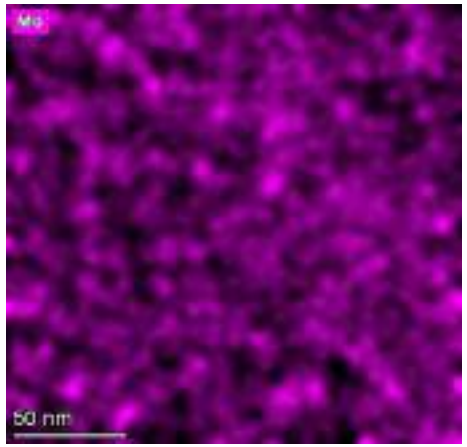

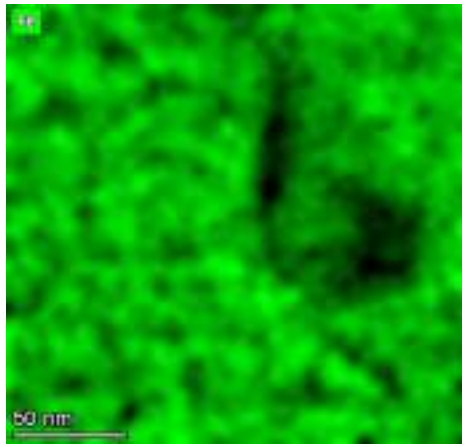

Austenite Reversion during Aging. 540 ºC

EOS condition

40 microns

CW laser mode

STEM mode

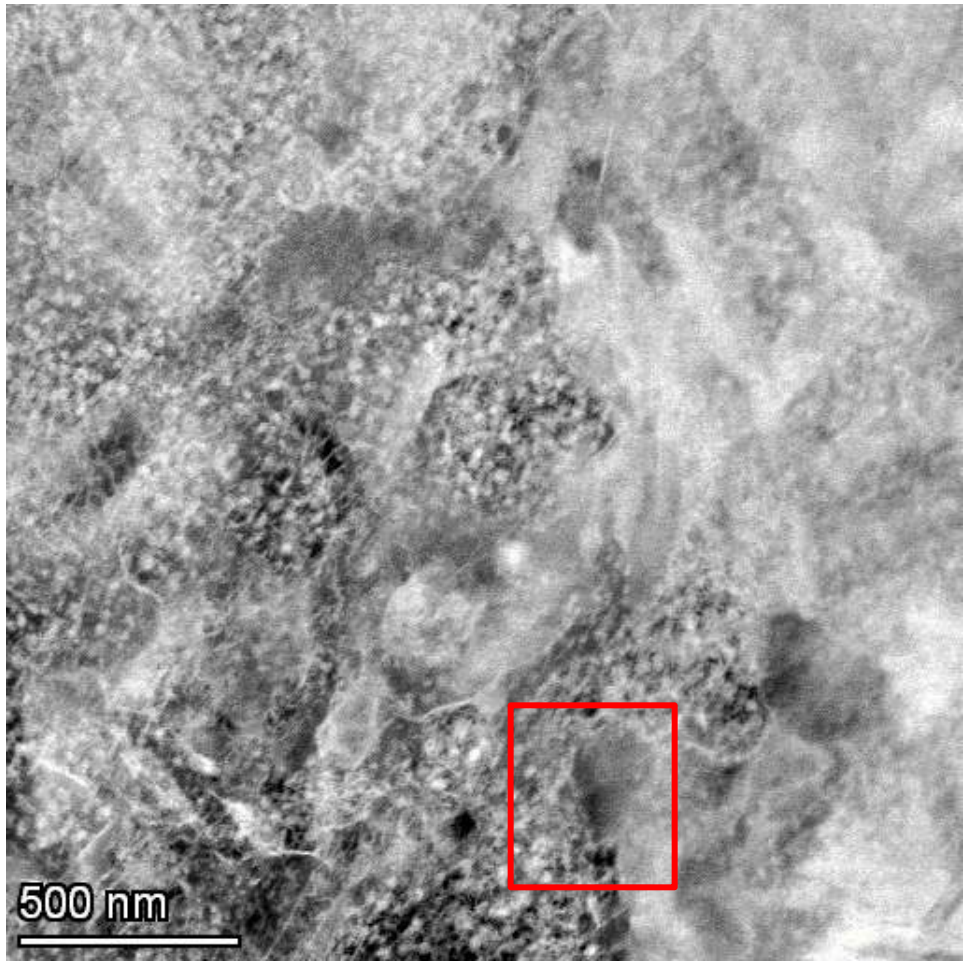

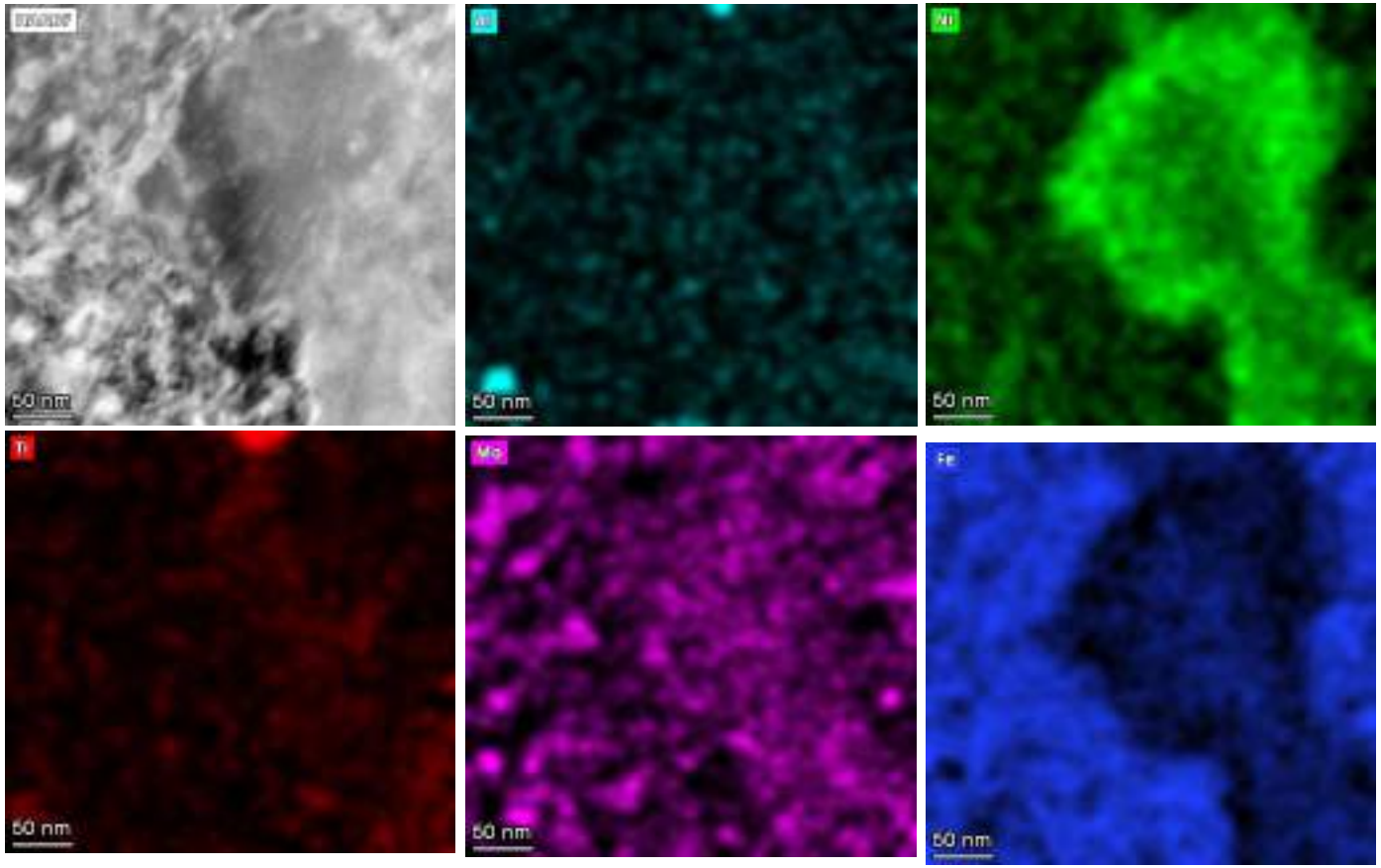

Hardness of LPBF Maraging Steel

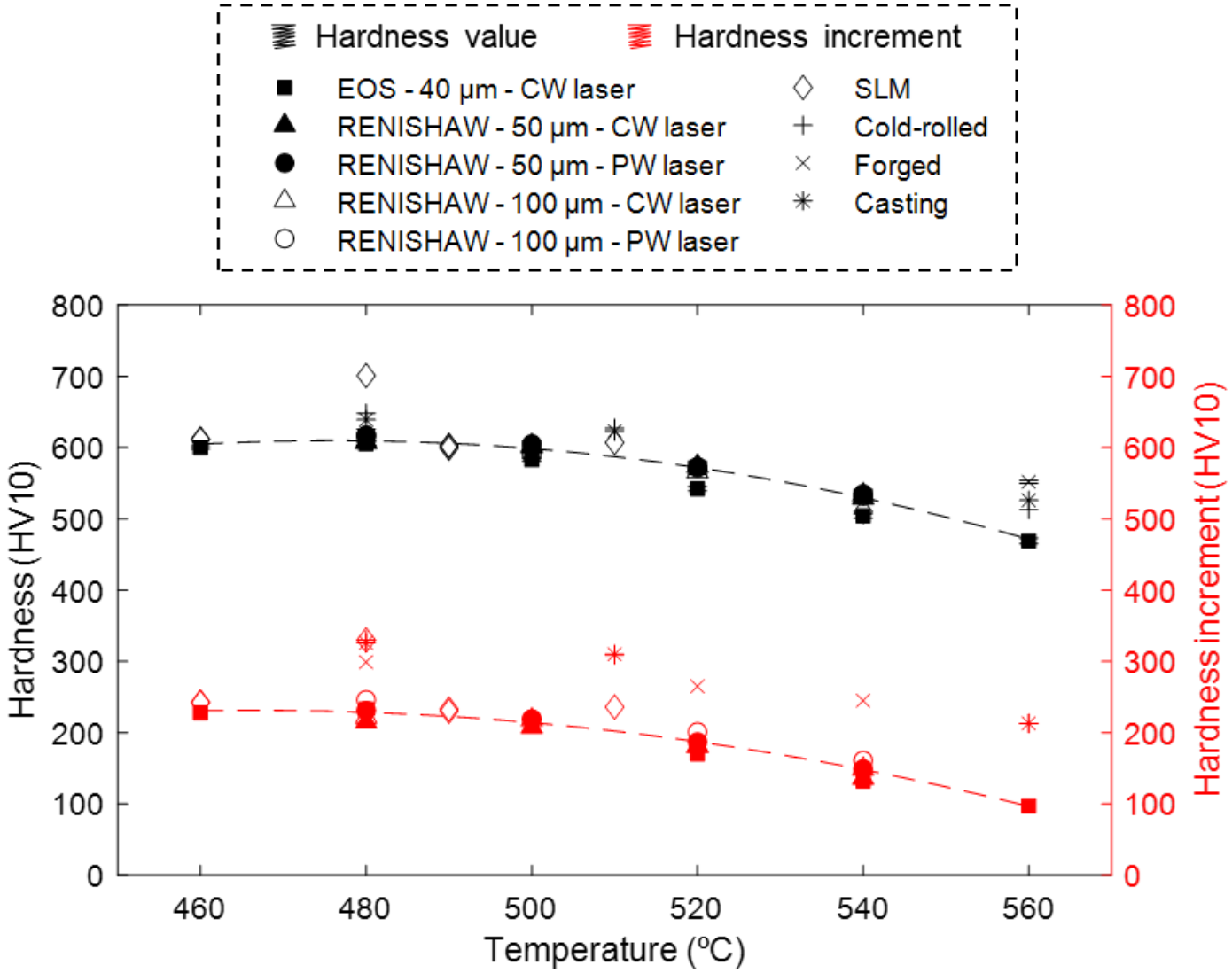

Content:

- ✓ Revealing the complexity of non-equilibrium, and non-uniform microstructures formed during LPBF process of maraging steels.
- ✓ Precipitation of intermetallic phases and austenite growth/reversion during ageing of LPBF maraging steels.
- ✓ Promoting thermal stabilization of austenite in microstructure by preheating and/or post-heat-treatment in a specially designed tool steels for LPBF manufacturing.

Laser Powder Bed Fusion with Base Plate Preheating

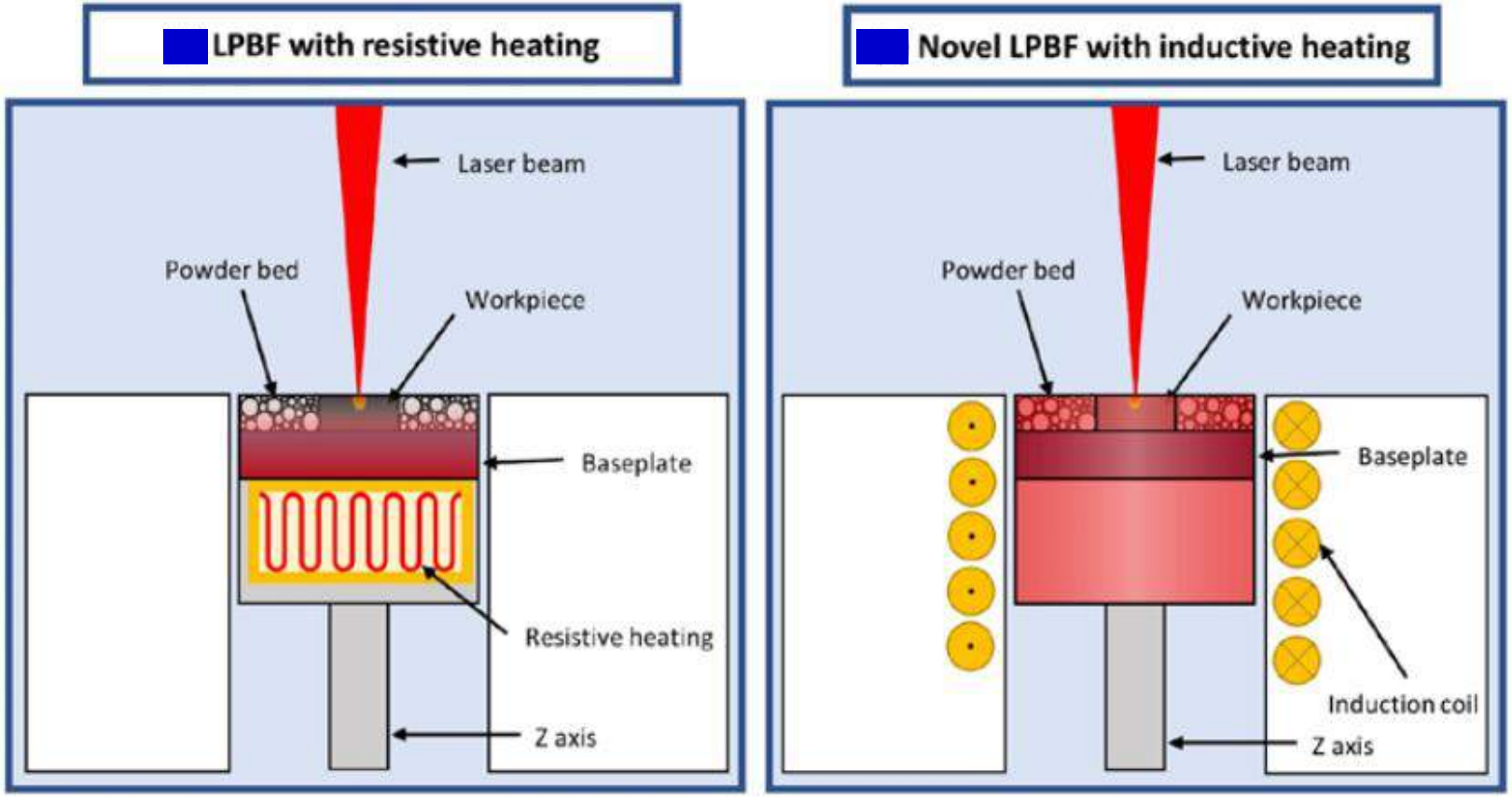

Base plate preheating is added to the process of LPBF. This tool aims at a reduction of thermal stresses in LPBF parts, achieved by decreasing the thermal gradients during processing.

Preheating effect on as-built structures in a tool steel

220 W and 600 mm/s

No PH

PH=350ºC

PH=450ºC

Preheating effect on as-built structures in a tool steel

220 W and 600 mm/s

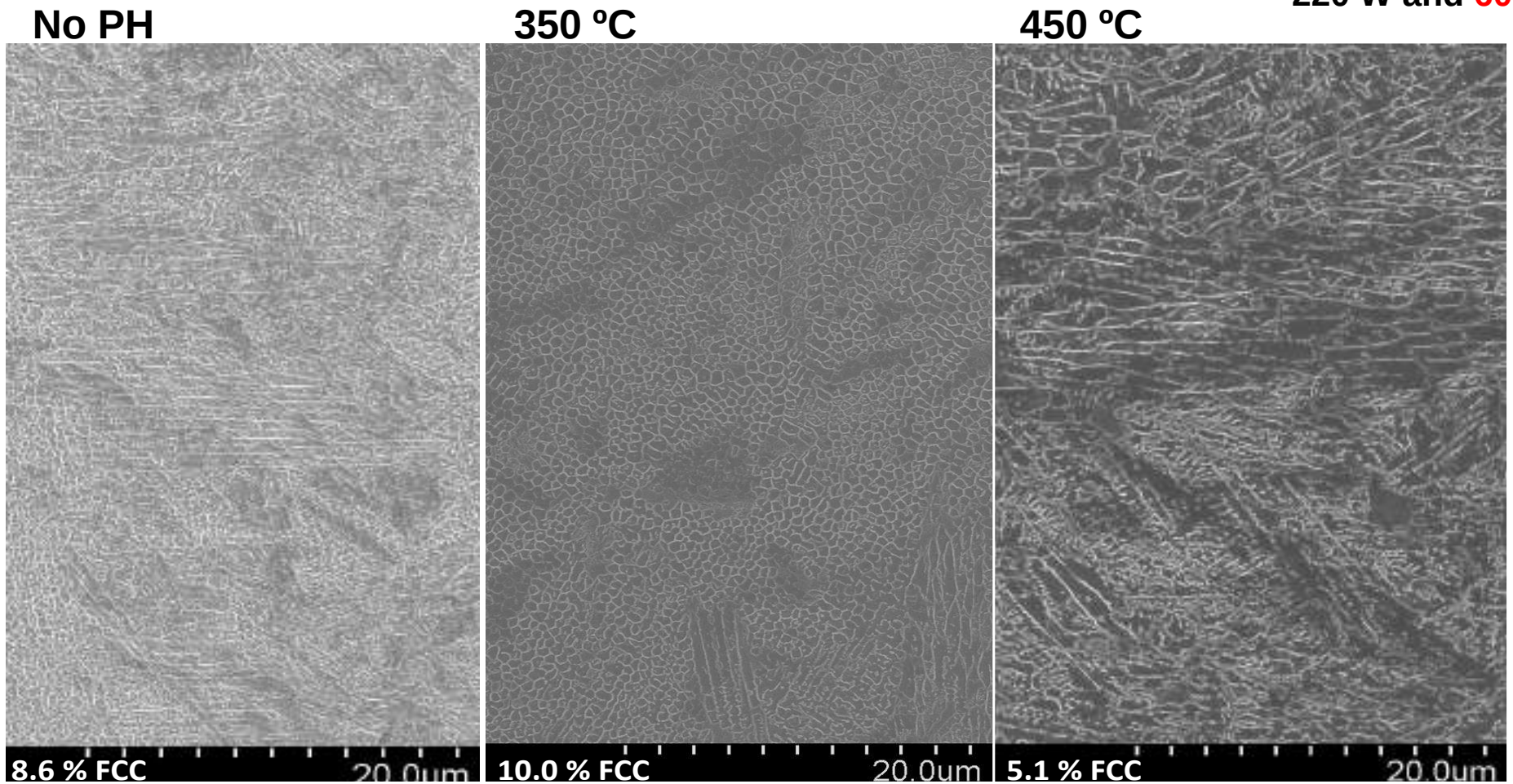

For pre-heating up to 350ºC, which is around the Ms temperature of the steel, the same cellular solidification structure and martensitic microstructure is found.

Changes in the microstructure are more evident if keeping the part above Ms temperature, where a bainitic microstructure is formed.

Preheating effect on as-built structures in a tool steel

220 W and 600 mm/s

No PH

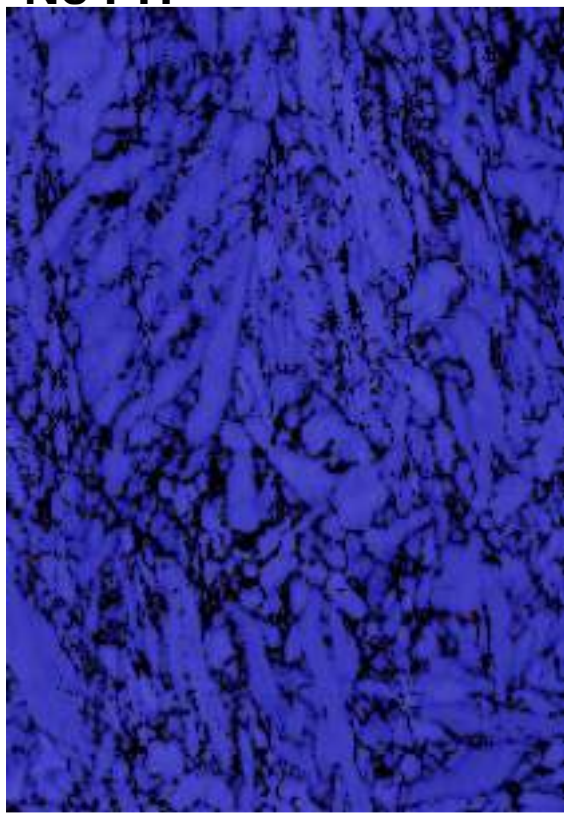

350 ºC

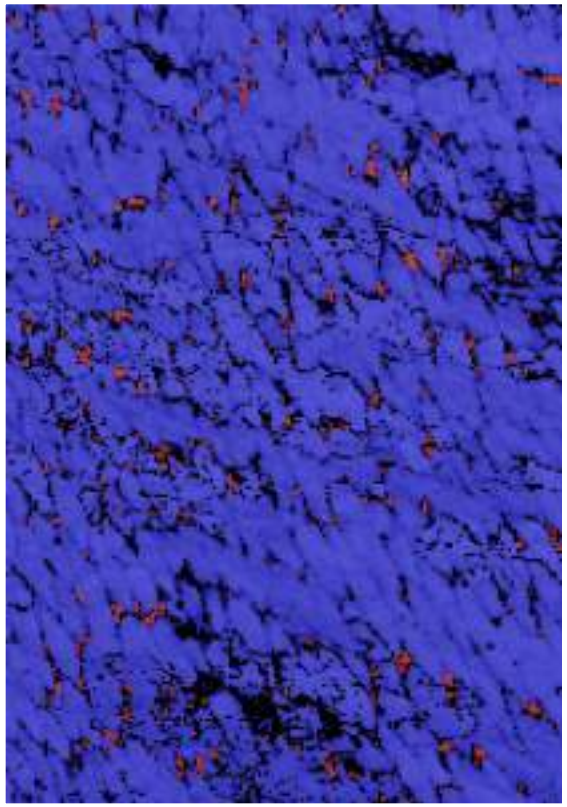

450 ºC

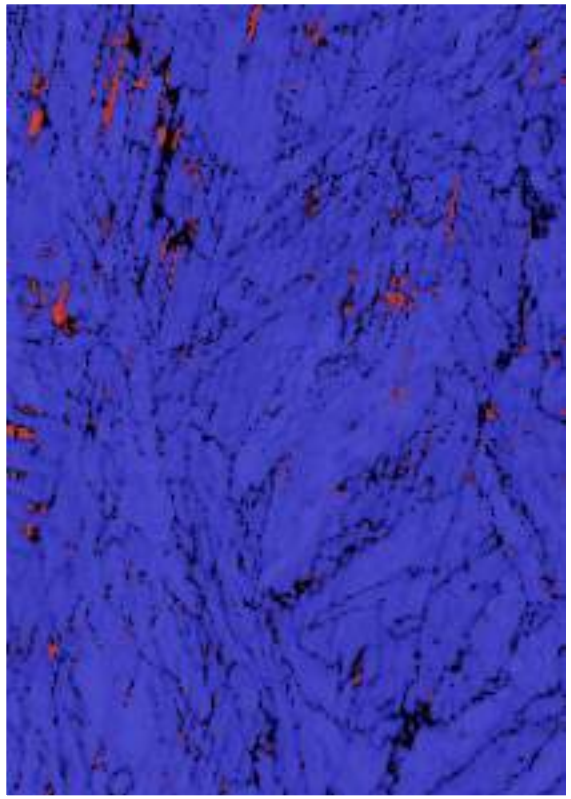

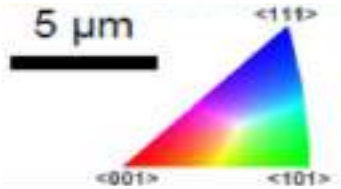

Phase identification by EBSD reveals that retained austenite is related to segregation at cellular boundaries.
The highly distorted crystal structure in the non preheated sample does not allow to resolve any retained austenite.

Preheating effect on as-built structures. Retained austenite content by XRD analysis

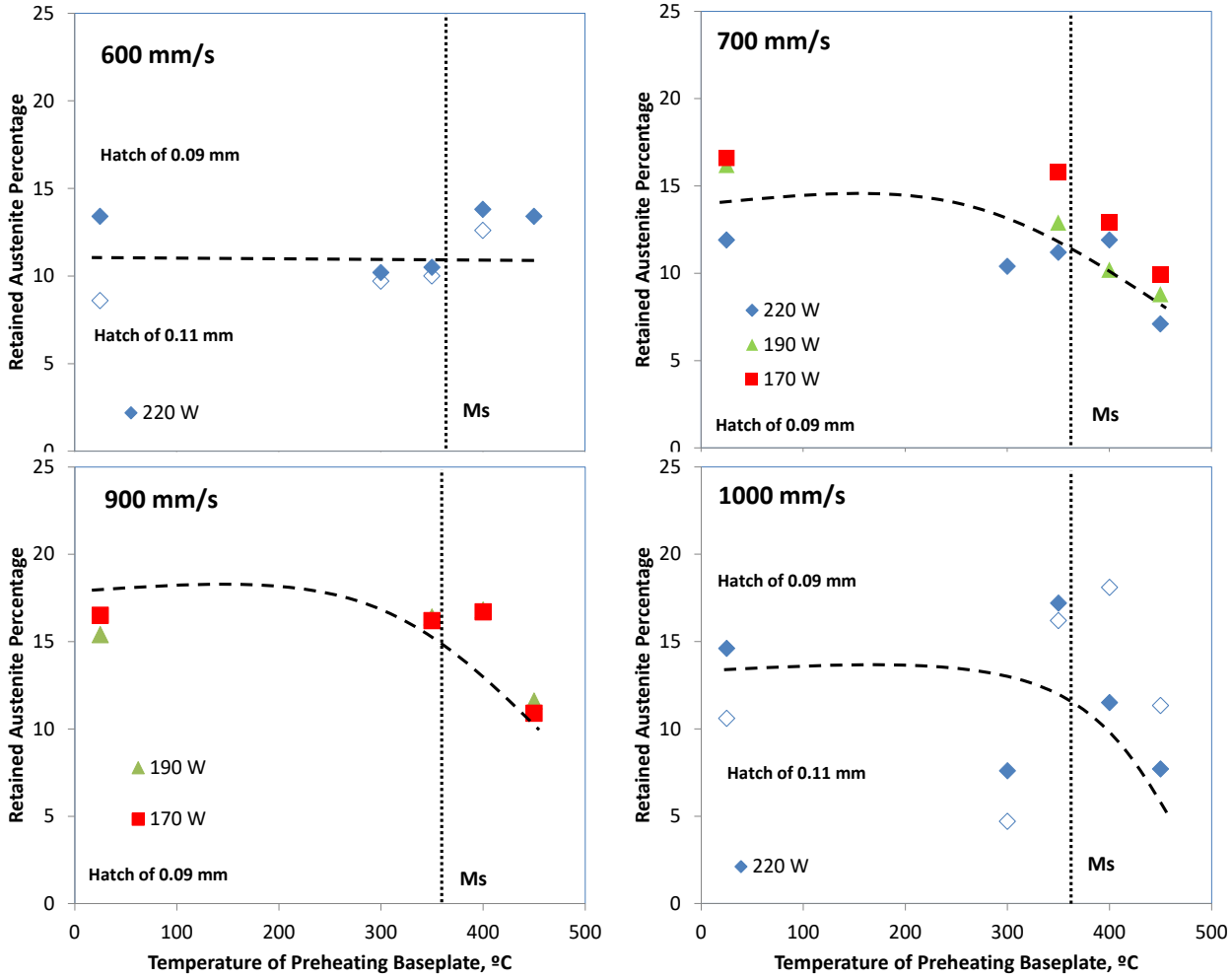

The effect of preheating on the stabilization of austenite to RT seems to be more pronounce at higher laser speed.

Hardness in as-cast and LPBF material

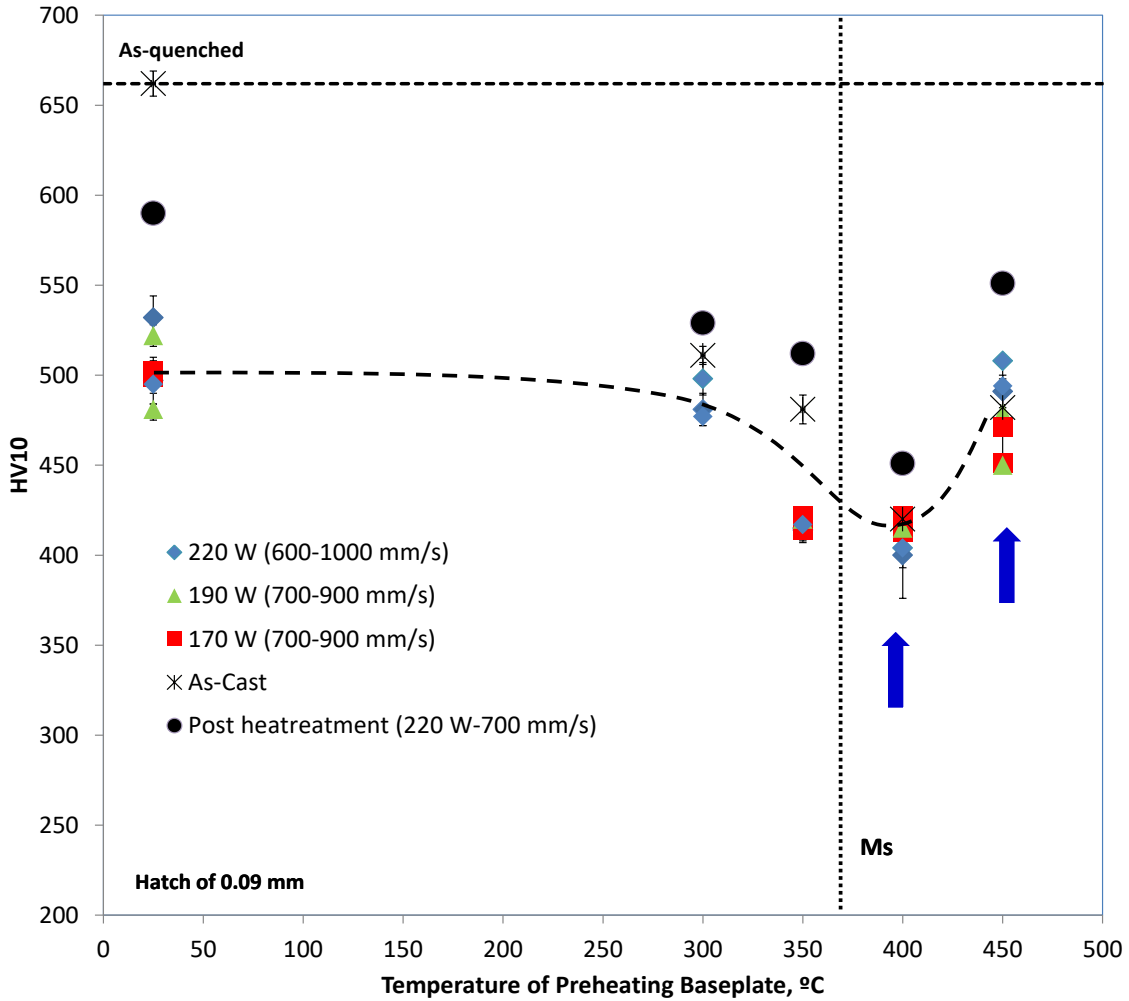

The effect of preheating on hardness seems to be independent of the LPBF processing parameters

As-cast material and isothermal heat treatment at 400 ℃

LPBF (220 W – 700 mm/s) Post heat treatment at 400 ℃

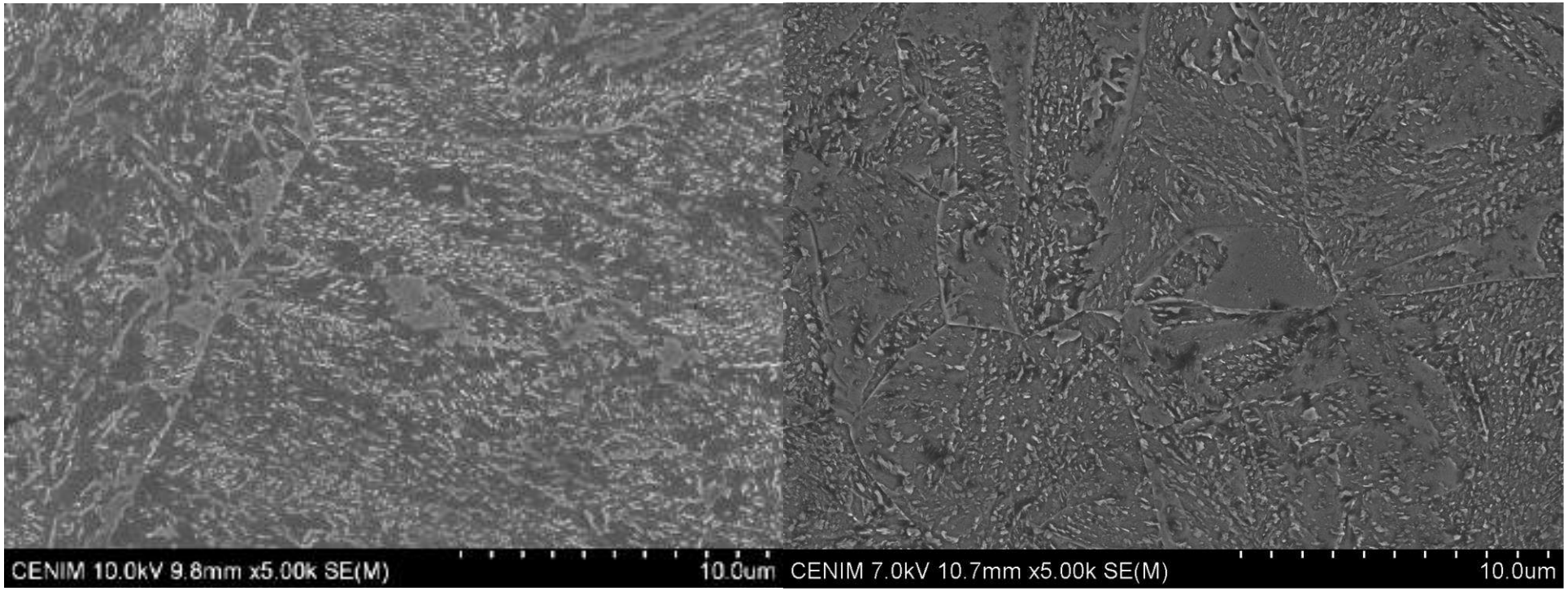

The degree of bainite transformation is lower in LPBF material for the same temperature. This explains the observed differences on hardness.

As-cast material and isothermal heat treatment at 450 ℃

LPBF (220 W – 700 mm/s) Post heat treatment at 450 ℃

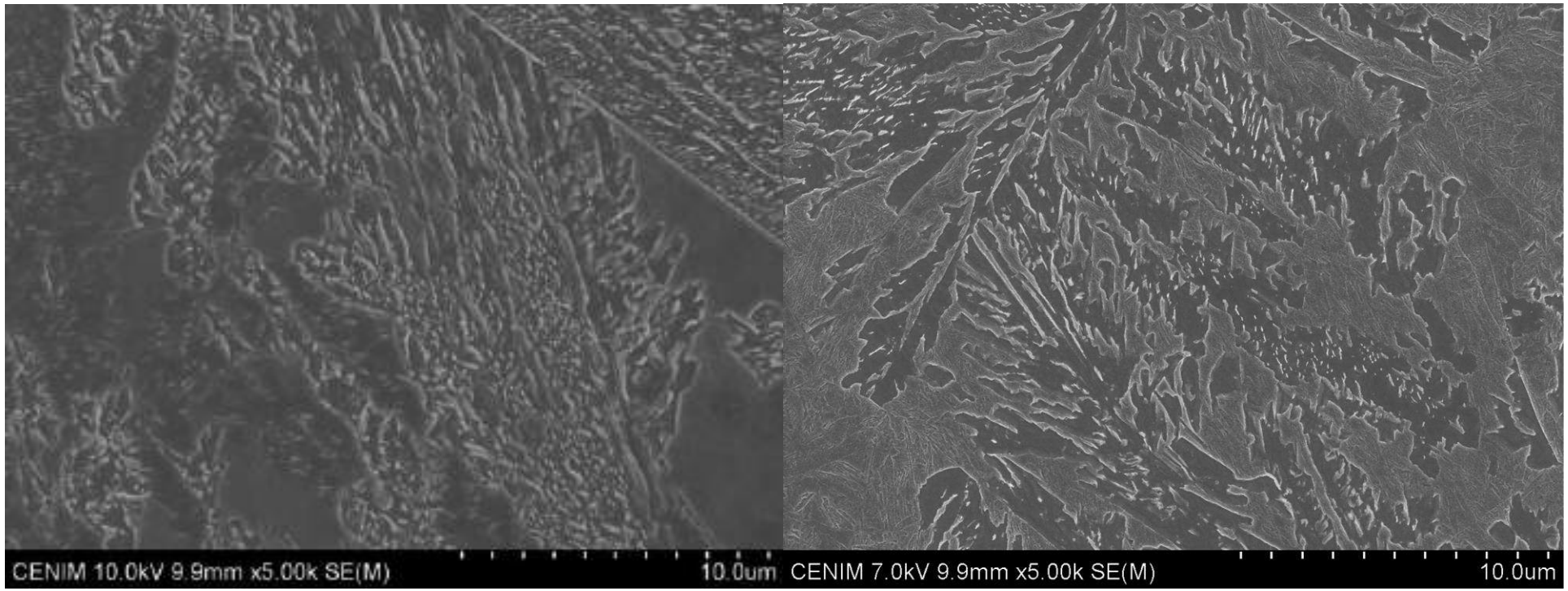

The degree of bainite transformation is lower in LPBF material for the same temperature. This explains the observed differences on hardness.

Remarks

- ✓ Refined cellular microstructure is a unique feature in alloys fabricated by laser powder bed fusion. Results evidenced the importance of layer thickness as a key parameter to modify the solidification cell size of the as-built samples.
- ✓ Solute segregation in additive manufacturing of steels leads to complex microstructures formed by a tetragonal martensitic matrix and a heterogeneous distribution of retained austenite.
- ✓ The high dislocation density in combination with solute segregation in the as-fabricated material can promote the precipitation of intermetallic phases that are responsible for the high strength.
- ✓ It is not clear if the austenite growth/reversion and the precipitation of the intermetallic phases during ageing occur as competitive or collaborative phase transformations.
- ✓ The amount of retained austenite can be controlled with the process parameters (laser speed, hatch...) and by preheating and/or post-heat-treatment.

Thanks for your attention

Blank

Thermal cycles

- **P.A. Hooper measured melt pool temperatures between 1,700 and 3,700 ºC by a high-speed temperature imaging system in laser powder bed fusion process [Additive Manufacturing, 2018, vo. 22, 548-559].**
- **Kosiba et al. determined the cooling rate inherent to high-power laser powder bed fusion between 14,000 and 90,000 ºC/s based on the average spacing of the lamellae of the eutectic microstructure of a Al-33Cu (wt%) specimen [Journal of Alloys and Compounds, 2023, vol. 967, 171773.**

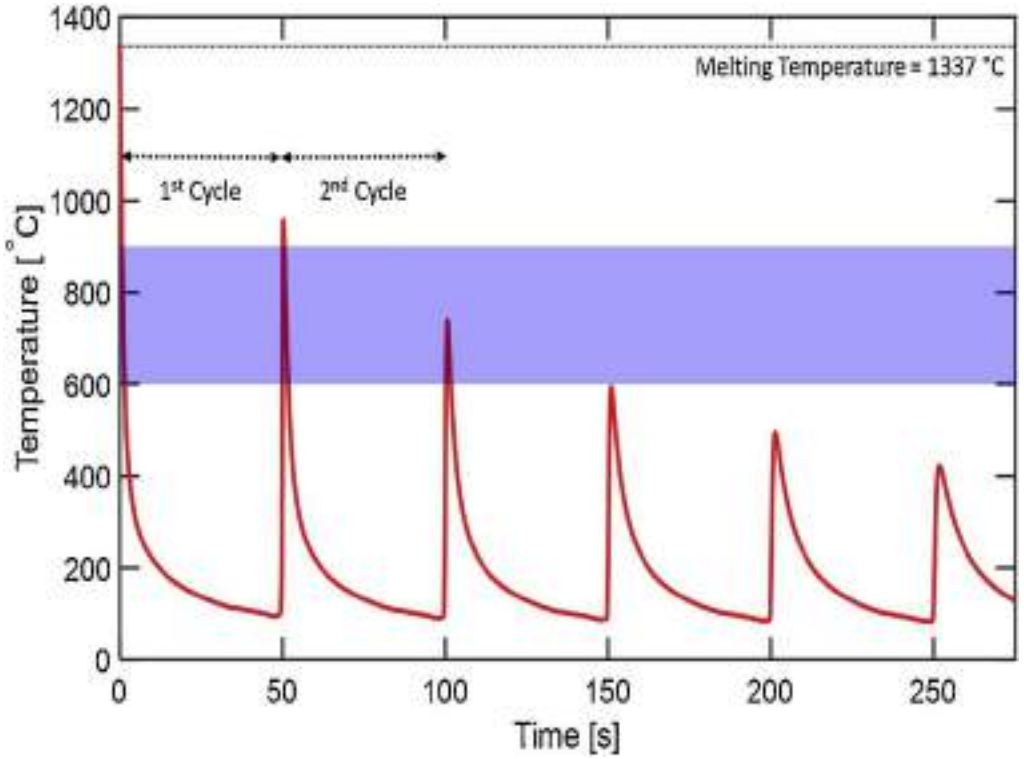

Kumara et al., 'Microstructure modelling of laser metal powder directed energy deposition of Ni alloy 718', Additive Manufacturing, 2019, vol. 25, 357-364.

Preheating effect on as-built structures in a tool steel

220 W and 600 mm/s

No PH

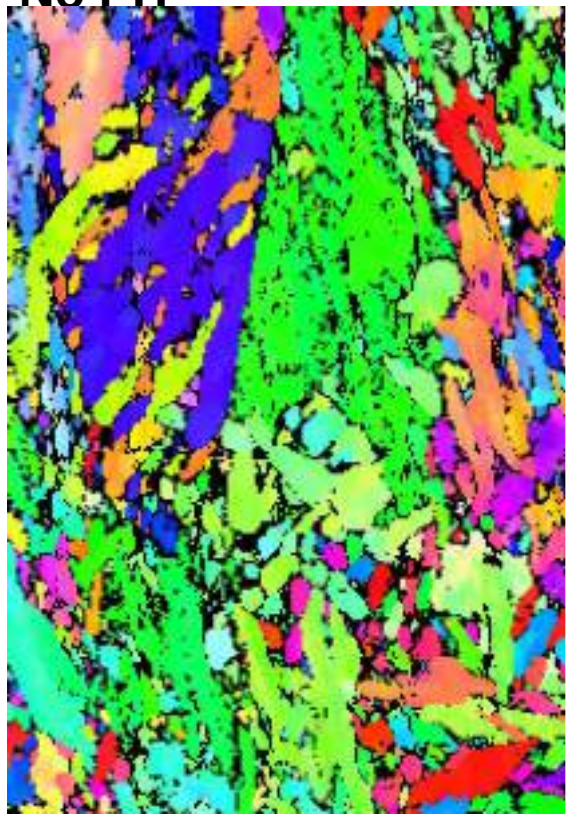

350 ºC

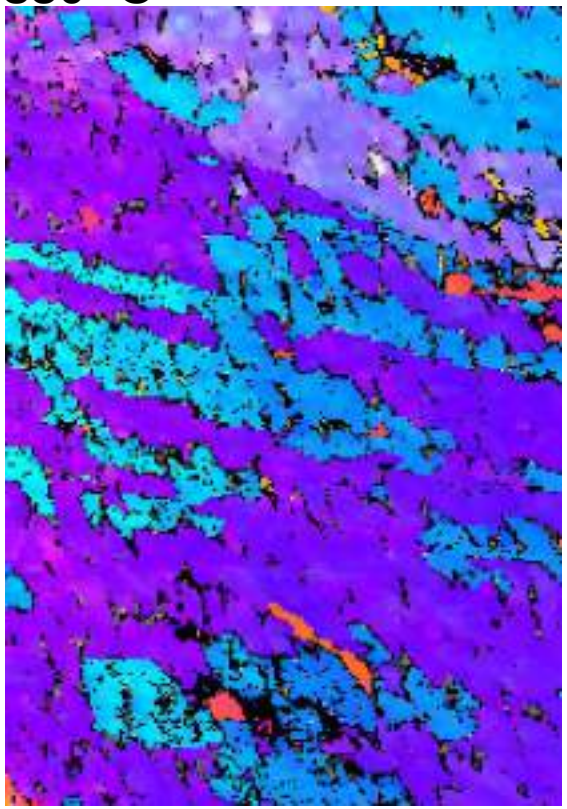

450 ºC

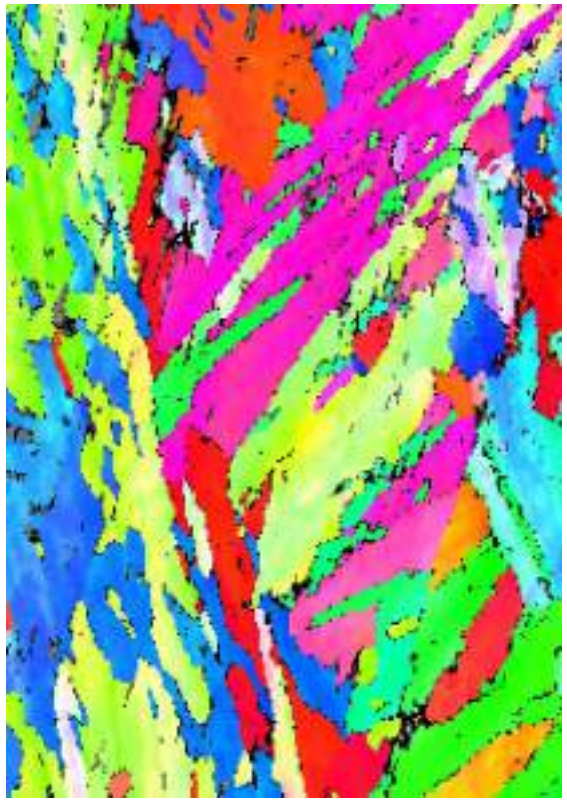

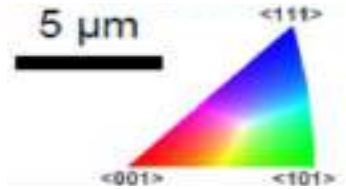

Ferrite crystals occupy several solidification substructures holding an orientation relationship between them and the retained austenite.

All the possible orientations variants are observed to form regardless the pre-heating temperature.

Preheating effect on as-built structures at nanoscale

No PH

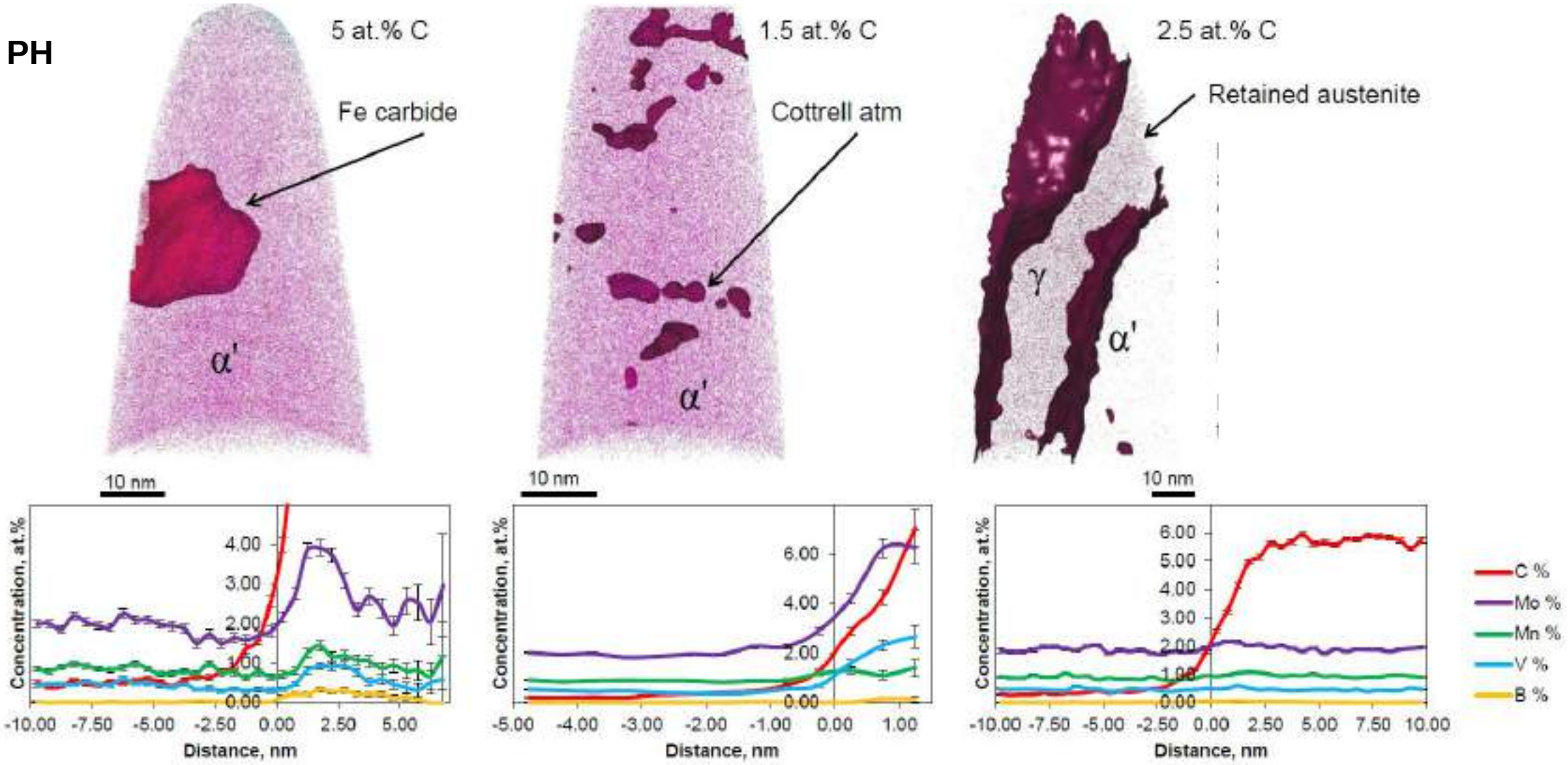

Slight partitioning towards carbides, strong partitioning towards Cottrell atmospheres, but no solute partitioning towards retained austenite. Carbon clusters are also identified with no solute segregation. The amount of carbon in martensite is below the nominal content (i.e. it is tempered).

Preheating effect on as-built structures at nanoscale

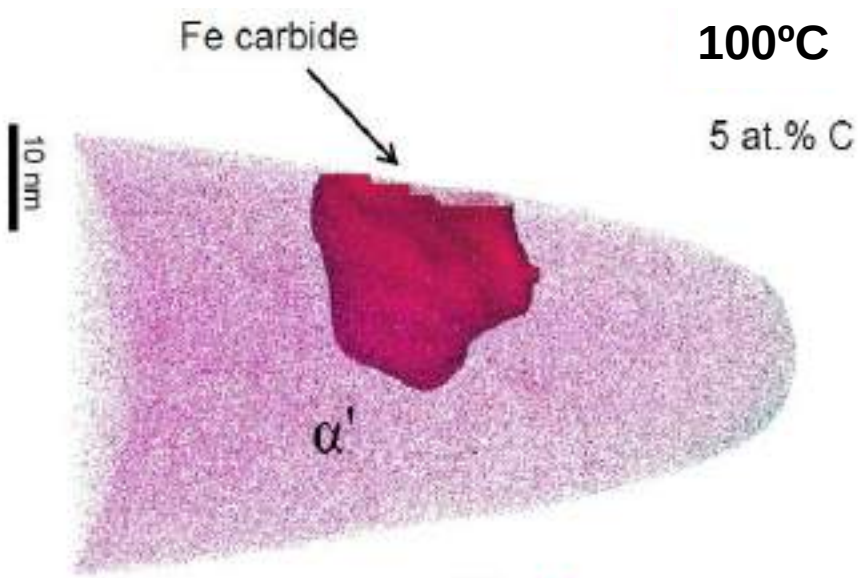

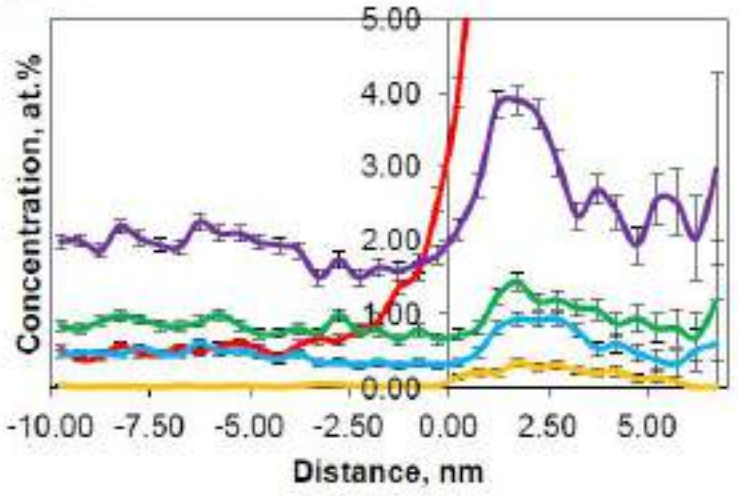

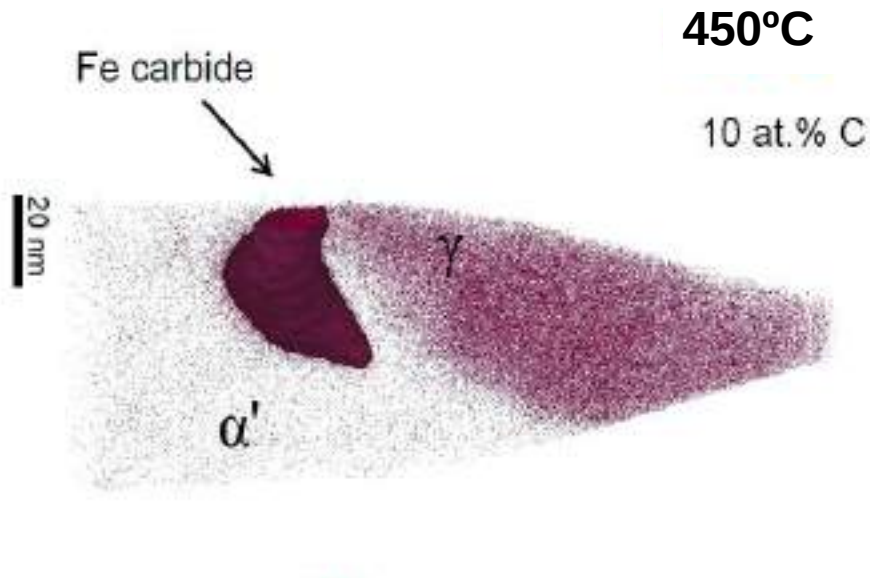

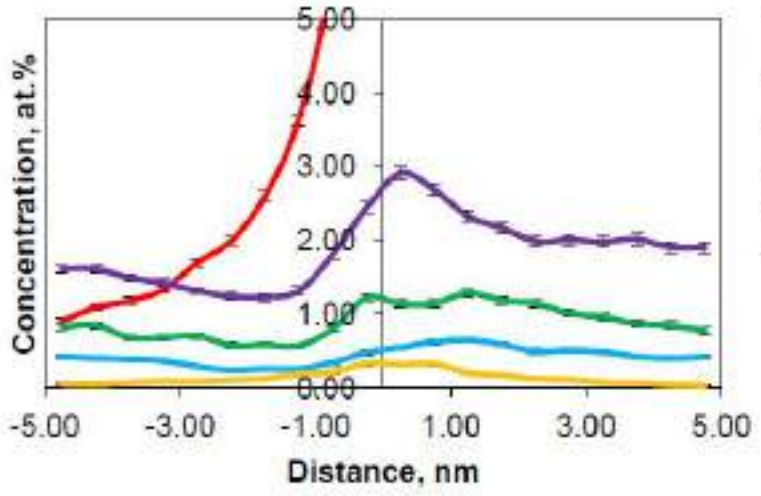

Iron carbides precipitated at 100 and 450ºC have a carbon content of 20 at.% (approx. cementite) and shown slight solute partitioning with spikes of solute enrichment at the interface.

Preheating effect on as-built structures at nanoscale

350 ºC

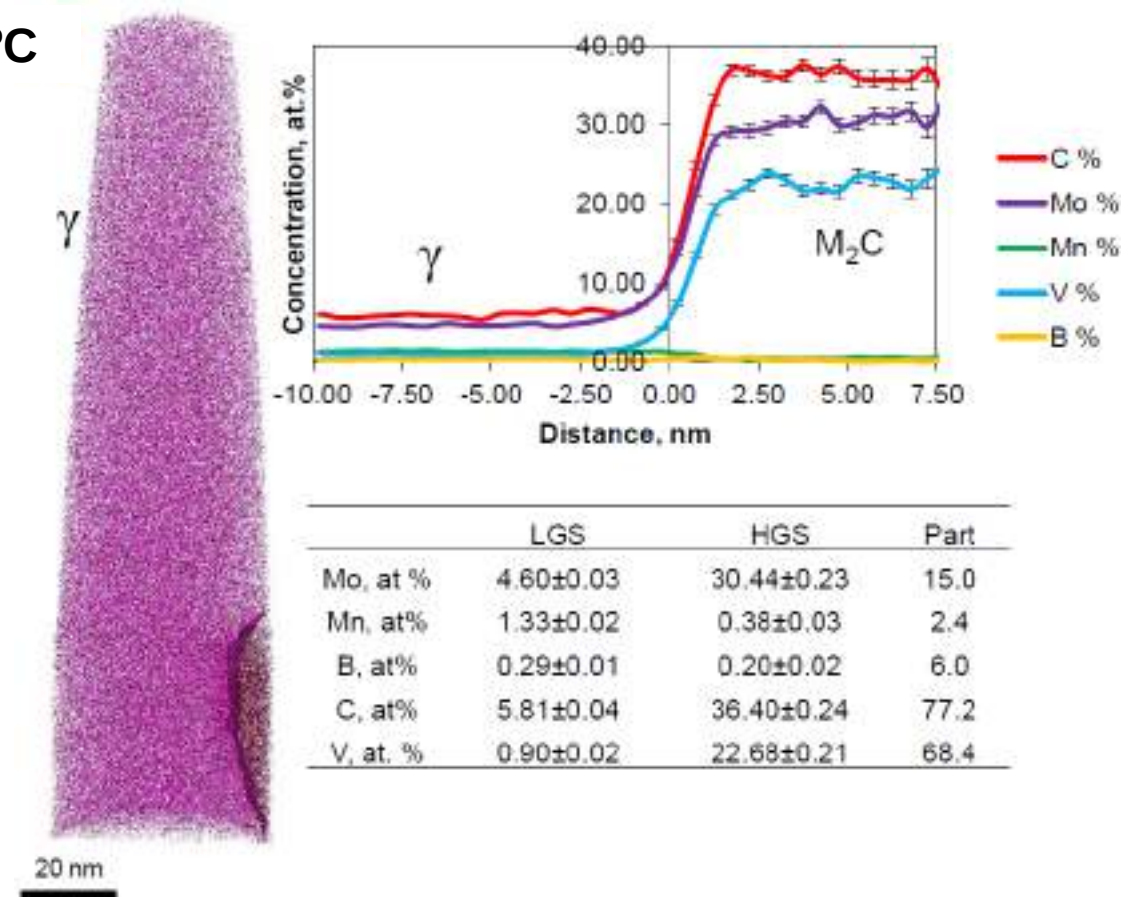

	LGS	HGS	Part
Mo, at %	4.60±0.03	30.44±0.23	15.0
Mn, at%	1.33±0.02	0.38±0.03	2.4
B, at%	0.29±0.01	0.20±0.02	6.0
C, at%	5.81±0.04	36.40±0.24	77.2
V, at. %	0.90±0.02	22.68±0.21	68.4

450 ºC

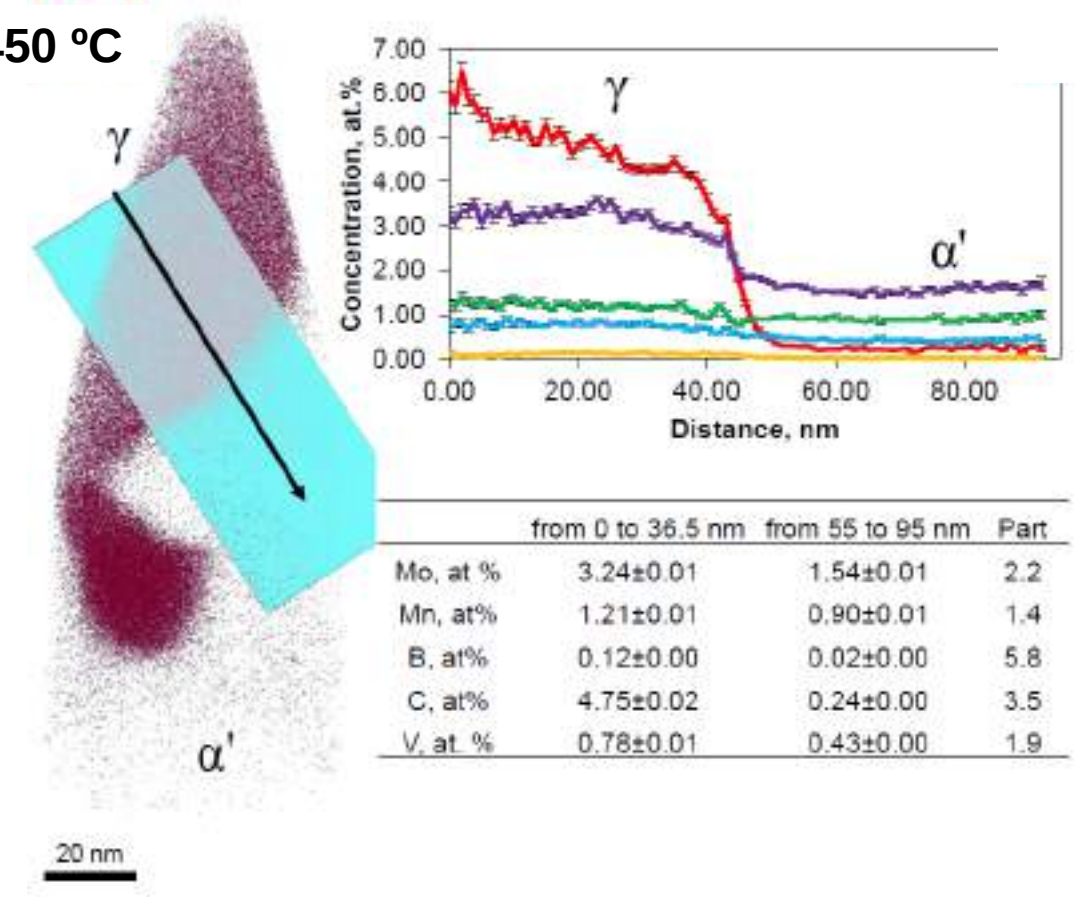

	from 0 to 36.5 nm	from 55 to 95 nm	Part
Mo, at %	3.24±0.01	1.54±0.01	2.2
Mn, at%	1.21±0.01	0.90±0.01	1.4
B, at%	0.12±0.00	0.02±0.00	5.8
C, at%	4.75±0.02	0.24±0.00	3.5
V, at. %	0.78±0.01	0.43±0.00	1.9

Molybdenum–vanadium carbides are detected at 350ºC. In this steel, carbon segregation is mainly responsible of the stabilization of the austenitic phase at the boundaries.